PHYSICAL REVIEW D **81,** 085030 (2010)

Gauge-invariant and infrared-improved variational analysis of the Yang-Mills vacuum wave functional

Hilmar Forkel

Institut für Physik, Humboldt-Universität zu Berlin, D-12489 Berlin, Germany

(Received 13 January 2010; published 22 April 2010; publisher error corrected 29 April 2010)

We study a gauge-invariant variational framework for the Yang-Mills vacuum wave functional. Our approach is built on gauge-averaged Gaussian trial functionals which substantially extend previously used trial bases in the infrared by implementing a general low-momentum expansion for the vacuum-field dispersion (which is taken to be analytic at zero momentum). When completed by the perturbative Yang-Mills dispersion at high momenta, this results in a significantly enlarged trial-functional space which incorporates both dynamical mass generation and asymptotic freedom. After casting the dynamics associated with these wave functionals into an effective action for collections of soft vacuum-field orbits, the leading infrared improvements manifest themselves as four-gradient interactions. Those turn out to significantly lower the minimal vacuum energy density, thus indicating a clear overall improvement of the vacuum description. The dimensional transmutation mechanism and the dynamically generated mass scale remain almost quantitatively robust, however, which ensures that our prediction for the gluon condensate is consistent with standard values. Further results include a finite group velocity for the soft gluonic modes due to the higher-gradient corrections and indications for a negative differential color resistance of the Yang-Mills vacuum.

DOI: 10.1103/PhysRevD.81.085030 PACS numbers: 11.15.−q, 11.15.Tk, 12.38.Lg

I. INTRODUCTION

The variational approach was among the first theoretical methods developed to study nonperturbative ground-state properties of quantum systems [1]. Soon after the inception of QCD, it was brought to bear on the physics of the gluon vacuum as well [2–6], making increasingly use of its capabilities to treat nonperturbative problems analytically, at real time and at strong coupling (in contrast, e.g., to semiclassical approximations). Indeed, variational techniques remain applicable even in nonstatic and curved spacetimes [7,8] as well as in nonequilibrium [9] situations [11]. Since variational problems are naturally formulated in the Schrödinger picture, furthermore, they often invoke quantum-mechanical intuition to shed new light on field-theoretic states, as encoded, e.g., in the node number of their wave functionals [4,12] or in the action of transformation groups [7]. On the other hand, field-theoretic applications have to implement the UV field modes and their dynamics exactly [12], they must deal with the standard renormalization issues in the Schrödinger representation [13,14], and they require a manageable way of calculating matrix elements by functionally integrating over physical intermediate states. For gauge theories, maintaining gauge invariance becomes an additional mandatory requirement which, in the Hamiltonian formulation, amounts to preserving Gauss' law. Traditionally, the latter is implemented in combination with (almost) complete gauge fixing to Coulomb gauge [2,15,16], although generally without full account of the gauge-group topology and the resulting Gribov copies. In addition, this gauge-fixed approach has to deal with a nonlocal Hamiltonian [17] and must take special precautions to avoid gauge-symmetry breaking approximations [18].

Alternatively, the variational problem can be formulated in a (residual) gauge-invariant manner which, at least under certain approximations, remains analytically tractable [18]. The mechanism of dimensional transmutation becomes manifestly gauge invariant and particularly transparent from this perspective [19], and the dynamical mass gap [20] emerges already from a minimal parametrization of the Gaussian ''core'' wave functional [18]. The projection onto the gauge-singlet component of this core functional may furthermore generate an area law for spacelike Wilson loops and thereby account for linear quark confinement [18,19,21], although experience from compact electrodynamics suggests that the vacuum wave functional will need nonminimal adjustments to describe the charged sector [22]. Another attractive feature of this approach is that it re-expresses the infrared dynamics in terms of gauge-invariant matrix fields (which subsume whole families of gauge-field orbits [23]) and that it preserves traceable links of heuristic value between these soft collective fields and the underlying Yang-Mills fields. Moreover, the gauge-invariant reformulation preserves the global, i.e., topological properties of the gauge fields. The contributions from all vacuum homotopy classes as well as instanton-mediated transitions between them, for example, are explicitly and transparently taken into account without recourse to the semiclassical approximation [7,18,23,24]. Besides such sets of (multi-) instanton and meron orbits, the dynamics contained in the vacuum wave functional sustains a rich variety of additional gauge-invariant infra-

red modes, including Faddeev-Niemi knots and other topological as well as nontopological solitons [23,25].

Our main objective in the present article will be to improve the vacuum description provided by the gauge-invariant variational approach. To this end, we develop a trial-functional family which accommodates a rather general momentum distribution for the infrared vacuum modes while remaining analytically tractable. Because of the explicit representation of the ground state, structural aspects of the Yang-Mills dynamics and their impact on the vacuum can then be understood in terms of the resulting gauge-field population. Moreover, our generalized trial basis will aid in the full exploration of the gauge-projected Gaussian functional space, e.g., by evaluating and analyzing relevant amplitudes, and thereby in the assessment of its limitations and further improvement potential. In the longer run, this type of analysis should reveal the extent to which Yang-Mills vacuum physics can be captured by the most general Gaussian core functionals, their subsequent gauge projection and the mean-field treatment of the resulting soft-mode dynamics. One may hope that these insights will eventually help to find a systematic and manageable approximation to the Yang-Mills vacuum wave functional beyond the Gaussian ansatz.

After having set up our extended trial-functional space, the next major task will be to establish the framework for calculating the associated vacuum amplitudes. This will enable us, in particular, to evaluate the vacuum energy density and its reduction in the generalized trial space, thus providing a quantitative measure for the improvement of the vacuum description. The analysis of the infrared-mode distribution encoded in the energetically favored wave functional will further shed new light on the resulting vacuum physics. It will, in particular, reveal the physical significance of the variational parameters and clarify the impact of their optimized values on the soft-mode dynamics. We will furthermore examine the influence of the enlarged trial space on the phase structure and the order-disorder phase transition of the underlying infrared dynamics (which has, as the Yang-Mills dynamics, its origin in the imposition of gauge invariance). In fact, the robustness of this phase transition ensures a reliable variational determination of the ground-state energy. Our analysis of the resulting vacuum properties will be complemented by evaluating the lowest-dimensional gluon condensate, which also provides a quantitative test of the dynamically generated mass scale and its relation to the underlying trace anomaly. Beyond the evaluation and analysis of specific amplitudes, finally, the extended variational framework will furnish a transparent theoretical laboratory well suited to build up nonperturbative real-time intuition about the Yang-Mills vacuum [26].

The paper is organized as follows: in Sec. II, we introduce our infrared-generalized, gauge-invariant trial-functional family for the Yang-Mills ground state. In Sec. III we rewrite the associated vacuum overlap amplitude in terms of an effective bare action, summarize our strategy for calculating the variational bound on the Yang-Mills vacuum energy, and review the perturbative integration over the hard modes which results in a renormalized soft-mode action. In Sec. IV, we develop the theoretical framework for calculating relevant amplitudes by integrating over the soft modes, and in Sec. V, we derive explicit expressions for the 2- and 4-point functions. Their further evaluation is prepared in Sec. VI, where we set up the saddle-point expansion for the integral over the soft modes. We further derive the corresponding gap equation and find its solutions, which provide quantitative information on the phase structure of the soft-mode dynamics. In Sec. VII, we calculate the various contributions to the vacuum energy density (both in the ordered and disordered phase) which we minimize in Sec. VIII. We further compute the gluon condensate, discuss the physical implications of our results and suggest a few directions for future work. In Sec. IX, finally, we collect our principal results and our main conclusions.

II. VACUUM WAVE FUNCTIONAL

The success of variational estimates depends mostly on the choice of the underlying trial function(al) space. Ideally, it should be both comprehensive enough to accommodate the relevant physics and concise enough to remain analytically tractable and reasonably transparent. In the following sections we establish the basis of our subsequent analysis by introducing a gauge-invariant trial-functional family for the Yang-Mills ground state which is designed to compromise between these conflicting goals. Although our trial space expands the minimal one used in Ref. [18] substantially, the ensuing variational analysis will turn out to require only a moderate increase in computational effort.

Our basis implements Feynman's three requirements for trial wave functionals of gauge theories, i.e., the at least approximate calculability of matrix elements, the correct UV asymptotics and gauge invariance [12]. The major methodological advance of Ref. [18] was to show that a trial space of manifestly gauge-invariant wave functionals, namely, gauge-projected Gaussians, still permits an (approximately) analytically manageable variational analysis. In the following sections we first discuss the essential features of the minimal ansatz of Ref. [18], and then generalize its momentum distribution for the infrared vacuum modes.

A. Gauge invariance by projection

Variational analyses are naturally set up in the Hamiltonian formulation of Yang-Mills theory and in the ''coordinate'' Schrödinger picture. This restricts gauge transformations to a fixed reference time, thereby effectively decoupling them from the dynamical time evolution.

In the temporal (or Weyl) gauge $A_0^a = 0$ which we adopt in the following, the residual gauge transformations are static, furthermore, and problems with negative-norm states (as, e.g., in covariant gauges) are avoided from the outset [27]. The gauge invariance of the vacuum wave functional is imposed by Gauss' law which acts as a subsidiary condition in Fock space. This is particularly crucial for variational treatments because the Yang-Mills Hamiltonian becomes unique only when acting on physical states. Hence, as pointed out in Ref. [18], trying to minimize the vacuum expectation value of the Hamiltonian in the whole space of normalizable functionals could favor contributions from unphysical parts of the Hilbert space which may be almost arbitrarily enhanced by adding functionals of gauge-group generators to a given Hamiltonian.

Starting from an approximate and hence typically gauge-dependent core functional ψ_0 to be specified in Sec. II B (ψ_0 depends on the static gauge fields $\vec{A}(\vec{x})$, i.e., on half of the canonical variables), we impose gauge invariance by projecting on its gauge-singlet component, which amounts to averaging over the gauge group [29]. The result is a trial vacuum wave functional of the form

$$\Psi_0[\vec{A}] = \sum_{Q\in Z} e^{iQ\theta} \int D\mu[U^{(Q)}]\psi_0[\vec{A}^{U^{(Q)}}] =: \int DU\,\psi_0[\vec{A}^U], \tag{1}$$

where $d\mu$ is the invariant Haar measure of the SU(N_c) gauge group [30], Q is the homotopy degree or winding number of the group element $U^{(Q)}$, and θ is the vacuum angle. The expression (1) acquires the obligatory θ phase under large (i.e., topologically nontrivial) gauge transformations and renders Gauss' law manifest.

Instead of dealing with the gauge-invariant trial functional (1), one may alternatively evaluate the energy density of gauge-*dependent* Gaussian wave functionals and then correct for the lack of gauge invariance before miniziation. This approach was pursued in Ref. [31] where the spurious kinetic energy due to gauge rotations was subtracted by Thouless-Valatin projection (as originally developed for the treatment of deformed nuclei). The main advantages of the approach based on wave functionals of the type (1) are that gauge invariance of subsequent calculations and approximations is maintained exactly, and that it applies universally to *all* matrix elements.

B. Gaussian core wave functional

In order to determine the gauge-invariant trial functionals (1) and the related amplitudes completely, it remains to adopt a core-functional family ψ_0. As in any variational calculation, this choice generally remains an uncontrolled approximation without systematic improvement strategy. In order to motivate our choice for ψ_0 and to discuss the underlying physics, we first recall that the vacuum wave functional cannot have nodes, i.e., that $\psi_0[A] \geq 0$ for all A [4]. (This provides an example for how quantum-mechanical insights remain applicable to field theory in the Schrödinger representation as long as its infinitely many degrees of freedom do not generate qualitatively new effects.) Hence, one may write without loss of generality

$$\psi_0[\vec{A}] = \frac{1}{\mathcal{N}} e^{-\Phi[\vec{A}]}, \tag{2}$$

where $\mathcal{N}$ is a generally infinite normalization constant, and Φ is a real and typically nonlocal functional of the gauge field. In order to find a viable approximation for Φ, we represent it as a functional power series in A and determine physically reasonable and analytically tractable truncations. The first two terms of this series are generally discarded: constant terms can be absorbed into the normalization constant $\mathcal{N}$, while the term linear in the gauge field (by itself) corresponds to a coherent vacuum state which is known to be unstable [32].

The next term is quadratic in A and plays several crucial roles. The first originates from an ambiguity in Φ which is due to the invariance of the Haar measure in Eq. (1) under right (or left) multiplication by any given group element. As a consequence, infinitely many choices for $\Phi[A]$ lead up to an unphysical redefinition of the normalization constant to the same Ψ_0 [21]. This ambiguity can be removed, however, by prescribing the quadratic term of Φ. Furthermore, this term leads to a product of Gaussian vacuum wave functionals of the Abelian $U(1)$ gauge theory [33] which asymptotic freedom renders exact in the ultraviolet. Finally, and from the practical perspective most importantly, the Gaussian functional ψ_0 resulting from a quadratic term can be integrated over A analytically, while higher-order contributions may at best be treated perturbatively [35]. Hence, one generally truncates the series for Φ after the quadratic term, which leads to the "squeezed" approximation for the core functional, i.e., to the Gaussian

$$\psi_0^{(G)}[\vec{A}] = \frac{1}{\mathcal{N}_G} \exp\Big[-\frac{1}{2}\int d^3x \int d^3y A_i^a(\vec{x}) \times G_{ij}^{-1ab}(\vec{x}-\vec{y})A_j^b(\vec{y})\Big], \tag{3}$$

with the normalization factor $\mathcal{N}_G^{-1} = [\det(G/2)]^{-1/4}$ and a real kernel or "covariance" G^{-1} which satisfies a normalizability condition [cf. Eq. (8)]. Equation (3) appears to be the "richest" core-functional family whose matrix elements can be dealt with by the currently available analytical methods of field theory. [Adding c number sources to the variable A would still allow for an analytical treatment and generate finite vacuum expectation values for A in gauge-fixed approaches, while such local "condensates" (except of the time component) are not sustained in

our residually gauge-invariant vacuum and would be rendered mute by the gauge projection in Eq. (1).]

As already mentioned, the core functional (3) represents an infinite product of Gaussians, one for each Fourier mode of the gauge field with momentum $\vec{k}$. Hence, the components of the Fourier-transformed covariance

$$\omega_{ij}^{ab}(\vec{k}) := G_{ij}^{-1,ab}(\vec{k}) = g_1^{ab}(k)\delta_{ij} + g_2^{ab}(k)\hat{k}_i\hat{k}_j \quad (4)$$

(where $\hat{k}_i := k_i/k$ with $k := \sqrt{k_i k_i}$) turn after diagonalization into mode frequencies or energies. The squeezed state thus generalizes the ground state of the quantum-mechanical harmonic oscillator. In our context, it corresponds to a vacuum consisting of color-singlet gauge-field pairs which may be regarded as the protostate of a glueball condensate [36]. (This should be contrasted to the ''condensation'' of single gluons in a coherent state.)

Since Gaussian functionals transform nontrivially under non-Abelian gauge groups, the gauge averaging in Eq. (1) is an integral part of our approximation to the physical vacuum state. Gauge-fixed variational analyses in Coulomb gauge (for references see, e.g., [2,5,6,15,16]) are generally based on Gaussian functionals as well, however. They were found to generate a mass gap [2,15] and, when multiplied by the inverse square root of the Faddeev-Popov determinant, an approximately linearly rising confinement potential [16].

C. General properties and UV asymptotics of the covariance

We are now going to specify the properties of the covariance (4) which characterizes the members of our core trial-functional family (3) and which contains the variational parameters whose values will be adapted below to optimally approximate the Yang-Mills vacuum wave functional. Translational invariance implies $G_{ij}^{-1,ab}(\vec{x},\vec{y}) = G_{ij}^{-1,ab}(\vec{x}-\vec{y})$ and was already anticipated in Eq. (3). Without loss of generality at the perturbative level (and beyond, since the integration over the gauge group in Eq. (1) averages out longitudinal contributions), we will further specialize to a purely transverse covariance with $g_2 \equiv 0$ [18], i.e.,

$$G_{ij}^{-1,ab}(k) = \delta_{ij}G^{-1,ab}(k), \quad (5)$$

which allows for a direct comparison with the results of Ref. [18] and should be sufficient for our explorative purposes. (The impact of longitudinal contributions $\propto g_2^{ab}$ was discussed in Refs. [19,37], and a specific prescription for g_2^{ab} was shown to reproduce the 1-loop Yang-Mills β function. Because of the ambiguity of the core functional mentioned in Sec. II B, a longitudinal term in the covariance can always be removed from Φ without changing the physical part of the vacuum wave functional, although generally in exchange for terms containing higher powers of the gauge field [21].)

In order to motivate the color structure of our covariance, we note that only the homogeneous part of the gauge transformations keeps the exponent Φ of the core-functional bilinear in A. Gauge transformations which vary little over distances for which $G^{-1}(\vec{x}-\vec{y})$ has appreciable support therefore leave the Gaussian part of the exponent with a covariance of the form [18]

$$G^{-1,ab}(k) = \delta^{ab}G^{-1}(k) \quad (6)$$

approximately invariant. This will hold, in particular, for those gauge-group elements which determine our soft-mode dynamics (see below). Since the same color structure is appropriate for the hard gauge-field modes, which we will treat perturbatively in the small bare coupling g_b, we adopt Eq. (6) for the remainder of this paper. As a consequence, the core functionals ψ_0 become invariant both under global $U(N_c)$ transformations and under $N_c^2 - 1$ copies of the $U(1)$ gauge group.

Combining the spacial (5) and color (6) structures, our covariance assumes the form

$$G_{ij}^{-1ab}(\vec{x},\vec{y}) = \delta^{ab}\delta_{ij}G^{-1}(\vec{x}-\vec{y}) = \delta^{ab}\delta_{ij}\int\frac{d^3k}{(2\pi)^3}e^{i\vec{k}(\vec{x}-\vec{y})}G^{-1}(k), \quad (7)$$

which is symmetric in each of the three ''index'' pairs. The covariance is further restricted by the requirement that wave functionals of physical states have to be normalizable. Since the norm of the functional (3) involves an integral over the Fourier modes $A(k)$, this implies that the integrand $\psi_0^*(k)\psi_0(k)$ has to damp large gauge fields $A(k)$ for all k. The corresponding localization in field space is implemented by demanding

$$G^{-1}(k) > 0, \quad (8)$$

which ensures vacuum stability and a positive energy spectrum of the associated quantum field theory. The condition (8) will limit the domain of the variational parameters to be introduced below.

As noted by Feynman, a further mandatory requirement is that all trial functionals reproduce the asymptotically free gauge dynamics for $k \to \infty$ exactly [12]. This prevents the infinitely many ultraviolet modes (which are irrelevant for the vacuum physics) from artificially dominating the soft-mode energy density through their IR-mode couplings. In order to implement the correct UV behavior, we factorize the unprojected core functional (3) as

$$\psi_0^{(G)}[\vec{A}] = \psi_0^{(G_<)}[\vec{A}_<]\psi_0^{(G_>)}[\vec{A}_>] \quad (9)$$

by splitting the $\vec{k}$ integration domain in the exponentials into soft/hard regions with momenta $k \gtrless \mu$ relative to a separation scale μ, i.e.,

$$\psi_0^{(G_{\lessgtr})}[\vec{A}_{\lessgtr}] = \exp\Big\{-\frac{1}{2}\int\frac{d^3k}{(2\pi)^3}\theta(\pm\mu^2\mp\vec{k}^2) \times A^a_{\lessgtr,i}(k)G^{-1}_{\lessgtr}(k)A^a_{\lessgtr,i}(k)\Big\}. \quad (10)$$

This allows to incorporate the asymptotic freedom of Yang-Mills theory (i.e., the Gaussian UV fixed point) by requiring that G approaches the noninteracting, massless static vector field propagator $G_0(k) = 1/k$ when $k \to \infty$. As long as $\mu \gg \Lambda_{\rm YM}$ where $\Lambda_{\rm YM}$ is the Yang-Mills scale, a natural approximation is therefore [38]

$$G^{-1}_{>}(k) = k, \quad (11)$$

which we adopt in the following [39]. More specifically, the value of μ must be chosen large enough for perturbative corrections from the hard modes, or equivalently the renormalization-group (RG) improved running coupling $\alpha(\mu) = g^2(\mu)/(4\pi)$, to remain small. (RG-improved perturbative corrections to the leading $k \to \infty$ behavior will enter when integrating out the hard modes perturbatively, cf. Sec. VII A and Appendix A 2.) Since μ will be treated as a variational parameter, this has to be checked *a posteriori*, i.e., for the value μ^* which turns out to minimize the vacuum energy. For the infrared momenta $k < \mu$, finally, the nonperturbative Yang-Mills dynamics is expected to induce a qualitatively different covariance $G^{-1}_{<}(k)$ which will be the subject of the following section.

D. Generalized IR (soft-mode) covariance

Because of the logarithmically slow running of the Yang-Mills coupling in the ultraviolet, the high-momentum behavior of our trial-functional family is rather accurately reproduced by the hard-mode covariance (11). Hence, only the IR covariance $G^{-1}_{<}(k)$, which encodes the more complex and less understood nonperturbative vacuum physics, remains to be determined variationally. To this end, we have to implement a parametrization for $G^{-1}_{<}$ which is sufficiently "rich" to accommodate the relevant physics without impeding an analytically tractable variational analysis. The minimal choice

$$G^{-1}_{<,\rm KK}(k) = \mu \quad (12)$$

was adopted in the pioneering study [18] and shown to generate a mass gap when the separation scale μ is simultaneously utilized as a variational parameter. While it therefore provides an efficient starting point for describing the Yang-Mills vacuum, one may also worry about too much bias since it leaves only one characteristic vacuum mass scale to be determined by energy minimization. This involves the risk of essentially "building in" the mass gap without gaining much further insight into the underlying vacuum structure.

In the following, we will therefore rely on a more comprehensive parametrization of $G^{-1}_{<}$ which better accommodates the $k < \mu$ mode dynamics while still allowing for a variational analysis without the need for solving a functional differential equation. It is based on the under reasonable analyticity assumptions general gradient expansion [23]

$$G^{-1}_{<}(\vec{x}-\vec{y}) = m_g\Big[1 + c_1\frac{\partial_x^2}{\mu^2} + c_2\Big(\frac{\partial_x^2}{\mu^2}\Big)^2 + c_3\Big(\frac{\partial_x^2}{\mu^2}\Big)^3 + \ldots\Big]\delta^3_{<}(\vec{x}-\vec{y}), \quad (13)$$

which can be efficiently truncated to yield a manageable trial basis for the $k^2 \ll \mu^2$ soft-mode physics. Besides μ, the variational parameter space then contains the IR gluon mass $m_g > 0$ and a few of the low-momentum constants c_n which characterize dispersive properties of the vacuum (cf. Sec. VIII C). [The parameters c_n should be considered as renormalized at μ since they do not receive UV contributions from integrating over the $k > \mu$ modes.] The derivatives in Eq. (13) act on the regularized delta function

$$\delta^3_{<}(\vec{x}-\vec{y}) := \int\frac{d^3k}{(2\pi)^3}\theta(\mu^2-\vec{k}^2)e^{i\vec{k}(\vec{x}-\vec{y})}, \quad (14)$$

which encodes the slow variation $\|\partial A_<\|/\|A_<\| \le \mu$ of the soft modes and ensures that the higher-order terms of the above expansion are parametrically suppressed. It further restricts the support of $G^{-1}_{<}$:

$$G^{-1}_{<}(\vec{x}) \sim 0 \quad \text{for } |\vec{x}| > \frac{1}{\mu}. \quad (15)$$

Together with the hard-mode covariance (11), Eq. (13) provides a rather general parametrization of the core functional (3) which includes the minimal one-parameter ansatz (12) for $c_n = 0$ and $m_g = \mu$.

Note, incidentally, that the perturbative covariance (11) has a branch point at $k^2 = 0$ and thus cannot be directly expanded as in Eq. (13). Note further that the expression (13) can be extended beyond the limited spacial tensor structure (5) by writing

$$G^{-1}_{<,ij}(\vec{x}-\vec{y}) = G^{(L)-1}_{<,ij}(\vec{x}-\vec{y}) + G^{(T)-1}_{<,ij}(\vec{x}-\vec{y}), \quad (16)$$

with ($X \equiv L, T$)

$$G^{(X)-1}_{<,ij}(\vec{x}-\vec{y}) = m_g^{(X)}\Big[1 + c_1^{(X)}\frac{\partial_x^2}{\mu^2} + c_2^{(X)}\Big(\frac{\partial_x^2}{\mu^2}\Big)^2 + c_3^{(X)}\Big(\frac{\partial_x^2}{\mu^2}\Big)^3\ldots\Big]\delta^3_{X,ij}(\vec{x}-\vec{y}), \quad (17)$$

where

$$\delta^3_{X,ij}(\vec{x}) = \int\frac{d^3k}{(2\pi)^3}\theta(\mu^2-\vec{k}^2)\delta_{X,ij}(\hat{k})e^{i\vec{k}\vec{x}}, \quad (18)$$

with $\delta_{T,ij}(\hat{k}) \equiv \delta_{ij} - k_ik_j/\vec{k}^2$ and $\delta_{L,ij}(\hat{k}) \equiv k_ik_j/\vec{k}^2$. This decouples the longitudinal and transverse contributions and implies, in particular,

$$\partial_{x,i} G_{ij}^{(T)-1}(\vec{x}-\vec{y}) = 0. \tag{19}$$

For $m_g^{(T)} = m_g^{(L)}$ and $c_n^{(T)} = c_n^{(L)}$ the more general expression (16) simplifies to Eq. (13). In the following analysis we adopt the latter, in order not to compromise transparency by additional parameters and to allow for a direct comparison with the results of Ref. [18].

In momentum space Eq. (13) becomes

$$G_<^{-1}(k) = m_g\Big[1 - c_1\frac{k^2}{\mu^2} + c_2\Big(\frac{k^2}{\mu^2}\Big)^2 - c_3\Big(\frac{k^2}{\mu^2}\Big)^3 + \ldots\Big]\theta(\mu^2 - k^2), \tag{20}$$

which renders the relation between the parameters c_n and the dispersion properties of the IR quasigluons (cf. Sec. VIII C) more explicit. It further implies that the effective IR gluon propagator

$$G_<(k) = \frac{1}{m_g}\Big[1 + c_1\frac{k^2}{\mu^2} + (c_1^2 - c_2)\frac{k^4}{\mu^4} + (c_1^3 - 2c_1c_2 + c_3)\frac{k^6}{\mu^6} + \ldots\Big]\theta(\mu^2 - k^2), \tag{21}$$

resulting from $G_<^{-1}(k)G_<(k) = 1$, is analytic at $k^2 = 0$. (The finiteness of $G_<$ at zero momentum, $G_<(0) = m_g^{-1}$, is reminiscent of lattice results for the gluon propagator in Landau gauge [40].) The adjustable parameters m_g, μ and c_n are to be determined variationally (cf. Sec. VIII). Their physically sensible domain is restricted by several constraints, however. Indeed, as a consequence of the normalizability condition (8) the low-momentum constants must satisfy the bounds

$$c_1 < 1, \qquad c_2 > -1, \ldots \tag{22}$$

(for $m_g > 0$). The value of the IR gluon mass $m_g > 0$ is further constrained by requiring continuity of $G^{-1}(k)$ at the matching point $k = \mu$ between soft and hard momenta. This fixes m_g as a function of the other variational parameters. When approximating the series (20) by the truncation $c_{n\geq 2} = 0$, for example, one has

$$m_g(\mu, c_1) = \frac{\mu}{1 - c_1}. \tag{23}$$

Note that the requirement of a non-negative IR gluon mass then restricts the c_1 domain to $c_1 < 1$, in agreement with the bound (22) from normalizability. The singularity of $m_g(\mu, c_1)$ for $c_1 \to 1$ reflects the onset of the vacuum instability and is inherited by $G_<^{-1}(k)$, cf. Eq. (20).

In addition to the lowest-order approximation (12), our expansion (13) encompasses another previously used ansatz for the IR covariance, namely, the inverse of the noninteracting massive vector propagator,

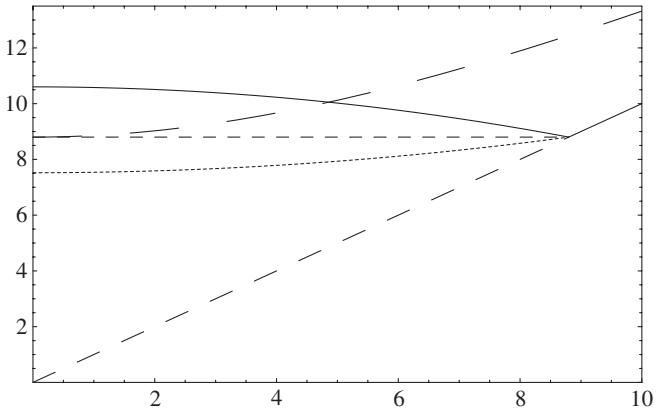

FIG. 1. The generalized IR covariance $G_<^{-1}(k) = \mu(1 - c_1k^2/\mu^2)/(1 - c_1)$ for $c_1 = 0.17$ (full line) and $c_1 = -0.17$ (dotted), together with the UV covariance $G_>^{-1}(k) = k$, and in comparison with $G_0^{-1}(k) = k$ (medium dashed), $G_{0,m_g=\mu}^{-1}(k) = \sqrt{k^2 + \mu^2}$ (long dashed) and $G_{\mathrm{KK}}^{-1}(k) = \mu$ (short dashed) [all curves in units of Λ_{YM} and for $\mu = 8.8\Lambda_{\mathrm{YM}}$].

$$G_0^{-1}(k;\mu) = \sqrt{k^2 + \mu^2} \overset{k<\mu}{=} \mu\Big[1 + \frac{1}{2}\frac{k^2}{\mu^2} - \frac{1}{8}\Big(\frac{k^2}{\mu^2}\Big)^2 + \frac{1}{16}\Big(\frac{k^2}{\mu^2}\Big)^3 - \ldots\Big], \tag{24}$$

which obviously corresponds to $m_g = \mu$, $c_1^{(0)} = -1/2$, $c_2^{(0)} = -1/8$, etc. Its truncation to $c_{n\geq 2} = 0$ was adopted as the basis of a gauge-invariant saddle-point expansion for the IR amplitudes and found to reproduce the soft-mode action (cf. Sec. III) at its saddle points within a few percent accuracy [23]. (Lattice simulations similarly found the Landau-gauge gluon propagator to behave like a massive vector propagator at intermediate momenta [41].)

In Fig. 1 we compare the expressions (12) and (24) for the IR covariance to Eq. (20) with $c_1 = \pm 0.15$ (the positive value will turn out to minimize the vacuum energy, cf. Sec. VIII A) and $c_{n\geq 2} = 0$. A more detailed discussion of the physics encoded in the covariance (20) will be postponed until the variationally optimized values of the low-momentum constants are found (cf. Sec. VIII C).

In summary, the Gaussian ansatz (3) for the core functional encodes the correct ultraviolet asymptotics, can be partly motivated in the infrared and is amenable to existing analytical methods of field theory. As such, it provides the best currently available, analytically manageable and gauge-invariant approximation to the Yang-Mills vacuum wave functional.

III. ENERGY AND SOFT-MODE DYNAMICS OF THE TRIAL-FUNCTIONAL FAMILY

A. Calculational strategy

Variational analyses à la Rayleigh-Ritz amount to minimizing the expectation value of a given Hamiltonian in a

suitable space of trial states. In our context, the energy density of the trial vacuum is

$$\langle \mathcal{H}(A,E)\rangle = \frac{\int D\vec{A}\Psi_0^*[\vec{A}]\mathcal{H}(\vec{A}^a, \frac{i\delta}{\delta\vec{A}^a(\vec{x})})\Psi_0[\vec{A}]}{\int D\vec{A}\Psi_0^*[\vec{A}]\Psi_0[\vec{A}]}, \quad (25)$$

where $\mathcal{H}$ is the Yang-Mills Hamiltonian [cf. Eq. (131)] in temporal gauge and Ψ_0 the generalized vacuum wave-functional family introduced in Sec. II. This expectation value is most efficiently evaluated by means of a generating functional, as summarized in Appendix A. In the present section we prepare for the calculation of Eq. (25) by sketching our basic strategy (which straightforwardly generalizes to more general matrix elements, cf. Appendix A).

After inserting the gauge-projected vacuum wave functional (1) into Eq. (25) and interchanging the order of the integration over fields and group elements, the gauge invariance of the $\vec{A}$ integral allows to factor out one gauge-group volume. Equation (25) can be then be rewritten as

$$\langle \mathcal{H}(A,E)\rangle = \frac{\int DU \int D\vec{A}\psi_0[\vec{A}^U]\mathcal{H}(\vec{A}^a, \frac{i\delta}{\delta\vec{A}^a(\vec{x})})\psi_0[\vec{A}]}{\int DU \int D\vec{A}\psi_0[\vec{A}^U]\psi_0[\vec{A}]} \quad (26)$$

[where DU is the functional SU(N_c) measure as defined in Eq. (1)]. After evaluating the functional derivatives contained in $\mathcal{H}$, the Gaussian integration over A can be performed exactly (cf. Appendix A for more details), resulting in

$$\langle \mathcal{H}\rangle = \frac{\int DU\langle\langle\langle \mathcal{H}\rangle\rangle\rangle \exp\{-\Gamma_b[U]\}}{\int DU \exp\{-\Gamma_b[U]\}}, \quad (27)$$

where we introduced the abbreviation

$$\langle\langle\langle \vec{A}\ldots\vec{A}\ldots\vec{E}\ldots\vec{E}\rangle\rangle\rangle \exp\{-\Gamma_b[U]\} \equiv \int D\vec{A}\psi_0[\vec{A}^U]\vec{A}\ldots\vec{A}\ldots\frac{i\delta}{\delta\vec{A}}\ldots\frac{i\delta}{\delta\vec{A}}\psi_0[\vec{A}]. \quad (28)$$

The above expression defines an effective bare action $\Gamma_b[U]$ which describes dynamical correlations originating from the gauge projection of the functional ψ_0. More specifically, from the normalization $\langle\langle\langle 1\rangle\rangle\rangle = 1$ it follows that

$$\Gamma_b[U] = -\ln\int D\vec{A}\psi_0^*[\vec{A}^U]\psi_0[\vec{A}]. \quad (29)$$

This gauge-invariant, three-dimensional Euclidean action would become U independent if ψ_0 were gauge invariant by itself. Hence, $\Gamma_b[U]$ gathers all those gauge-field contributions to the generating functional whose approximate vacua ψ_0 at $t = \pm\infty$ differ by a relative gauge orientation U. The variable U thus represents the contributions from a specifically weighted ensemble of all gluon field orbits to the vacuum overlap and is gauge invariant by construction.

After splitting $U(\vec{x}) = U_<(\vec{x})U_>(\vec{x})$ with $U_>(\vec{x}) = \exp(-ig\phi^a(\vec{x})\lambda^a/2)$ into hard- and soft-mode contributions and integrating over the hard UV modes ϕ perturbatively (as done in Ref. [18] which used the same UV covariance (11), cf. Appendix A), one arrives at

$$\langle \mathcal{H}\rangle = \frac{\int DU_< \int D\phi\langle\langle\langle \mathcal{H}\rangle\rangle\rangle \exp\{-\Gamma_b[\phi, U_<]\}}{\int DU_< \int D\phi \exp\{-\Gamma_b[\phi, U_<]\}}. \quad (30)$$

After further defining

$$\langle\langle\mathcal{O}\rangle\rangle \exp\{-\Gamma_<[U_<]\} := \int D\phi\langle\langle\langle\mathcal{O}\rangle\rangle\rangle \exp\{-\Gamma_b[\phi, U_<]\} \quad (31)$$

and, in particular, the effective soft-mode action

$$\Gamma_<[U_<] := -\ln\int D\phi \exp\{-\Gamma_b[\phi, U_<]\}, \quad (32)$$

we end up with a reformulation of the matrix element (25) in terms of the dynamics for the $U_<$ field, i.e., for the low-momentum components of the integration variable originating from the gauge projection of the vacuum functional (1):

$$\langle \mathcal{H}\rangle = \frac{\int DU_<\langle\langle \mathcal{H}\rangle\rangle \exp\{-\Gamma_<[U_<]\}}{\int DU_< \exp\{-\Gamma_<[U_<]\}}. \quad (33)$$

Hence, the calculation of $\langle\mathcal{H}\rangle$ boils down to an integral over $U_<$ in which the "reduced" (i.e., fixed $U_<$) matrix element $\langle\langle\mathcal{H}\rangle\rangle$ is weighted by a Boltzmann factor containing just the soft-mode action $\Gamma_<[U_<]$. This action is governed by our IR expansion (13) of the covariance $G_<^{-1}$ which produces interactions to be determined in Sec. III B. Since $\langle\langle\mathcal{H}\rangle\rangle$ consists of nonlocal functionals of the soft modes $U_<$, furthermore, the evaluation of Eq. (33) amounts to calculating (equal-time) soft-mode correlation functions. The necessary framework for such calculations will be set up in Sec. IV.

B. Soft-mode action

In this section we derive explicit expressions for the low-momentum dynamics (32) induced by the wave functional (1) with the Gaussian core (3) and the generalized covariance (11) and (13). After specializing the expression (29) for the bare action to the core functional (3), the integral over the gauge fields can be carried out exactly (cf. Appendix A). The result is the action of a three-dimensional, bilocal nonlinear sigma model:

$$\Gamma_b[U] = \frac{1}{2g_b^2}\int d^3x\int d^3y L_i^a(\vec{x})\mathcal{D}^{ab}(\vec{x}-\vec{y})L_i^b(\vec{y}). \quad (34)$$

(Above we have omitted a term of higher order in the small bare coupling g_b, cf. Appendix A.) The U fields enter Γ_b both in terms of the left-invariant SU(N_c) Maurer-Cartan forms

$$L_i(\vec{x}) = U^\dagger(\vec{x})\partial_i U(\vec{x}) =: L_i^a(\vec{x})\frac{\lambda^a}{2i} \tag{35}$$

[with real components L_i^a and the SU(N_c) Gell-Mann matrices λ^a] and through higher-order corrections to the bilocal operator

$$\mathcal{D}^{ab} = [(G + G^U)^{-1}]^{ab} \simeq \tfrac{1}{2}G^{-1}\delta^{ab} + \ldots, \tag{36}$$

where $G^U = G^{ab}(\vec{x} - \vec{y})U^\dagger(\vec{x})t^a U(\vec{x}) \otimes U(\vec{y})t^b U^\dagger(\vec{y})$ and $t^a = \lambda^a/2$. The above reformulation of the vacuum functional overlap can alternatively be obtained by a saddle-point evaluation [19] of the Gaussian integral in Eq. (29).

According to the strategy outlined in Sec. III A, the calculation of infrared amplitudes involves an effective action (32) which only retains soft field modes explicitly. After factorizing $U = U_< U_>$, the hard modes $U_>$ with $k^2 > \mu^2$ can be integrated out of Eq. (32) perturbatively (cf. Appendix A) as long as the renormalized coupling [42]

$$g(\mu) = g_b + \frac{g_b^3 N_c}{(2\pi)^2}\ln\frac{\Lambda_{\mathrm{UV}}}{\mu} + O(g_b^5) \tag{37}$$

[for $G_>(k) = k^{-1}$] stays sufficiently small. Note that Eq. (37) exhibits asymptotic freedom and differs from the one-loop Yang-Mills coupling only by a small correction factor $1/11$ which could, e.g., be generated by an anisotropic component for $G_>^{-1}$ [19,37]. The one-loop integration over the high-momentum modes was found to be reliable down to $\mu \simeq 1.3$ GeV [42]. In this range, the resulting renormalized soft-mode action

$$\Gamma_<[U_<] = \frac{1}{4g^2(\mu)}\int d^3x \int d^3y L_{<,i}^a(\vec{x})G_<^{-1}(\vec{x} - \vec{y})L_{<,i}^a(\vec{y}) \tag{38}$$

[cf. Eq. (A48)] is obtained from Eq. (34) by replacing the bare coupling g_b with the running coupling $g(\mu)$. One may further simplify the action (38) by exploiting the strongly local support of the IR covariance (13) [compared to the minimal soft-mode wavelength μ^{-1}] which manifests itself in the regularized delta function (14) and its derivatives. Indeed, this allows to apply the unitarity constraint for the $U_<$ approximately at neighboring points, i.e.,

$$G^{-1}(\vec{x} - \vec{y})U_<^\dagger(\vec{x})U_<(\vec{y}) \simeq G^{-1}(\vec{x} - \vec{y}), \tag{39}$$

which could be systematically improved by Taylor expansion of the slowly varying soft modes. To leading order, one may therefore replace Eq. (38) by the $2U$ contribution

$$\Gamma_<^{(2U)}[U_<] = \frac{1}{2g^2(\mu)}\int d^3x \int d^3y\, \mathrm{tr}\{\partial_i U_<(\vec{x}) \times G^{-1}(\vec{x} - \vec{y})\partial_i U_<^\dagger(\vec{y})\}. \tag{40}$$

Inserting our full expansion (13) of the generalized IR covariance into the low-momentum dynamics (38), on the other hand, yields the complete soft-mode action in the form

$$\Gamma_<[U_<] = \int d^3z[\mathcal{L}_{<,0}(\vec{z}) + \mathcal{L}_{<,c_1}(\vec{z}) + \mathcal{L}_{<,c_2}(\vec{z}) + \ldots], \tag{41}$$

where the $\mathcal{L}_{<,c_n}(\vec{z})$ are (quasi-) local Lagrangians. [A saddle-point expansion of this dynamics, with the c_n determined by the massive vector covariance (24), was employed in Ref. [23] to identify gluonic IR degrees of freedom.] The leading-order, two-derivative Lagrangian

$$\begin{aligned}\mathcal{L}_{<,0}(\vec{z}) &= -\frac{m_g}{2g^2}\,\mathrm{tr}\{U_<^\dagger(\vec{z})\partial_i U_<(\vec{z})U_<^\dagger(\vec{z})\partial_i U_<(\vec{z})\} \\ &= \frac{m_g}{2g^2}\,\mathrm{tr}\{\partial_i U_<^\dagger\partial_i U_<\}\end{aligned} \tag{42}$$

(where we used $U_<^\dagger U_< = 1$ and neglected a surface term) is just the standard nonlinear σ model. The $c_n \neq 0$ corrections (with the low-momentum constants c_n restricted by the requirements of a positive static action and a bounded vacuum energy, cf. Sec. II D) generate $2(n+1)$-derivative interactions which are, relative to the leading term (42), suppressed by n powers of k^2/μ^2:

$$\mathcal{L}_{<,c_n}(\vec{z}) = \frac{c_n m_g}{2g^2\mu^{2n}}\,\mathrm{tr}\{U_<^\dagger(\vec{z})\partial_i U_<(\vec{z})\partial^{2n}[\partial_i U_<^\dagger(\vec{z})U_<(\vec{z})]\}. \tag{43}$$

The action (41), based on the Lagrangians (42) and (43), exhibits the dynamics generated both by the generalized IR covariance (20) and by gauge projection. It encodes, in particular, information on the vacuum topology which shows up in the form of instanton [43] (through the Atiyah-Manton holonomy [44]), meron [45], monopole [46], Fadeev-Niemi-Cho knot [47,48] etc. contributions and can be made explicit [23]. The approximation (39) can be used to reduce the $c_n \neq 0$ interaction terms to their bilinear (i.e., $2U$) parts

$$\mathcal{L}_{<,c_n}^{(2U)}(\vec{z}) = \frac{c_n m_g}{2g^2\mu^{2n}}\,\mathrm{tr}\{\partial_i U_<^\dagger(\vec{z})\partial^{2n}[\partial_i U_<(\vec{z})]\}, \tag{44}$$

furthermore, which will turn out to generate the dominant contributions to the vacuum energy density and other matrix elements.

We close this section by recalling that the soft-mode dynamics (41) follows uniquely from the adopted vacuum wave functional and preserves traceable links between the $U_<$ fields and the underlying gauge fields [23]. Nevertheless, it remains reasonably transparent and allows for efficient and controlled truncations resulting, e.g., in the analytical expressions for the vacuum energy to be derived below. These benefits originate in large part from re-expressing the dynamics in terms of the gauge-invariant fields U which gather collective contributions from whole gauge-field orbits instead of dealing with each gauge field individually [23].

IV. SOFT-MODE CORRELATION FUNCTIONS

As outlined in Sec. III A, the calculation of the vacuum energy density requires the evaluation of the reduced matrix element $\langle\langle \mathcal{H} \rangle\rangle$ which contains correlations functions of the soft-mode fields $U_<$. In the following section we set up our framework for evaluating these correlators.

A. Generating functional

Soft-mode correlation functions, as they appear in the integrand $\langle\langle \mathcal{H} \rangle\rangle$ of the vacuum expectation value (33) and in the gap equation to be derived below, are efficiently calculated by means of the generating functional

$$Z[j, j^\dagger] = \int DU_< \exp[-\Gamma_<[U_<] - \int d^3z \,\mathrm{tr}\{jU_<^\dagger + j^\dagger U_<\}], \tag{45}$$

where j, $j^\dagger$ are matrix sources. In order to prepare for the (approximate) integration over the soft modes in Eq. (45), we first release the unitarity constraint on the $U_<$ fields in the usual manner by inserting a delta functional, i.e.

$$Z[j, j^\dagger] = \int DV \delta[V^\dagger V - 1] \exp[-\Gamma_<[V] - \int d^3z \,\mathrm{tr}\{jV^\dagger + j^\dagger V\}], \tag{46}$$

$$= \int D\Sigma \int DV \exp[-\Gamma_<[V] - \Gamma_\Sigma[V, \Sigma] - \int d^3z \,\mathrm{tr}\{jV^\dagger + j^\dagger V\}], \tag{47}$$

where the Hermitian matrix fields $\Sigma(\vec{x})$ act as Lagrange multipliers (with a normalization chosen for later convenience) and where $\Gamma_\Sigma[V, \Sigma]$ contains the interactions between the Σ and V fields,

$$\Gamma_\Sigma[V, \Sigma] = \int d^3x \mathcal{L}_\Sigma(\vec{z}) = \frac{m_g}{2g^2} \int d^3x \,\mathrm{tr}[\Sigma(V^\dagger V - 1)]. \tag{48}$$

The integral over the unconstrained complex matrices V has a linear Euclidean measure DV. Hence, after pulling out the subleading (cf. Sec. III B), non-Gaussian $4U$ interactions as functional derivatives with respect to the sources, it can be performed analytically. This results in

$$Z[j, j^\dagger] = \int D\Sigma DV \exp\Big\{ - \int d^3z [\mathcal{L}_{<,0} + \mathcal{L}_\Sigma + \mathcal{L}_{<,c_1} + \mathcal{L}_{<,c_2} + \ldots + \mathrm{tr}\{jV^\dagger + j^\dagger V\}]\Big\}, \tag{49}$$

$$= \int D\Sigma DV \exp\Big[- \int d^3z (\mathcal{L}^{(4U)}_{<,c_1} + \mathcal{L}^{(4U)}_{<,c_2} + \ldots)\Big] \times \exp\Big[- \int d^3z (\mathcal{L}^{(2U)} + \mathrm{tr}\{jV^\dagger + j^\dagger V\})\Big], \tag{50}$$

$$= \mathcal{V}^{(4U)}\Big[\frac{\delta}{\delta j}, \frac{\delta}{\delta j^\dagger}\Big] Z^{(2U)}[j, j^\dagger], \tag{51}$$

where we have gathered the part of the generating functional which originates from the bilinear Lagrangian

$$\mathcal{L}^{(2U)} := \mathcal{L}_{<,0} + \mathcal{L}^{(2U)}_{<,c_1} + \mathcal{L}^{(2U)}_{<,c_2} + \ldots + \mathcal{L}_\Sigma = =: \mathrm{tr}\{V^\dagger \Delta V\} - \frac{m_g}{2g^2} \mathrm{tr}\{\Sigma\}, \tag{52}$$

with the kernel

$$\Delta(\vec{x} - \vec{y}; \{c_n\}, \Sigma) := - \frac{m_g}{2g^2}\Big(\partial_x^2 + \frac{c_1}{\mu^2}\partial_x^4 + \frac{c_2}{\mu^4}\partial_x^6 + \ldots - \Sigma\Big)\delta^3_<(\vec{x} - \vec{y}) \tag{53}$$

(which defines the inverse soft-mode propagator) as

$$Z^{(2U)}[j, j^\dagger] = \int D\Sigma DV \times \exp\Big[- \int d^3z (\mathcal{L}^{(2U)} + \mathrm{tr}\{jV^\dagger + j^\dagger V\})\Big]. \tag{54}$$

All contributions from the $4U$ vertices, on the other hand, are collected in the functional potential

$$\mathcal{V}^{(4U)}[U^\dagger, U] = \exp\Big[- \int d^3z (\mathcal{L}^{(4U)}_{<,c_1} + \mathcal{L}^{(4U)}_{<,c_2} + \ldots)\Big]. \tag{55}$$

The Gaussian integral over the V fields in Eq. (54) can then be performed analytically, with the result

$$\frac{Z^{(2U)}[j, j^\dagger]}{Z^{(2U)}[0, 0]} = \int D\Sigma \exp\Big[\int d^3x \int d^3y \times \mathrm{tr}\{j^\dagger(\vec{x})\Delta^{-1}(\vec{x} - \vec{y}; \{c_n\}, \Sigma) j(\vec{y})\}\Big]. \tag{56}$$

The whole Σ dependence of the correlators, as well as the c_n dependence originating from the $2U$ interactions, is now concentrated in the gauge-invariant soft-mode propagator Δ^{-1} which we will analyze in Sec. IV C. The perturbative treatment of the $4U$ vertices for $|c_n| \ll 1$ starts from the expansion

$$\mathcal{V}^{(4U)}\Big[\frac{\delta}{\delta j}, \frac{\delta}{\delta j^\dagger}\Big] \equiv \exp\Big[- \int d^3z \mathcal{L}^{(4U)}_{<,c_1}\Big(\frac{\delta}{\delta j}, \frac{\delta}{\delta j^\dagger}\Big) - \ldots\Big], \tag{57}$$

$$= 1 - \int d^3z \mathcal{L}^{(4U)}_{<,c_1}\left(\frac{\delta}{\delta j}, \frac{\delta}{\delta j^\dagger}\right) + O(c_1^2, c_{n\geq 2}) \quad (58)$$

of the functional potential which contains the c_n dependence induced by the $4U$ interactions.

B. Mean-field approximation and vacuum phases

After having rewritten the generating functional as an integral over the auxiliary field Σ, we evaluate the latter in the saddle-point or mean-field approximation (cf. Appendix A 3). When the integrand in Eq. (47) is expressed as a Boltzmann factor

$$\exp\{-\tilde{\Gamma}[\Sigma]\} := \int DV \exp\{-\Gamma_<[V] - \Gamma_\Sigma[V, \Sigma]\} \quad (59)$$

(in the present section we are interested only in the vacuum overlap amplitude and therefore set all sources to zero), the saddle-point equation takes the form

$$\frac{\delta\tilde{\Gamma}[\Sigma]}{\delta\Sigma(\vec{x})} = \exp\tilde{\Gamma}[\Sigma] \int DV \frac{\delta\Gamma_\Sigma[V, \Sigma]}{\delta\Sigma(\vec{x})} \times \exp\{-\Gamma_<[V] - \Gamma_\Sigma[V, \Sigma]\}, \quad (60)$$

$$= \frac{m_g}{2g^2} \exp\tilde{\Gamma}[\Sigma] \int DV[V^\dagger(\vec{x})V(\vec{x}) - 1] \times \exp\{-\Gamma_<[V] - \Gamma_\Sigma[V, \Sigma]\} = 0, \quad (61)$$

which ensures that its solutions extremize the effective action $\tilde{\Gamma}$. To leading order in the saddle-point expansion, integrals over Σ are then approximated by their integrands where Σ is replaced by a solution $\Sigma^{(\mathrm{mf})}$ of Eq. (61). This turns Eq. (61) into

$$\langle U^\dagger(\vec{x})U(\vec{x})\rangle = 1, \quad (62)$$

in particular, and thereby restores the unitarity constraint at the mean-field level. In a homogeneous vacuum one expects the solution of Eq. (62) to be a constant field. The interactions (48) then turn into a mass term for V which triggers dimensional transmutation [as in $O(n)$ models] and generates a mass gap. Hence, Eq. (62) plays the role of a gap equation. Since for $\Sigma > 0$ the $\mathrm{SU}_L(N_c) \times \mathrm{SU}_R(N_c)$ symmetry of the soft-mode action (41) is unbroken, the mean-field solution should further be proportional to the unit matrix, i.e.,

$$\Sigma^{(\mathrm{mf})} = \bar{\Sigma} \times 1, \quad (63)$$

where $\bar{\Sigma}$ is a real constant.

In order to exhibit the vacuum phase structure encoded in the wave functional (1) more fully, an analogous mean-field treatment of the V integral in Eq. (47) [which reproduces its Gaussian part exactly] turns out to be useful as well. Defining the associated effective action (again for vanishing sources) by

$$\exp\{-\tilde{\Gamma}[V]\} := \int D\Sigma \exp\{-\Gamma_<[V] - \Gamma_\Sigma[V, \Sigma]\}, \quad (64)$$

one obtains the corresponding saddle-point equation

$$\frac{\delta\tilde{\Gamma}[V]}{\delta V^\dagger(\vec{x})} = \exp\tilde{\Gamma}[V] \int D\Sigma \frac{\delta\{\Gamma_<[V] + \Gamma_\Sigma[V, \Sigma]\}}{\delta V^\dagger(\vec{x})} \times \exp\{-\Gamma_<[V] - \Gamma_\Sigma[V, \Sigma]\}, \quad (65)$$

$$\to \frac{m_g}{2g^2} \exp\tilde{\Gamma}[\bar{V}][\bar{\Sigma}\ \bar{V}] \exp\{-\Gamma_\Sigma[\bar{V}, \bar{\Sigma}]\} = 0. \quad (66)$$

In the second line we have saturated the Σ integral with the constant (i.e., vacuum) mean fields $\bar{V}$ and $\bar{\Sigma}$. This implies $\Gamma_<[\bar{V}] = 0$, in particular, since $\Gamma_<$ only contains derivative interactions. Hence, Eq. (66) reduces to

$$\langle \Sigma U(\vec{x})\rangle = 0. \quad (67)$$

(The $\mathrm{SU}_L(N_c) \times \mathrm{SU}_R(N_c)$ symmetry of Γ [under which U, V transform as $V \to RVL^\dagger$] turns a nonzero mean field $\bar{V}$ into a continuous family of degenerate saddle points. The associated Goldstone zero-mode contributions are not suppressed by the Gaussian weight and have to be integrated exactly.)

The solutions of the saddle-point Eqs. (62) and (67) characterize the vacuum phases of the effective σ model (41). The gap equation (62) determines the auxiliary mean field $\bar{\Sigma}$ and will be solved in Sec. VI. The saddle-point Eq. (67) shows that the vacuum can exist in two phases, as expected on general grounds and confirmed by lattice simulations [49,50] and the ε expansion [51]. More specifically, with increasing "analog temperature" $g^2(\mu)$ or decreasing μ one expects the vacuum to pass through an order-disorder phase transition, as in the analogous statistical spin model. In the ordered low-temperature (i.e., weakly coupled) phase one has

$$\langle U\rangle \neq 0, \qquad \langle\Sigma\rangle = 0, \quad (68)$$

i.e., the $\mathrm{SU}_L(N_c) \times \mathrm{SU}_R(N_c)$ symmetry is broken to its diagonal subgroup and $N_c^2 - 1$ massless Goldstone bosons are generated. In the disordered high-temperature (strong-coupling) phase with

$$\langle U\rangle = 0, \qquad \langle\Sigma\rangle \neq 0, \quad (69)$$

on the other hand, the symmetry of the action is restored [52]. The disorder-order transition occurs when $\langle\Sigma\rangle$ reaches zero in the disordered phase. As usual, it is the result of a competition between the ordering tendency of the energy and the disordering propensity of the entropy. Our above arguments imply, furthermore, that the *qualitative* phase structure is independent of the detailed interactions (43) as long as the soft-mode dynamics contains only derivative interactions. (This is guaranteed by the unitarity of the $U_<$ fields.) As a consequence of $\Gamma_<[\bar{V}] = 0$, in particular, the mean-field equations and hence the qualita-

tive phase structure have no *explicit* dependence on the low-momentum constants c_n.

C. Soft-mode propagator

The static soft-mode propagator Δ^{-1} determines the Gaussian part (56) of the generating functional and thereby encapsulates most of the impact of the higher-derivative interactions on vacuum structure and amplitudes. From the Fourier transform

$$\Delta(\vec{x}-\vec{y}) = \frac{m_g}{2g^2}\int\frac{d^3k}{(2\pi)^3}\theta(\mu^2-k^2) \times\left(k^2-\frac{c_1}{\mu^2}k^4+\frac{c_2}{\mu^4}k^6-\ldots+\bar{\Sigma}\right)e^{i\vec{k}(\vec{x}-\vec{y})} \tag{70}$$

of its inverse (53), which we have specialized to the constant mean field (63), the propagator is obtained as the solution of

$$\int d^3z\,\Delta^{-1}(\vec{x}-\vec{z})\Delta(\vec{z}-\vec{y}) = \delta^3_<(\vec{x}-\vec{y}), \tag{71}$$

where $\delta^3_<$ is the regularized delta function (14). In terms of the dimensionless variables

$$\vec{\kappa}\equiv\frac{\vec{k}}{\mu}, \qquad \xi\equiv\frac{\sqrt{\bar{\Sigma}}}{\mu}, \tag{72}$$

one therefore has

$$\Delta^{-1}(\vec{x}-\vec{y}) = \int\frac{d^3\kappa}{(2\pi)^3}e^{i\mu\vec{\kappa}(\vec{x}-\vec{y})}\Delta^{-1}(\kappa), \tag{73}$$

with

$$\Delta^{-1}(\kappa) = \frac{2g^2\mu}{m_g}\frac{\theta(1-\kappa^2)}{\kappa^2+\xi^2+\mathcal{M}^2(\kappa^2)}. \tag{74}$$

The Fourier representation of the soft-mode propagator can be simplified by performing the angular integrals analytically,

$$\Delta^{-1}(\vec{x}-\vec{y}) = \frac{g^2}{\pi^2 m_g}\frac{1}{|x-y|}\int_0^1 d\kappa\,\frac{\kappa\sin(\kappa\mu|x-y|)}{\kappa^2+\xi^2+\mathcal{M}^2(\kappa^2)}, \tag{75}$$

which becomes useful for numerical implementations and demonstrates that the isotropic regularization (i.e., $\kappa\leq 1$) preserves

$$\Delta^{-1}(\vec{x}-\vec{y}) = \Delta^{-1}(\vec{y}-\vec{x}). \tag{76}$$

Equation (74) reveals that the higher-derivative interactions generate a momentum-dependent self-energy

$$\mathcal{M}^2(\kappa^2) = -c_1\kappa^4+c_2\kappa^6-c_3\kappa^8+\ldots \tag{77}$$

for the soft modes. Hence, the propagator (74) may be regarded as the resummation of a static self-energy (i.e., $\mathcal{M}^2$) insertion. This geometric series converges for $|\mathcal{M}^2(\kappa^2)/(\kappa^2+\xi^2)|<1$. Expecting the c_1 contribution to dominate at small momenta $k\ll\mu$ and therefore truncating to $c_{n\geq 2}=0$ (see below), this implies

$$|c_1|<\frac{\kappa^2+\xi^2}{\kappa^4}. \tag{78}$$

For $\kappa\in[0,1]$ and $\xi\geq 0$, the above inequality is satisfied as long as $|c_1|<1$. This does not additionally constrain the parameter space, however, since $c_1<1$ guarantees the normalizability of the vacuum wave functional [cf. Eq. (22)] and $|c_1|\ll 1$ ensures the validity of our perturbative $O(c_1)$ treatment (58) of the residual $4U$ interactions.

In order to analyze the singularity structure of the soft-mode propagator, we rewrite Eq. (74) for $c_{n\geq 2}=0$ as

$$\Delta^{-1}(\kappa) = \frac{2g^2\mu}{m_g}\frac{\theta(1-\kappa^2)}{\kappa^2(1-c_1\kappa^2)+\xi^2} = \frac{2g^2\mu}{m_g}\frac{\theta(1-\kappa^2)}{\sqrt{1+4c_1\xi^2}}\left(\frac{1}{\kappa^2-\kappa_2^2}-\frac{1}{\kappa^2-\kappa_1^2}\right), \tag{79}$$

which reveals two poles at the momenta

$$\kappa^2_{1,2}(\xi,c_1) = \frac{1}{2c_1}(1\pm\sqrt{1+4c_1\xi^2}). \tag{80}$$

The pole position κ_1^2 [with the positive sign in Eq. (80)] diverges for $c_1\to 0$ but decreases monotonically for $c\to 1$ to reach $\kappa_1^2(\xi,c_1=1)\geq 1$. Hence, the pole at κ_1^2 lies outside of the integration range $\kappa\in[0,1]$ for all $c_1\in[-\infty,1]$ (and even for $\xi\to 0$). The second pole at κ_2^2 lies inside the integration range for $c_1>-\infty$ and $\xi=0$. For $c_1=0$, in particular, it turns into the standard infrared pole of the $c_n=0$ propagator, showing that the momentum-dependent self-energy does not create singularities beyond the $\xi\to 0$ pole of the uncorrected soft-mode propagator.

V. EVALUATION OF THE 2- AND 4-POINT CORRELATORS FOR $c_{n\geq 2}=0$

Having established our calculational framework for the generating functional, we now derive explicit expressions for the soft modes' two- and four-point functions. The results will underlie our subsequent evaluation of the matrix elements $\langle U^\dagger_<(\vec{x})U_<(\vec{x})\rangle$ in the gap equation (62) and $\langle L^a_{<,i}(\vec{x})L^a_{<,i}(\vec{y})\rangle$ in the chromo-electric contribution (142) to the vacuum energy density.

As stated previously, among the contributions from the higher-derivative interactions (43) those associated with c_1 are expected to dominate at small momenta $k^2\ll\mu^2$. This expectation is further supported by evidence from Ref. [23] where relevant infrared physics was found to be captured by the truncation of the covariance expansion (13) to $c_{n\geq 2}=0$. (More specifically, the first correction term $\mathcal{L}_{<,c_1}$ turned out to reproduce the full [nonlocal] IR action

(38) at its saddle points with better than 10% accuracy.) Furthermore, the $c_{n\geq 2}$ corrections (although straightforward to implement) obscure the (e.g., graphical) analysis of the vacuum energy density and the interpretation of other amplitudes. Hence, we will restrict the remainder of our investigation to the c_1 corrections, associated with the four-gradient interactions

$$\mathcal{L}_{<,c_1}(\vec{z}) = \frac{c_1 m_g}{2g^2\mu^2}\,\mathrm{tr}\{U^\dagger_<(\vec{z})\partial_i U_<(\vec{z})\partial^2[\partial_i U^\dagger_<(\vec{z})U_<(\vec{z})]\}, \tag{81}$$

$$= \mathcal{L}^{(2U)}_{<,c_1}(\vec{z}) + \mathcal{L}^{(4U)}_{<,c_1}(\vec{z}) \tag{82}$$

(where derivatives are implied to act on the nearest field only), which we have split as in Sec. III B into the dominant $2U$ interaction term $\mathcal{L}^{(2U)}_{<,c_1}$, given by Eq. (44) for $n = 1$, and the $4U$ contribution

$$\mathcal{L}^{(4U)}_{<,c_1}(\vec{z}) = \frac{c_1 m_g}{2g^2\mu^2}\,\mathrm{tr}\{U^\dagger_<\partial_i U_<[2\partial_i\partial_k U^\dagger_<\partial_k U_< + \partial_i U^\dagger_<\partial^2 U_<]\}. \tag{83}$$

As discussed in Sec. IV A, we will evaluate the $2U$ contributions to the relevant n-point functions exactly and treat the residual contributions from the $4U$ vertices perturbatively [54] to $O(c_1)$. The latter has to be justified *a posteriori*, by showing that the variational results favor small enough coupling values $|c_1^*| \ll 1$ (cf. Sec. VIII A).

A. The 2-point function

In this section we evaluate the 2-point soft-mode correlator (for $c_{i\geq 2} = 0$) which simultaneously provides the basis for the calculation of the 4-point correlator in the next section. Since we are working to $O(c_1)$ in the $4U$ interactions, we will only keep one insertion of the $\mathcal{L}^{(4U)}_{<,c_1}$ vertex in the functional potential operator (58), which thus reduces to

$$\mathcal{V}^{(4U,c_1)}\left[\frac{\delta}{\delta j},\frac{\delta}{\delta j^\dagger}\right] = 1 - \frac{c_1 m_g}{2g^2\mu^2}\int d^3z\,\partial^2\left[\frac{\partial_i\delta}{\delta j_{MN}(\vec{z})}\times\frac{\delta}{\delta j^\dagger_{PM}(\vec{z})}\right]\frac{\delta}{\delta j_{QP}(\vec{z})}\,\frac{\partial_i\delta}{\delta j^\dagger_{NQ}(\vec{z})} \tag{84}$$

[where the notation $(\partial_i\delta)/\delta j(\vec{z})$ implies that the partial derivative is acting *only* on the result of the associated functional derivative]. The 2-point function is then obtained by taking derivatives of the generating functional (51) with respect to the matrix sources j and $j^\dagger$, i.e.,

$$\langle U^\dagger_{<,AB}(\vec{x})U_{<,CD}(\vec{y})\rangle = \frac{-\delta}{\delta j_{BA}(\vec{x})}\,\frac{-\delta}{\delta j^\dagger_{DC}(\vec{y})}\,\mathcal{V}^{(4U,c_1)}\left[\frac{\delta}{\delta j},\frac{\delta}{\delta j^\dagger}\right]\times\frac{Z^{(2U)}[j,j^\dagger]}{Z^{(2U)}[0,0]}\bigg|_{j,j^\dagger=0}, \tag{85}$$

where the superscript $(2U)$ indicates as in Eq. (54) that the corresponding quantity is evaluated by using only the $2U$ contribution to the full soft-mode action. Equation (85) can then be rewritten as

$$\langle U^\dagger_{<,AB}(\vec{x})U_{<,CD}(\vec{y})\rangle = \langle U^\dagger_{<,AB}(\vec{x})U_{<,CD}(\vec{y})\rangle^{(2U)} - \left\langle U^\dagger_{<,AB}(\vec{x})\int d^3z\,\mathcal{L}^{(4U)}_{<,c_1}[U^\dagger_<(\vec{z}),U_<(\vec{z})]U_{<,CD}(\vec{y})\right\rangle^{(2U)}, \tag{86}$$

where

$$\langle U^\dagger_{<,AB}(\vec{x})U_{<,CD}(\vec{y})\rangle^{(2U)} = \frac{\delta^2}{\delta j_{BA}(\vec{x})\delta j^\dagger_{DC}(\vec{y})}\,\frac{Z^{(2U)}[j,j^\dagger]}{Z^{(2U)}[0,0]}\bigg|_{j,j^\dagger=0} = \delta_{AD}\delta_{BC}\Delta^{-1}(\vec{y},\vec{x}) \tag{87}$$

is determined by the $2U$ part of the higher-derivative interactions only, while the $4U$ dynamics generates the perturbative $O(c_1)$ correction

$$\langle U^\dagger_{<,AB}(\vec{x})\int d^3z\,\mathcal{L}^{(4U)}_{<,c_1}(\vec{z})U_{<,CD}(\vec{y})\rangle^{(2U)} = \frac{c_1 m_g}{2g^2\mu^2}\,\frac{\delta^2}{\delta j_{BA}(\vec{x})\delta j^\dagger_{DC}(\vec{y})}\,v[j,j^\dagger]|_{j,j^\dagger=0}, \tag{88}$$

which is due to the insertion of the vertex

$$v[j,j^\dagger] := \frac{2g^2\mu^2}{c_1 m_g}\int d^3z\,\mathcal{L}^{(4U)}_{<,c_1}\left(\frac{\delta}{\delta j},\frac{\delta}{\delta j^\dagger}\right)\frac{Z^{(2U)}[j,j^\dagger]}{Z^{(2U)}[0,0]}, \tag{89}$$

$$= \int d^3z\,\partial^2\left[\frac{\partial_i\delta}{\delta j_{MN}(\vec{z})}\,\frac{\delta}{\delta j^\dagger_{PM}(\vec{z})}\right]\frac{\delta}{\delta j_{QP}(\vec{z})}\,\frac{\partial_i\delta}{\delta j^\dagger_{NQ}(\vec{z})}\times\frac{Z^{(2U)}[j,j^\dagger]}{Z^{(2U)}[0,0]} \tag{90}$$

(where ∂^2 acts only on the square bracket).

After evaluating the functional derivatives in Eq. (90), the contributions to the vertex v can be grouped according to the number of included source fields as

$$v[j,j^\dagger] = \frac{Z^{(2U)}[j,j^\dagger]}{Z^{(2U)}[0,0]}(v_d + v_{jj^\dagger}[j,j^\dagger] + v_{jj^\dagger jj^\dagger}[j,j^\dagger]). \tag{91}$$

The constant $v_d = v[0,0]$ is the IR-divergent, disconnected part which originates from the "8" vacuum-bubble diagram, with all four legs of the vertex $v[j,j^\dagger]$ closed among themselves, and reads

$$v_d = -N^3\mu^6\left(\frac{g^2}{\pi^2 m_g}\right)^2\tilde{\imath}_2^2(\xi,c_1)(2\pi)^3\delta^3(0) \tag{92}$$

[the integral $\tilde{\imath}_2(\xi, c_1)$ is defined in Appendix B]. More generally, disconnected contributions to the n-point functions arise when all functional derivatives associated with external lines hit the $Z^{(2U)}[j, j^\dagger]v_d$ part of $v[j, j^\dagger]$. The resulting products of free Green functions with v_d will play no role in our following discussion. All remaining terms require one (two) pair(s) $(\delta/\delta j)(\delta/\delta j^\dagger)$ to hit $v_{jj^\dagger}$ $(v_{jj^\dagger jj^\dagger})$ and thus contribute exclusively to the *connected* 2-(4-)point function. The 2-line connected part of the vertex thus becomes

$$\begin{aligned} v_{jj^\dagger}[j, j^\dagger] = & -\frac{g^2 N \mu^3}{\pi^2 m_g} \tilde{\imath}_2(\xi, c_1) \\ & \times \int d^3z [-j^\dagger_{MN} \Delta^{-1} \partial^2 \Delta^{-1} j_{NM} \\ & + (\partial_i \Delta^{-1} j_{MN}) j^\dagger_{NM} \Delta^{-1} \overleftarrow{\partial}_i] \end{aligned} \tag{93}$$

(where the ∂_i ($\overleftarrow{\partial}_i$) act on the first (second) argument of Δ^{-1} and integrals over the arguments of Δ^{-1} folded with a source are implied but not written explicitly). The 4-line connected part, finally, is

$$\begin{aligned} v_{jj^\dagger jj^\dagger}[j, j^\dagger] = & \int d^3z (\partial_i \Delta^{-1} j_{QN}) j^\dagger_{PQ} \Delta^{-1} \\ & \times [2(\partial_j \Delta^{-1} j_{MP})(j^\dagger_{NM} \Delta^{-1} \overleftarrow{\partial}_i \overleftarrow{\partial}_j) \\ & + (\partial^2 \Delta^{-1} j_{MP})(j^\dagger_{NM} \Delta^{-1} \overleftarrow{\partial}_i)] \end{aligned} \tag{94}$$

and contributes only to $n \geq 4$ point functions. (In both of the above expressions the "open" arguments (i.e., those not integrated over) are always the vertex coordinates $\vec{z}$ with $\partial_i \equiv \partial/\partial z_i$.)

We now proceed with the calculation of the 2-point (and $2n$-point) functions by evaluating the $4U$-vertex-induced functional

$$\begin{aligned} \Pi^{(2)}_{ABCD}[j, j^\dagger](\vec{x}, \vec{y}) := & \frac{-\delta}{\delta j_{BA}(\vec{x})} \frac{-\delta}{\delta j^\dagger_{DC}(\vec{y})} v[j, j^\dagger] \\ =: & \frac{Z^{(2U)}[j, j^\dagger]}{Z^{(2U)}[0, 0]} \bar{\Pi}^{(2)}_{ABCD}[j, j^\dagger](\vec{x}, \vec{y}), \end{aligned} \tag{95}$$

which yields

$$\begin{aligned} \bar{\Pi}^{(2)}_{ABCD}[j, j^\dagger](\vec{x}, \vec{y}) = & \delta_{AD} \Delta^{-1}_{CB}(\vec{y} - \vec{x})(v_{jj^\dagger} + v_{jj^\dagger jj^\dagger}) + \int d^3z'' j^\dagger_{AB}(\vec{z}'') \Delta^{-1}(\vec{z}'' - \vec{x}) \\ & \times \int d^3z' \Delta^{-1}(\vec{y} - \vec{z}') j_{CD}(\vec{z}')(v_{jj^\dagger} + v_{jj^\dagger jj^\dagger}) + \int d^3z' \Delta^{-1}(\vec{y} - \vec{z}') j_{CD}(\vec{z}') \\ & \times \frac{\delta(v_{jj^\dagger}[j, j^\dagger] + v_{jj^\dagger jj^\dagger}[j, j^\dagger])}{\delta j_{BA}(\vec{x})} + \int d^3z'' j^\dagger_{AB}(\vec{z}'') \Delta^{-1}(\vec{z}'' - \vec{x}) \frac{\delta(v_{jj^\dagger}[j, j^\dagger] + v_{jj^\dagger jj^\dagger}[j, j^\dagger])}{\delta j^\dagger_{DC}(\vec{y})} \\ & + \frac{\delta^2(v_{jj^\dagger}[j, j^\dagger] + v_{jj^\dagger jj^\dagger}[j, j^\dagger])}{\delta j_{BA}(\vec{x}) \delta j^\dagger_{DC}(\vec{y})}. \end{aligned} \tag{96}$$

The 2-point function is obtained from $\Pi^{(2)}$ by setting the sources j, $j^\dagger$ to zero. Since then $v_{jj^\dagger}[0, 0] = v_{jj^\dagger jj^\dagger}[0, 0] = 0$ and also the one-derivative terms as well as the term with two derivatives on $v_{jj^\dagger jj^\dagger}$ vanish, one is left with

$$\Pi^{(2)}_{ABCD}[0, 0](\vec{x}, \vec{y}) = \frac{\delta^2 v_{jj^\dagger}[j, j^\dagger]}{\delta j_{BA}(\vec{x}) \delta j^\dagger_{DC}(\vec{y})} \tag{97}$$

(the right-hand side is independent of j, $j^\dagger$—hence one does not have to impose j, $j^\dagger = 0$ explicitly). It thus remains to calculate

$$\begin{aligned} \frac{\delta^2 v_{jj^\dagger}[j, j^\dagger]}{\delta j_{BA}(\vec{x}) \delta j^\dagger_{DC}(\vec{y})} = & \delta_{AD} \delta_{CB} \frac{4Ng^4}{\pi^2} \frac{\mu}{m_g^2} \tilde{\imath}_2(\xi, c_1) \partial_x^2 \frac{-\partial}{\partial \xi^2} \\ & \times \Delta^{-1}(\vec{y} - \vec{x}), \end{aligned} \tag{98}$$

$$= -\delta_{AD} \delta_{BC} \frac{2g^2}{m_g} \frac{\gamma}{\zeta \mu} \bar{\Delta}^{-1}(\vec{x} - \vec{y}), \tag{99}$$

where we used the symmetry property (76) and defined the "$4U$-vertex-inserted" soft-mode propagator

$$\begin{aligned} \bar{\Delta}^{-1}(\vec{x}) := & 2\tilde{\imath}_2 \mu \partial_x^2 \frac{\partial}{\partial \xi^2} \Delta^{-1}(\vec{x}) \\ = & \frac{4g^2 \mu^4}{m_g} \tilde{\imath}_2(\xi, c_1) \int \frac{d^3\kappa}{(2\pi)^3} \\ & \times \frac{\kappa^2 \theta(1 - \kappa^2) e^{i\vec{\kappa}\mu\vec{x}}}{[\kappa^2(1 - c_1\kappa^2) + \xi^2]^2}, \end{aligned} \tag{100}$$

as well as the dimensionless parameters

$$\xi = \frac{\sqrt{\bar{\Sigma}}}{\mu}, \qquad \gamma \equiv \frac{g^2 N_c}{\pi^2} = 4N_c \frac{\alpha}{\pi}, \qquad \zeta \equiv \frac{m_g}{\mu}. \tag{101}$$

Hence, the c_1 correction (88) to the connected 2-point function, which originates from the perturbative insertion of the $4U$ part (83) of the four-derivative interactions, becomes

$$\left\langle U^\dagger_{<,AB}(\vec{x}) \int d^3z \mathcal{L}^{(4U)}_{<,c_1}(\vec{z}) U_{<,CD}(\vec{y}) \right\rangle^{(2U)} = \frac{c_1 m_g}{2g^2\mu^2} \Pi^{(2)}_{ABCD}[0,0](\vec{x},\vec{y}) = -\delta_{AD}\delta_{BC} \frac{c_1\gamma}{\zeta\mu^3} \bar{\Delta}^{-1}(\vec{x}-\vec{y}). \quad (102)$$

Our final result for the 2-point function is therefore

$$\langle U^\dagger_{<,AB}(\vec{x}) U_{<,CD}(\vec{y})\rangle = \delta_{AD}\delta_{BC}\left[\Delta^{-1}(\vec{x}-\vec{y}) + \frac{c_1\gamma}{\zeta\mu^3}\bar{\Delta}^{-1}(\vec{x}-\vec{y})\right]. \quad (103)$$

Its diagonal dependence on the group indices reflects the $\mathrm{SU}_L(N_c) \times \mathrm{SU}_R(N_c)$ symmetry of the soft-mode dynamics (41).

B. The 4-point function

In the following section we sketch the analogous evaluation of the 4-point function. Although our main goal of computing c_n corrections to the vacuum energy density involves (in our approximation) only the 2-point function, the explicit expression for the 4-point function

$$\delta_4 \equiv \langle U^\dagger_{<,AB}(\vec{z}_1) U_{<,CD}(\vec{z}_2) U^\dagger_{<,EF}(\vec{z}_3) U_{<,GH}(\vec{z}_4)\rangle, \quad (104)$$

$$= \frac{-\delta}{\delta j_{BA}(\vec{z}_1)} \frac{-\delta}{\delta j^\dagger_{DC}(\vec{z}_2)} \frac{-\delta}{\delta j_{FE}(\vec{z}_3)} \times \frac{-\delta}{\delta j^\dagger_{HG}(\vec{z}_4)} \mathcal{V}^{(4U,c_1)}\left[\frac{\delta}{\delta j}, \frac{\delta}{\delta j^\dagger}\right] \frac{Z^{(2U)}[j,j^\dagger]}{Z^{(2U)}[0,0]} \Big|_{j,j^\dagger=0}, \quad (105)$$

$$=: \delta_4^{(2U)} - \delta_4^{(4U,O(c_1))} + \ldots \quad (106)$$

will be useful, too, because it allows for consistency checks and an alternative estimate of the nonperturbative energy density. Above, we have defined

$$\delta_4^{(2U)} \equiv \langle U^\dagger_{<,AB}(\vec{z}_1) U_{<,CD}(\vec{z}_2) U^\dagger_{<,EF}(\vec{z}_3) U_{<,GH}(\vec{z}_4)\rangle^{(2U)}, \quad (107)$$

$$= \frac{\delta^4}{\delta j_{FE}(\vec{z}_3)\delta j^\dagger_{HG}(\vec{z}_4)\delta j_{BA}(\vec{z}_1)\delta j^\dagger_{DC}(\vec{z}_2)} \frac{Z^{(2U)}[j,j^\dagger]}{Z^{(2U)}[0,0]} \Big|_{j,j^\dagger=0}, \quad (108)$$

$$= \delta_{AD}\delta_{CB}\Delta^{-1}(\vec{z}_2,\vec{z}_1)\delta_{EH}\delta_{GF}\Delta^{-1}(\vec{z}_4,\vec{z}_3) + \delta_{AH}\delta_{GB}\Delta^{-1}(\vec{z}_4,\vec{z}_1)\delta_{ED}\delta_{CF}\Delta^{-1}(\vec{z}_2,\vec{z}_3), \quad (109)$$

which shows that in the absence of $4U$ interactions the 4-point function factorizes as

$$\langle U^\dagger_{LAB}(\vec{z}_1) U_{LCD}(\vec{z}_2) U^\dagger_{LEF}(\vec{z}_3) U_{LGH}(\vec{z}_4)\rangle = \langle U^\dagger_{LAB}(\vec{z}_1) U_{LCD}(\vec{z}_2)\rangle\langle U^\dagger_{LEF}(\vec{z}_3) U_{LGH}(\vec{z}_4)\rangle + \langle U^\dagger_{LAB}(\vec{z}_1) U_{LGH}(\vec{z}_4)\rangle\langle U^\dagger_{LEF}(\vec{z}_3) U_{LCD}(\vec{z}_2)\rangle, \quad (110)$$

and

$$\delta_4^{(4U,O(c_1))} \equiv \left\langle U^\dagger_{<,AB}(\vec{z}_1) U_{<,CD}(\vec{z}_2) \times \int d^3z \mathcal{L}^{(4U)}_{<,c_1}(\vec{z}) U^\dagger_{<,EF}(\vec{z}_3) U_{<,GH}(\vec{z}_4) \right\rangle^{(2U)}, \quad (111)$$

$$= \frac{c_1 m_g}{2g^2\mu^2} \frac{\delta^4 v[j,j^\dagger]}{\delta j_{FE}(\vec{z}_3)\delta j^\dagger_{HG}(\vec{z}_4)\delta j_{BA}(\vec{z}_1)\delta j^\dagger_{DC}(\vec{z}_2)} \Big|_{j,j^\dagger=0}, \quad (112)$$

$$=: -\frac{c_1 m_g}{2g^2\mu^2} \Pi^{(4)}_{ABCDEFGH}(\vec{z}_1,\vec{z}_2,\vec{z}_3,\vec{z}_4). \quad (113)$$

The above reordering of the functional derivatives reveals that Eq. (95) from the calculation of the 2-point function can be used as an intermediate step for the further evaluation. Indeed, to $O(c_1)$ the correction due to the $4U$ interaction becomes

$$\Pi^{(4)}_{ABCDEFGH}(\vec{z}_1,\vec{z}_2,\vec{z}_3,\vec{z}_4) := \frac{\delta}{\delta j_{FE}(\vec{z}_3)} \frac{\delta}{\delta j^\dagger_{HG}(\vec{z}_4)} \Pi^{(2)}_{ABCD}[j,j^\dagger](\vec{z}_1,\vec{z}_2)|_{j,j^\dagger=0}, \quad (114)$$

which simplifies in the zero-distance limit of some of its arguments (as it occurs in our context) and then renders, together with Eq. (109), the coordinate dependence of the 4-point function explicit.

VI. SOLUTION OF THE GAP EQUATION AND PHASE DIAGRAM

As explained in Sec. IV B, the above expressions for the 2- and 4-point functions are to be evaluated at the saddle point $\bar{\Sigma} =: (\mu\bar{\xi})^2$ of the integral over the auxiliary Σ field, i.e., at the minimal-action solution of the gap equation

$$\langle U^\dagger_{<,AB}(\vec{x}) U_{<,BC}(\vec{x})\rangle = \delta_{AC}. \quad (115)$$

After inserting the result (103) for the connected 2-point function (and recalling $\delta_{AA} = N_c$), Eq. (115) turns into

$$N_c\left[\Delta^{-1}(0) + \frac{c_1\gamma}{\zeta\mu^3}\bar{\Delta}^{-1}(0)\right] = 1. \quad (116)$$

The zero-distance limits of the propagator (73) and (74) and of the $4U$ correction (100) are then expressed in terms of the integrals $\tilde{\imath}_n$, $\tilde{\jmath}_n$ (defined and evaluated in Appendix B) as

$$\Delta^{-1}(0) = \frac{\gamma}{\zeta N_c}\tilde{\imath}_1(\xi, c_1), \quad (117)$$

$$\bar{\Delta}^{-1}(0) = \frac{2\gamma}{\zeta N_c}\mu^3 \tilde{\imath}_2(\xi, c_1)\tilde{j}_2(\xi, c_1) \tag{118}$$

[both are of $O(g^2/\zeta)$], so that the gap equation assumes its final form

$$\frac{\gamma}{\zeta}\left[\tilde{\imath}_1(\xi, c_1) + 2c_1\frac{\gamma}{\zeta}\tilde{\imath}_2(\xi, c_1)\tilde{j}_2(\xi, c_1)\right] = 1. \tag{119}$$

[For $c_1 = 0$ and $\zeta = 1$, Eq. (119) reduces as expected [18] to $\gamma\tilde{\imath}_1(\xi) = 1$ (except when γ diverges, see below).] This equation and the ξ dependence of the integrals (B1) and (B2) render the nonperturbative character of the solutions $\bar{\xi}(\mu, c_1, \zeta)$ explicit. As already mentioned, it reflects the infinite subset of diagrams required to generate a finite mass gap.

Before finding the solutions of Eq. (119) as functions of the variational parameters, we specialize ζ to the form required by continuity of $G^{-1}(k)$ at $k = \mu$ [cf. Eq. (23)],

$$\zeta_{\rm ct}(c_1) = \frac{m_g}{\mu} = \frac{1}{1 - c_1}, \tag{120}$$

and adopt the one-loop Yang-Mills coupling

$$\gamma(\mu) = \frac{g^2_{\rm YM}(\mu)N_c}{\pi^2} \overset{N_c=3}{=} \frac{24}{11\ln\frac{\mu}{\Lambda_{\rm YM}}} \tag{121}$$

to render the μ dependence of γ explicit. The coupling $g_{\rm YM}(\mu)$ is just 11/10 times larger [37,42] than the coupling (37) obtained from integrating out the high-momentum modes [42] governed by the UV covariance (11). (This discrepancy can be mended by admitting nontransverse modes to the UV covariance [19].) We prefer to use the Yang-Mills coupling because it facilitates direct comparison with the numerical results of Ref. [18].

The above considerations imply that the solutions of Eq. (119) depend on just two variational parameters, i.e., the RG scale $\mu \geq 0$ which enters through the coupling (121) and $c_1 < 1$ which controls the leading momentum dependence of the infrared covariance $G^{-1}_<(k)$. Our next task will be to determine the critical line $\mu(c_1)$ in this parameter space, i.e., the subspace which joins the points where the phase transition takes place and where thus the (dis-)order parameter vanishes,

$$\bar{\xi}(\mu(c_1), c_1) = 0. \tag{122}$$

This line can be found analytically since for $\xi = 0$ the integrals $\tilde{\imath}_1$, $\tilde{\imath}_2$ and $\tilde{j}_2$ in the gap equation (119) simplify to (cf. Appendix B 2)

$$\tilde{\imath}(c_1) := \tilde{\imath}_1(0, c_1) = \frac{\operatorname{arctanh}\sqrt{c_1}}{\sqrt{c_1}}, \qquad \tilde{\imath}_2(0, c_1) = \frac{\tilde{\imath}(c_1) - 1}{c_1} \tag{123}$$

and

$$\tilde{j}_2(0, c_1) = \frac{1}{2}\left[\frac{1}{1 - c_1} + \tilde{\imath}(c_1)\right]. \tag{124}$$

In order to exhibit the μ dependence, we first resolve the $\xi = 0$ gap equation for $\gamma(\mu)$, which yields

$$\frac{1}{\zeta^2_{\rm ct}}\left(\frac{\tilde{\imath} - 1}{1 - c_1} + \tilde{\imath}(\tilde{\imath} - 1)\right)\gamma^2 + \frac{\tilde{\imath}}{\zeta_{\rm ct}}\gamma - 1 = 0. \tag{125}$$

The two solutions of this equation can then be resolved for μ and combine into the critical line $\mu(c_1)$. With $\gamma(\mu)$ from Eq. (121) it takes the explicit form

$$\frac{\mu_{c,1,2}(c_1)}{\Lambda_{\rm YM}} = \exp\left[\frac{48}{11}\frac{(1 - c_1)[1 - \tilde{\imath}(c_1)][1 + (1 - c_1)\tilde{\imath}(c_1)]}{(1 - c_1)\tilde{\imath}(c_1) \pm \sqrt{5\tilde{\imath}^2(c_1)(1 - c_1)^2 - 4(1 - c_1)[1 - c_1\tilde{\imath}(c_1)]}}\right]. \tag{126}$$

In order to facilitate the discussion of the vacuum phase structure encoded in Eq. (126), we plot the phase boundary in Fig. 2. It reveals that Eq. (122) is satisfied by two values of μ for each c_1 for which a solution exists, except at the maximal and minimal values where μ becomes unique. *Vice versa*, there are two c_1 for each μ for which Eq. (122) holds. The critical line (126) covers the limited parameter ranges

$$0.5 \lesssim \frac{\mu}{\Lambda_{\rm YM}} \lesssim 8.86 \tag{127}$$

and

$$-0.48 \lesssim c_1 < 1. \tag{128}$$

This prevents the minimal-energy solution $\bar{\xi}^*$ (to be determined in Sec. VIII A) from attaining unacceptably large values of μ and $|c_1|$. The normalizability condition $c_1 < 1$ is automatically satisfied in the existence region of gap-equation solutions. Equation (126) further shows that nontrivial (i.e., nonzero) solutions of the gap equation exist only when the gauge coupling exceeds a critical value, i.e., for

$$g^2(\mu) > g^2(c_1), \tag{129}$$

as expected on physical grounds. The maximal critical coupling corresponds to $c_1 = 0$:

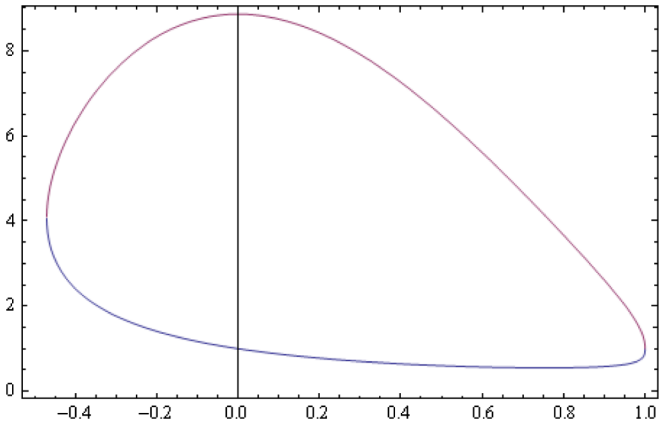

FIG. 2 (color online). Vacuum phase diagram: inside the plotted phase boundary $\mu_c(c_1)/\Lambda_{\rm YM}$ the theory is in its strongly coupled disordered phase. (Our treatment is approximately valid in the range $\mu \gtrsim 4\Lambda_{\rm YM}$ and $c_1 \in \{-0.5, 0.5\}$).

$$g^2(c_1) \leq g^2(c_1 = 0) = \frac{\pi^2}{N_c}. \tag{130}$$

Only part of the critical line (126) is physically trustworthy, however. Indeed, its validity range is limited to $|c_1| \ll 1$ for which the $O(c_1)$ evaluation of the $4U$ correction included in Eq. (126) is accurate, and to $\mu/\Lambda_{\rm YM} \gtrsim 5-6$ which justifies the $O(g)$ approximation. These two restrictions eliminate most of the $\mu_{c,1}$ branch and the lower-μ part of the $\mu_{c,2}$ branch. [Although the $c_1 = 0$ solution with $\mu/\Lambda_{\rm YM} \to 1$ and thus $g^2(\mu_c) \to \infty$ invalidates the $O(g)$ treatment, it nevertheless demonstrates that the gap equation does not reduce to $\gamma\tilde{\imath}_1(\xi) = 1$ for $c_1 \to 0$ if $\gamma(\mu)$ diverges simultaneously.]

In Fig. 3, finally, we plot the numerically generated solution $\bar{\xi}(\mu, c_1)$ of the gap equation (119) in the physically reliable parameter range. As expected, the $\bar{\xi} \geq 0$ region is surrounded by the critical line (126) and exists for $0.5 \lesssim \mu/\Lambda_{\rm YM} \lesssim 8.86$. In addition, Fig. 3 reveals that the (dis-)order parameter goes to zero continuously, i.e., that the transition from the disordered to the ordered phase is of second order [55].

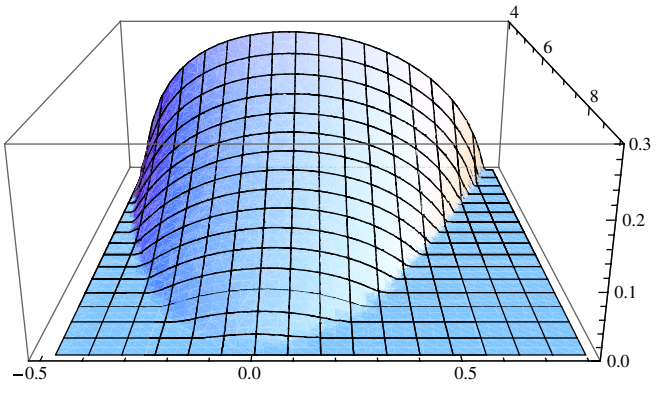

FIG. 3 (color online). The order-parameter solution $\bar{\xi}(\mu, c_1)$ of the gap equation in the variable ranges $\mu \in \{4, 9\}\Lambda_{\rm YM}$ and $c_1 \in \{-0.5, 0.8\}$.

VII. VACUUM ENERGY DENSITY

We have now assembled all the infrared-mode information necessary to evaluate the expectation value (25) of the Yang-Mills Hamiltonian density

$$\mathcal{H}_{\rm YM} = \tfrac{1}{2}(E_i^a E_i^a + B_i^a B_i^a) \tag{131}$$

in the generalized trial vacuum state (1). [We have adopted the $A_0 = 0$ gauge, and defined the chromo-electric and -magnetic fields as $E_i^a = F_{0i}^a$ and $B_i^a = \frac{1}{2}\varepsilon_{ijk}F_{jk}^a$.] Of course, the Hamiltonian (131) is formal and needs renormalization. Since we are interested in its matrix elements between Poincaré-invariant vacuum trial states with perturbative one-loop corrections only, a regularization of the vacuum matrix elements by a momentum cutoff $\Lambda_{\rm UV}$ will be sufficient [18]. In fact, the $\Lambda_{\rm UV}$ dependence of the vacuum energy density (25) can be completely removed by normal ordering the Hamiltonian (131) with respect to the noninteracting vacuum. This amounts to subtracting the ultraviolet-divergent energy density

$$\begin{aligned}\langle\mathcal{H}_{\rm YM}\rangle_0 &= 2(N_c^2-1)\frac{G_0^{-1}(\vec{x},\vec{x})}{2} \\ &= 2(N_c^2-1)\int\frac{d^3k}{(2\pi)^3}\theta(\Lambda_{\rm UV}^2-\vec{k}^2)\frac{\hbar\omega_k}{2} \\ &= \frac{N_c^2-1}{8\pi^2}\Lambda_{\rm UV}^4\end{aligned} \tag{132}$$

(where we wrote $\omega_k = k$ for the free gluon energy and reinstated $\hbar$) of the noninteracting vacuum, i.e., the sum over the zero-point energies of two transverse, massless vector modes, from $\langle\mathcal{H}_{\rm YM}\rangle$. [Recall that the momentum cutoffs are imposed on integrals over the gauge-invariant U modes and therefore do not compromise (residual) gauge invariance.]

A. Hard-mode contribution

According to our strategy for evaluating the trial energy density $\langle\mathcal{H}_{\rm YM}\rangle$ outlined in Sec. III A, the first step consists of integrating over the static gauge fields and the hard modes $U_>$. In the following section, this will be done for the chromo-electric $\langle E^2\rangle$ and -magnetic $\langle B^2\rangle$ contributions separately. We start from the intermediate matrix element

$$\begin{aligned}\langle\langle\langle E_i^a(\vec{x})E_j^b(\vec{y})\rangle\rangle\rangle &= \frac{\int D\vec{A}\,\psi_0[\vec{A}^U]\frac{i\delta}{\delta A_i^a(\vec{x})}\frac{i\delta}{\delta A_j^b(\vec{y})}\psi_0[\vec{A}]}{\int D\vec{A}\,\psi[\vec{A}^U]\psi[\vec{A}]} \\ &= \delta_{ij}\delta^{ab}G^{-1}(\vec{x},\vec{y}) \\ &\quad -\int d^3z_1\int d^3z_2 G^{-1}(\vec{x}-\vec{z}_1) \\ &\quad \times G^{-1}(\vec{y}-\vec{z}_2)\langle\langle\langle A_i^a(\vec{z}_1)A_j^b(\vec{z}_2)\rangle\rangle\rangle\end{aligned} \tag{133}$$

($E_i^a = i\delta/\delta A_i^a$, cf. Appendix A) for the chromoelectic 2-

point function. With the help of the expression (A21) for the gauge-field matrix element in terms of the functionals $a[U]$ and $\mathcal{M}[U]$ as defined in Eq. (A14), this specializes to

$$\begin{aligned}\langle\langle\langle E^2\rangle\rangle\rangle &:= \langle\langle\langle E_i^a(\vec{x})E_i^a(\vec{x})\rangle\rangle\rangle \\ &= 3(N_c^2-1)G^{-1}(\vec{x},\vec{x}) \\ &\quad - \int d^3z_1 d^3z_2 G^{-1}(\vec{x}-\vec{z}_1)G^{-1}(\vec{x}-\vec{z}_2) \\ &\quad \times [\mathcal{M}_{ii}^{-1aa}(\vec{z}_1,\vec{z}_2) + a_i^a(\vec{z}_1)a_i^a(\vec{z}_2)]. \end{aligned} \tag{134}$$

The analogous expression for the chromomagnetic contribution involves 2-, 3-, and 4-point functions of the gauge field. After rewriting them with $B_i^a = \varepsilon_{ijk}(\partial_j A_k^a + \frac{g}{2} f^{abc} A_j^b A_k^c)$ and Eqs. (A21)–(A23), one finds

$$\begin{aligned}\langle\langle\langle B^2\rangle\rangle\rangle &:= \langle\langle\langle B_i^a(\vec{x})B_i^a(\vec{x})\rangle\rangle\rangle \\ &= \varepsilon_{ijk}\varepsilon_{ilm}\partial_{z_{1j}}\partial_{z_{2l}}\mathcal{M}_{km}^{-1aa}(\vec{z}_1,\vec{z}_2)|_{\vec{z}_i=\vec{x}} + \varepsilon_{ijk}\varepsilon_{ilm}\partial_j a_k^a \partial_l a_m^a \\ &\quad + g\varepsilon_{ijk}\varepsilon_{ilm}f^{abc}[\mathcal{M}^{-1}(\vec{x},\vec{x})_{lm}^{bc}\partial_j a_k^a + \partial_{z_1,j}\mathcal{M}^{-1}(\vec{z}_1,\vec{x})_{km}^{ac}a_l^b + \partial_{z_1,j}\mathcal{M}^{-1}(\vec{z}_1,\vec{x})_{kl}^{ab}a_m^c + \partial_j a_k^a a_l^b a_m^c]_{z_i\to x} \\ &\quad + \frac{g^2}{4}f^{abc}f^{ade}[12\mathcal{M}^{-1bd}\mathcal{M}^{-1ce} + 8\mathcal{M}^{-1bd}a_i^c a_i^e + 2a_i^b a_j^c a_i^d a_j^e] \end{aligned} \tag{135}$$

(where all spacial arguments are set to $\vec{x}$ after taking the derivatives).

Now we compute the hard-mode contributions to the chromo-electric and -magnetic vacuum energies, as outlined in Sec. III A and Appendix A. This amounts to evaluating the intermediate matrix elements (31) for E^2 and B^2, i.e.,

$$\langle\langle E^2, B^2\rangle\rangle := \frac{\int D\phi[\langle\langle\langle E^2, B^2\rangle\rangle\rangle + O(g)]\exp\{-\Gamma_{b,>}[\phi]\}}{\int D\phi \exp\{-\Gamma_{,>}[\phi]\}} \tag{136}$$

to leading order in g. The hard-mode action $\Gamma_{b,>}[\phi]$ is defined in Eq. (A42). Since it is bilinear in ϕ, the integrals in Eq. (136) are Gaussian and can be calculated analytically, cf. Appendix A. This yields

$$\begin{aligned}\langle\langle E^2\rangle\rangle &= (N_c^2-1)\int\frac{d^3k}{(2\pi)^3}\theta(\Lambda_{\mathrm{UV}}^2-k^2)G^{-1}(k) \\ &\quad + \frac{1}{2}(N_c^2-1)\int\frac{d^3k}{(2\pi)^3}\theta(\mu^2-k^2)G^{-1}(k) \\ &\quad + \langle\langle E^2\rangle\rangle_{U_<} + O(g), \end{aligned} \tag{137}$$

which includes the contribution

$$\begin{aligned}\langle\langle E^2\rangle\rangle_{U_<} &:= -\frac{1}{4g^2}\int d^3z_1\int d^3z_2 G_<^{-1}(\vec{x}-\vec{z}_1)G_<^{-1}(\vec{x}-\vec{z}_2) \\ &\quad \times\langle\langle L_{<,i}^a(\vec{z}_1)L_{<,i}^a(\vec{z}_2)\rangle\rangle \end{aligned} \tag{138}$$

from the soft modes $U_<$, and

$$\langle\langle B^2\rangle\rangle = (N_c^2-1)\int\frac{d^3k}{(2\pi)^3}\theta(\Lambda_{\mathrm{UV}}^2-k^2)k^2G(k) + O(g). \tag{139}$$

With $\theta(k^2-\mu^2)G(k) = \theta(k^2-\mu^2)k^{-1}$ [cf. Eq. (11)] one finds the Λ_{UV} dependence of $\langle\langle E^2\rangle\rangle$ and $\langle\langle B^2\rangle\rangle$ to be identical. Hence, the lowest-dimensional gluon condensate $\langle F^2\rangle = 2[\langle B^2\rangle - \langle E^2\rangle]$ (to be discussed in Sec. VIII B) is Λ_{UV} independent by itself while the Λ_{UV} dependence of $\langle\langle\mathcal{H}_{\mathrm{YM}}\rangle\rangle$ has to be removed by renormalization. As noted above, at our level of approximation this amounts to normal ordering the Hamiltonian, i.e., to subtracting the noninteracting vacuum expectation values $\langle E^2\rangle_0 = \langle B^2\rangle_0 = (N_c^2-1)G_{m=0}^{-1}(\vec{x},\vec{x})$. The results are

$$\begin{aligned}\langle\langle{:}E^2{:}\rangle\rangle &= (N_c^2-1)\int\frac{d^3k}{(2\pi)^3}\theta(\mu^2-k^2)\left[\frac{3}{2}G^{-1}(k) - k\right] \\ &\quad + \langle\langle E^2\rangle\rangle_{U_<} + O(g) \end{aligned} \tag{140}$$

and

$$\begin{aligned}\langle\langle{:}B^2{:}\rangle\rangle &= (N_c^2-1)\int\frac{d^3k}{(2\pi)^3}\theta(\mu^2-k^2)[k^2G(k) - k] \\ &\quad + O(g). \end{aligned} \tag{141}$$

These expressions are indeed Λ_{UV} independent and exclusively receive contributions from momenta $k<\mu$. (Both properties have to become manifest at this stage because they are unaffected by the remaining integration over $U_<$.) Moreover, the above results provide a nontrivial check of the fact that by restoring residual gauge invariance the integration over ϕ has removed the longitudinal hard-mode contributions.

B. Soft-mode contribution in the disordered phase

It remains to calculate the chromo-electric soft-mode contribution (138) to the vacuum energy density. Here, the impact of the generalized IR covariance (13) becomes fully nonperturbative and the dependence on the variational parameters enters partly through the solutions of the gap equation. In order to evaluate Eq. (138), we first perform the remaining part of the $U_<$ integration [cf. Eq. (33)], i.e.,

we integrate over Σ, which yields

$$\langle E^2\rangle_{U_<} = -\frac{1}{4g^2}\int d^3z_1 \int d^3z_2 G_<^{-1}(\vec{x}-\vec{z}_1) \times G_<^{-1}(\vec{x}-\vec{z}_2)\langle L^a_{<,i}(\vec{z}_1)L^a_{<,i}(\vec{z}_2)\rangle. \quad (142)$$

[Recall that in the mean-field approximation of Sec. IV B the Σ integration amounts to evaluating $\langle\langle L^a_{<,i}(\vec{z}_1)L^a_{<,i}(\vec{z}_2)\rangle\rangle$ at the saddle-point solution $\bar{\Sigma}(\mu, c_1) = [\mu\bar{\xi}(\mu, c_1)]^2$ of the gap equation (119).] We further note that the integrals over $G^{-1}(\vec{x}-\vec{z}_1)G^{-1}(\vec{x}-\vec{z}_2)$ in Eq. (142) have most of their support at distances $|\vec{z}_1 - \vec{z}_2| < \mu^{-1}$ where $U_<(\vec{z}_2)U_<^\dagger(\vec{z}_1) \simeq 1$. This allows us to approximate

$$\langle L^a_{<,i}(\vec{z}_1)L^a_{<,i}(\vec{z}_2)\rangle = 2\langle \mathrm{tr}\{\partial_i U_<^\dagger(\vec{z}_2)U_<(\vec{z}_2)U_<^\dagger(\vec{z}_1)\partial_i U_<(\vec{z}_1)\}\rangle, \quad (143)$$

$$\simeq^{|\vec{z}_1-\vec{z}_2|<\mu^{-1}} 2\langle \mathrm{tr}\{\partial_i U_<^\dagger(\vec{z}_2)\partial_i U_<(\vec{z}_1)\}\rangle \quad (144)$$

[as in the $2U$ approximation (44) to the Lagrangian (43)]. From Eq. (103) one then has

$$\langle L^a_{<,i}(\vec{z}_1)L^a_{<,i}(\vec{z}_2)\rangle \simeq 2N_c^2\partial_{z_2,i}\Big[\Delta^{-1}(\vec{z}_2-\vec{z}_1) + \frac{c_1\gamma}{\zeta\mu^3}\bar{\Delta}^{-1}(\vec{z}_2-\vec{z}_1)\Big]\overleftarrow{\partial}_{z_1,i} \quad (145)$$

and with Eqs. (73) and (74) (specialized to $c_{n\geq 2} = 0$) and (100) further

$$\langle L^a_{<,i}(\vec{z}_1)L^a_{<,i}(\vec{z}_2)\rangle \simeq 4N_c\pi^2\frac{\gamma}{\zeta}\mu^2\int\frac{d^3\kappa}{(2\pi)^3}\kappa^2\theta(1-\kappa^2) \times e^{i\vec{\kappa}\mu(\vec{z}_2-\vec{z}_1)}\Big[\frac{1}{\kappa^2(1-c_1\kappa^2)+\bar{\xi}^2} + \frac{2c_1\gamma\zeta^{-1}\tilde{\imath}_2(\bar{\xi},c_1)\kappa^2}{[\kappa^2(1-c_1\kappa^2)+\bar{\xi}^2]^2}\Big], \quad (146)$$

which has the coincidence limit

$$\langle L^a_{<,i}(\vec{z})L^a_{<,i}(\vec{z})\rangle \simeq 2N_c\frac{\gamma}{\zeta}\mu^2\Big[\tilde{\imath}_2(\bar{\xi},c_1) + 2c_1\frac{\gamma}{\zeta}\tilde{\imath}_2(\bar{\xi},c_1)\tilde{\jmath}_3(\bar{\xi},c_1)\Big]. \quad (147)$$

With the explicit expression (13) for the generalized IR covariance (with $c_{i\geq 2} = 0$) Eq. (142) evaluates further to

$$\langle E^2\rangle_{U_<} = -\frac{m_g^2}{4g^2}\int\frac{d^3k}{(2\pi)^3}\theta(\mu^2-\vec{k}^2)\Big(1-c_1\frac{k^2}{\mu^2}\Big) \times\int\frac{d^3p}{(2\pi)^3}\theta(\mu^2-\vec{p}^2)\Big(1-c_1\frac{p^2}{\mu^2}\Big)\int d^3z_1 \times\int d^3z_2 e^{i\vec{k}(\vec{x}-\vec{z}_1)}e^{i\vec{p}(\vec{x}-\vec{z}_2)}\langle L^a_{<,i}(\vec{z}_1)L^a_{<,i}(\vec{z}_2)\rangle \quad (148)$$

and, after inserting Eq. (147), assumes its final form

$$\langle E^2\rangle_{U_<} = -\frac{N_c^2\zeta}{2\pi^2}\mu^4\Big[\tilde{\imath}_2 - 2c_1\tilde{\imath}_3 + c_1^2\tilde{\imath}_4 + 2c_1\frac{\gamma}{\zeta}\tilde{\imath}_2(\tilde{\jmath}_3 - 2c_1\tilde{\jmath}_4 + c_1^2\tilde{\jmath}_5)\Big], \quad (149)$$

where the integrals $\tilde{\imath}_n$, $\tilde{\jmath}_n$ are understood to be evaluated as $\tilde{\imath}_n(\bar{\xi}(\mu, c_1), c_1)$, $\tilde{\jmath}_n(\bar{\xi}(\mu, c_1), c_1)$. (Note that these integrals receive most of their contributions from vacuum modes with momenta $k \sim \mu$ [cf. Appendix A].)

The rather complex parameter dependence of Eq. (149) simplifies considerably for small $|c_1| \ll 1$. Indeed, after specializing the IR mass parameter ζ to $\zeta_{\mathrm{ct}}(c_1) = (1-c_1)^{-1} = 1 + c_1 + O(c_1^2)$ [which ensures a continuous covariance, cf. Eq. (120)] and using the small-c_1 expansions (B66) and (B67) of the integrals $\tilde{\imath}_n$ and $\tilde{\jmath}_n$, the soft-mode contribution $\varepsilon_{U_<} = \langle E^2\rangle_{U_<}/2$ to the energy density becomes

$$\varepsilon_{U_<}(\mu, c_1, \zeta_{\mathrm{ct}}; \bar{\xi}) = -\frac{N_c^2}{4\pi^2}\mu^4\{\tilde{\imath}_2(\bar{\xi}) + c_1[\tilde{\imath}_2(\bar{\xi}) - 2\tilde{\imath}_3(\bar{\xi}) + \tilde{\jmath}_4(\bar{\xi}) + 2\gamma\tilde{\imath}_2(\bar{\xi})\tilde{\jmath}_3(\bar{\xi})]\} + O(c_1^2), \quad (150)$$

$$\simeq -\frac{N_c^2}{4\pi^2}\mu^4(1+c_1)\tilde{\imath}_2(\bar{\xi}) \quad (151)$$

for $|c_1| \ll 1$. (The last expression provides a very reasonable approximation for $|c_1| \lesssim 0.1$.) With $c_1 = 0$ and $m_g = \mu$ (and approximating $N_c^2 - 1 \sim N_c^2$), finally, the above expression reduces to the result

$$\varepsilon_{U_<}(\mu, c_1 = 0, \zeta = 1; \bar{\xi}) = -\frac{N_c^2}{4\pi^2}\mu^4\tilde{\imath}_2(\bar{\xi}) = -\frac{N_c^2}{4\pi^2}\mu^4\Big[\frac{1}{3} - \bar{\xi}^2\Big(1 - \bar{\xi}\arctan\frac{1}{\bar{\xi}}\Big)\Big] \quad (152)$$

of Ref. [18], as it should.

C. Energy density in the disordered phase (i.e., for $\mu \ll \Lambda_{\mathrm{UV}}$)

The (normalized) integral over the auxiliary field Σ turns the matrix element $\langle\langle\mathcal{H}_{\mathrm{YM}}\rangle\rangle$ into the trial vacuum energy density $\langle\mathcal{H}_{\mathrm{YM}}\rangle$ [cf. Eq. (33)]. This integral is nontrivial only for the $U_<$ and hence ξ dependent part (138) of the integrand (137). Its evaluation in the previous section yielded Eq. (149). Combining these results and separating the complete vacuum energy density $\varepsilon = E/V = \langle\mathcal{H}_{\mathrm{YM}}\rangle$ into hard and soft contributions,

$$\varepsilon(\mu, c_1, \zeta; \bar{\xi}) = \langle\mathcal{H}_{\mathrm{YM}}\rangle = \varepsilon_>(\mu) + \varepsilon_<(\mu, c_1, \zeta; \bar{\xi}) \quad (153)$$

(with ζ still unspecified), one finds

$$\varepsilon_>(\mu) = \frac{1}{2}(N_c^2-1)\int\frac{d^3k}{(2\pi)^3}[\theta(\Lambda_{\rm UV}^2-k^2)-\theta(\mu^2-k^2)] \times [G_>^{-1}(k)+k^2G_>(k)] \tag{154}$$

and

$$\varepsilon_<(\mu,c_1,\zeta;\bar\xi) = \frac{1}{2}(N_c^2-1)\int\frac{d^3k}{(2\pi)^3}\theta(\mu^2-k^2) \times\left[\frac{3}{2}G_<^{-1}(k)+k^2G_<(k)\right] + \frac{1}{2}\langle E^2\rangle_{U_<}(\mu,c_1,\zeta;\bar\xi). \tag{155}$$

The energy density $\varepsilon_>$ of the hard modes involves only $G_>^{-1}(k)=k=k^2G_>(k)$ and evaluates further to

$$\varepsilon_>(\mu) = 2(N_c^2-1)\int\frac{d^3k}{(2\pi)^3}[\theta(\Lambda_{\rm UV}^2-k^2)-\theta(\mu^2-k^2)]\frac{k}{2} = \frac{N_c^2-1}{8\pi^2}(\Lambda_{\rm UV}^4-\mu^4), \tag{156}$$

which is the (regularized) zero-point energy density of the two transverse, *massless* vector modes with energy $\omega(k)=k$ (recall that the integration over ϕ has removed the longitudinal-mode contribution) and reflects the built-in asymptotic freedom of the $k>\mu$ modes. As anticipated, the subtraction of the free vacuum energy density (132) in the course of normal ordering cancels its $\Lambda_{\rm UV}$ dependence.

The soft-mode contribution is mainly of nonperturbative origin and therefore structurally more involved. Inserting the covariance (20) and its inverse (21) [for $c_{n\geq 2}=0$, as before, and $\zeta=m_g/\mu$] into Eq. (155) yields

$$\varepsilon_< = \frac{N_c^2-1}{4\pi^2}\left[\frac{\zeta}{2}\left(1-\frac{3c_1}{5}\right) -\frac{1}{\zeta c_1^2}\left(1+\frac{c_1}{3}-\frac{\operatorname{arctanh}\sqrt{c_1}}{\sqrt{c_1}}\right)\right]\mu^4+\frac{\langle E^2\rangle_{U_<}}{2}, \tag{157}$$

so that the total energy density (153), after dropping the constant zero-point contribution $(N_c^2-1)\Lambda_{\rm UV}^4/(8\pi^2)$, becomes

$$\varepsilon = \frac{N_c^2-1}{4\pi^2}\frac{\mu^4}{\zeta c_1^2}\left[-\frac{3(3\zeta c_1-5\zeta+5)\zeta c_1^2+10c_1+30}{30} +\frac{\operatorname{arctanh}\sqrt{c_1}}{\sqrt{c_1}}\right]+\frac{\langle E^2\rangle_{U_<}}{2}. \tag{158}$$

After further approximating $N_c^2-1\simeq N_c^2$, ensuring the continuity of $G_<(k)$ by imposing Eq. (120) and using Eq. (149), we obtain our final expression for the energy density in the disordered phase,

$$\bar\varepsilon(\mu,c_1) := \varepsilon(\mu,c_1,\zeta_{\rm ct}(c_1);\bar\xi(\mu,c_1)) = -\frac{N_c^2}{4\pi^2}\mu^4\left[\frac{4c_1^3+10c_1^2-50c_1+30}{30c_1^2(1-c_1)}-\frac{1-c_1}{c_1^2}\frac{\operatorname{arctanh}\sqrt{c_1}}{\sqrt{c_1}} +\frac{\tilde\imath_2-2c_1\tilde\imath_3+c_1^2\tilde\imath_4+2\gamma c_1(1-c_1)\tilde\imath_2(\tilde\jmath_3-2c_1\tilde\jmath_4+c_1^2\tilde\jmath_5)}{1-c_1}\right], \tag{159}$$

where the integrals $\tilde\imath_n$, $\tilde\jmath_n$ are evaluated at $\bar\xi(\mu,c_1)$. For $c_1\to 1$ several terms of the energy density (159) diverge and prevent the vacuum from encountering the limiting instability. For $|c_1|\ll 1$, on the other hand, the rather complex c_1 dependence of the full vacuum energy density (159) simplifies to

$$\bar\varepsilon(\mu,c_1) = \frac{N_c^2}{4\pi^2}\mu^4\left\{\frac{1}{5}-\tilde\imath_2(\bar\xi)-\left[\frac{1}{7}+\tilde\imath_4(\bar\xi)-2\tilde\imath_3(\bar\xi)+2\gamma\tilde\imath_2(\bar\xi)\tilde\jmath_3(\bar\xi)\right]c_1\right\}+O(c_1^2) \tag{160}$$

(where the solution $\bar\xi$ of the gap equation is evaluated at $c_1=0$). For $c_1=0$ and $\zeta=1$, finally, it reduces as expected to the energy density of Ref. [18],

$$\varepsilon(\mu,c_1=0,\zeta=1;\bar\xi(\mu,c_1=0)) = \frac{N_c^2}{4\pi^2}\mu^4\left[-\frac{2}{15}+\bar\xi^2\left(1-\bar\xi\arctan\frac{1}{\bar\xi}\right)\right]. \tag{161}$$

The full energy density (159) is plotted in Fig. 4 and will be discussed further in Sec. VIII A.

D. Energy density in the ordered phase (i.e., for $\mu\ggg\Lambda_{\rm YM}$)

As argued above, the mean-field approximation is reliable in the disordered phase, i.e., for those $\mu<\mu_c\leq 8.86\Lambda_{\rm YM}$ [cf. Eq. (127)] for which $\bar\xi$ is not too small. In order to get a more complete picture of the vacuum energy density and its μ dependence, however, one has to evaluate the soft-mode contributions in the ordered phase as well, i.e., for $\mu\ggg\Lambda_{\rm YM}$ where the mean-field approximation breaks down. However, in this phase the Yang-Mills coupling becomes small [56], i.e.,

$$g^2(\mu\ggg\Lambda_{\rm YM})\ll 1, \tag{162}$$

so that the soft-mode dynamics can instead be treated perturbatively. After restricting ourselves in accordance

with our previous approximation scheme to the $2U$ contributions in Eqs. (42) and (44) [again with $c_{i\geq 2} = 0$], this dynamics becomes

$$\Gamma_<^{(2U)}[U_<] = -\frac{m_g}{2g^2}\int d^3z\,\mathrm{tr}\Big\{U_<^\dagger\Big(\partial^2 + \frac{c_1}{\mu^2}\partial^4\Big)U_<\Big\}. \tag{163}$$

Since in the ordered phase fluctuations $\varphi_<^a$ around $U_< \sim 1$ are small, one can furthermore truncate the weak-coupling expansion of $U_<$, i.e.,

$$U_< = \exp(ig\varphi_<^a\lambda^a) = 1 + ig\varphi_<^a\lambda^a + O(g^2), \tag{164}$$

which to $O(g^2)$ yields (with $\mathrm{tr}\{\lambda^a\lambda^b\} = 2\delta^{ab}$ and denoting the Fourier transform of φ as $\tilde{\varphi}$) the bilinear action

$$\Gamma_<^{(2U)}[\varphi_<] = \frac{1}{2}\int\frac{d^3k}{(2\pi)^3}\Big[\tilde{\varphi}_<^a(-\vec{k})2m_g\Big(k^2 - \frac{c_1}{\mu^2}k^4\Big)\tilde{\varphi}_<^a(\vec{k}) + \ldots\Big]. \tag{165}$$

From this "kinetic" term one reads off the static $k < \mu$ propagator of the φ modes [which contains, in contrast to the soft-mode propagator (73) and (74) in the disordered phase and as a consequence of Goldstone's theorem, no mass term] as

$$\langle\varphi_<^a(\vec{z}_1)\varphi_<^b(\vec{z}_2)\rangle = \frac{\delta^{ab}}{2m_g}\int\frac{d^3k}{(2\pi)^3}\theta(\mu^2 - k^2)\frac{e^{-i\vec{k}(\vec{z}_1-\vec{z}_2)}}{k^2 - \frac{c_1}{\mu^2}k^4}. \tag{166}$$

The correlator (143), which determines the chromoelectric vacuum energy density due to the soft modes, then becomes (with $\delta^{aa} = N_c^2 - 1$)

$$\langle L_{<,i}^a(\vec{z}_1)L_{<,i}^a(\vec{z}_2)\rangle \simeq 2\langle\mathrm{tr}\{\partial_i U_<^\dagger(\vec{z}_1)\partial_i U_<(\vec{z}_2)\}\rangle \simeq 4g^2\langle\partial_i\varphi_<^a(\vec{z}_1)\partial_i\varphi_<^a(\vec{z}_2)\rangle, \tag{167}$$

$$= 2(N_c^2 - 1)\frac{g^2\mu^2}{\zeta}\int\frac{d^3\kappa}{(2\pi)^3}\frac{\theta(1-\kappa^2)}{1 - c_1\kappa^2}e^{-i\mu\vec{\kappa}(\vec{z}_1-\vec{z}_2)}. \tag{168}$$

After inserting this result into Eq. (148) one obtains

$$\langle E^2\rangle_{U_<} = -(N_c^2 - 1)\frac{\zeta\mu^4}{2}\int\frac{d^3\kappa}{(2\pi)^3}\theta(1-\kappa^2)(1 - c_1\kappa^2), \tag{169}$$

$$= -\frac{N_c^2 - 1}{4\pi^2}\zeta\mu^4\Big(\frac{1}{3} - \frac{1}{5}c_1\Big). \tag{170}$$

Hence, Eq. (157) yields the infrared contributions

$$\varepsilon_< = \frac{N_c^2 - 1}{4\pi^2}\frac{\mu^4}{\zeta c_1^2}\Big(\frac{-3\zeta^2c_1^3 + 5\zeta^2c_1^2 - 5c_1 - 15}{15} + \frac{\mathrm{arctanh}\sqrt{c_1}}{\sqrt{c_1}}\Big) \tag{171}$$

to the energy density which specialize with $\zeta_{\mathrm{ct}}(c_1) = (1 - c_1)^{-1}$ to

$$\varepsilon_< = \frac{N_c^2 - 1}{4\pi^2}\mu^4\frac{1 - c_1}{c_1^2}\Big[\frac{-8c_1^3 + 25c_1 - 15}{15(1 - c_1)^2} + \frac{\mathrm{arctanh}\sqrt{c_1}}{\sqrt{c_1}}\Big]. \tag{172}$$

Together with the hard-mode contribution (156) [which is identical in both vacuum phases] and after discarding the zero-point contribution, finally, the total vacuum energy density in the ordered phase becomes

$$\varepsilon(\mu, c_1) = \frac{N_c^2 - 1}{4\pi^2}\mu^4\frac{1 - c_1}{c_1^2}\Big[-\frac{c_1^3 + 15c_1^2 - 50c_1 + 30}{30(1 - c_1)^2} + \frac{\mathrm{arctanh}\sqrt{c_1}}{\sqrt{c_1}}\Big], \tag{173}$$

$$= \frac{N_c^2 - 1}{4\pi^2}\mu^4\Big[\frac{1}{30} + \frac{8}{105}c_1 + \frac{32}{315}c_1^2 + O(c_1^3)\Big]. \tag{174}$$

Several properties of Eq. (173) are noteworthy. First of all, in the $c_1 \to 0$ limit it reduces, as expected, to the result of Ref. [18] [cf. their Eq. (4.24)],

$$\varepsilon(\mu, c_1 = 0) = \frac{N_c^2 - 1}{120\pi^2}\mu^4. \tag{175}$$

The total energy density diverges for $c_1 \to 1$ where the vacuum wave functionals would become unnormalizable, furthermore, which prevents c_1 from growing beyond unity during energy minimization. Most importantly, however, for $\mu \gg \Lambda_{\mathrm{YM}}$ the negative hard-mode contribution to the energy density [i.e., Eq. (156) without the Λ_{UV}^4 term] is overcome by the positive contribution (172) from the soft modes. Indeed, the (large μ) vacuum energy density (173) is positive for all $c_1 < 1$ and hence a monotonically *increasing* function of μ. In addition, Eq. (173) increases monotonically with c_1 in the range $-2 < c_1 < 1$ which includes those $|c_1| \ll 1$ values for which our perturbative $O(c_1)$ treatment is reliable (and thus our variational result $c_1^* \simeq 0.15$ to be determined in Sec. VIII A). Under these circumstances it is reasonable to expect that the perturbative result (173) remains at least qualitatively reliable for μ values down to the phase transition [18] at $\mu \lesssim 8.86\Lambda_{\mathrm{YM}}$.

VIII. VARIATIONAL ANALYSIS

We are now prepared to minimize the vacuum energy density in our trial-functional family according to the Rayleigh-Ritz variational principle. Above we found that (inside the validity range of our approximations) the energy density (159) in the strongly coupled disordered phase decreases monotonically with increasing μ up to the phase transition, whereas its counterpart (173) in the ordered weak-coupling phase monotonically increases both with μ and c_1. The combination of these results indicates that

the vacuum energy density attains its minimum at the phase boundary in the disordered phase, where the number of massless particles becomes maximal. Indeed, the number $N_c^2 - 1$ of massless Goldstone modes in the ordered phase (at very large μ all other modes have $m \sim \Lambda_{\rm UV}$ and are too massive to contribute significantly) doubles at the transition where they are joined by degenerate parity partners. Hence, the massless particles generate roughly twice the internal energy at the second-order transition, which becomes maximal at the critical μ^* [18]. [This argument is not affected by the higher-gradient interactions (43) since those share the symmetries of the leading term (42).]

Our program for the following subsections will be as follows: after determining the energy minimum at the boundary of the disordered phase quantitatively (Sec. VIII A), we evaluate the associated, four-dimensional gluon condensate in Sec. VIII B. The resulting vacuum-field distribution and its physical interpretation are discussed in Sec. VIII C, and its impact on the phase structure of the soft-mode dynamics is subject of Sec. VIII D. In Sec. VIII E we comment on the qualitative role of the higher-gradient interactions in the soft-mode Lagrangian (43). Finally, in Sec. VIII F, we mention several options for improvements and future applications of the gauge-invariant variational framework.

A. Vacuum energy minimization

In Fig. 4 the energy density (159) of the disordered vacuum phase (calculated on the basis of the numerical solution of the gap equation, cf. Fig. 3) is plotted as a function of μ and c_1. The plot range of μ includes those regions in which (i) the one-loop evaluation of the hard-mode contributions remains reasonably accurate (corresponding roughly to $\mu \geq 4\Lambda_{\rm YM}$), (ii) the system stays in the disordered phase where the nontrivial solution $\bar{\xi}$ of the gap equation exists, and (iii) the mean-field approximation remains approximately valid. Together with Eq. (127) these conditions require

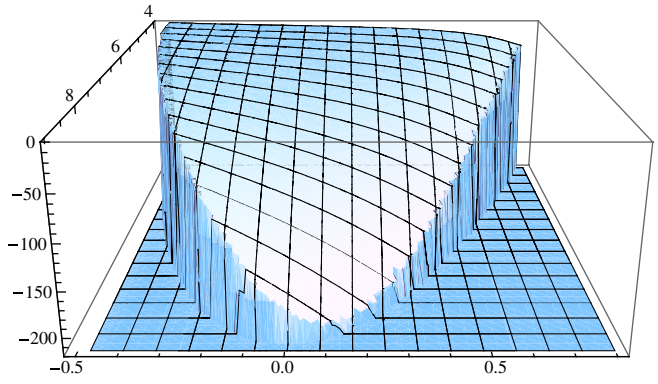

FIG. 4 (color online). The energy density $\bar{\varepsilon}(\mu, c_1)$ of the vacuum-field solution $\bar{\xi}(\mu, c_1)$ in the parameter ranges $\mu \in \{4, 9\}\Lambda_{\rm YM}$ and $c_1 \in \{-0.5, 0.8\}$. Note the minimum of the energy surface at $c_1 \simeq 0.15$.

$$4\Lambda_{\rm YM} \lesssim \mu \lesssim 8.86\Lambda_{\rm YM}. \tag{176}$$

For illustrative purposes the plot range of c_1 is chosen to cover almost the full existence range $-0.48 \lesssim c_1 \lesssim 0.95$ of gap-equation solutions, on the other hand, although our perturbative treatment of the $4U$ interactions becomes questionable close to the upper limit.

The arguably most prominent qualitative feature of the vacuum energy density $\bar{\varepsilon}\,(\mu, c_1)$ in the disordered phase is its monotonic decrease with both μ and c_1 which continues until the nontrivial solution of the gap equation ceases to exist at the second-order phase transition (cf. Fig. 4). This essential feature manifests itself already in the linearization (160) of the c_1 dependence around $c_1 = 0$. As a consequence, the energy of the disordered vacuum is minimized at $\bar{\xi} = 0_+$, i.e., at the disorder-order phase transition, for each admissible value of c_1. In order to find the precise minimum of $\bar{\varepsilon}$ and the corresponding parameter values μ^* and c_1^*, we plot the energy density along the critical line, i.e.,

$$\bar{\varepsilon}(c_1) := \bar{\varepsilon}(\mu_c(c_1), c_1), \tag{177}$$

in the range $c_1 \in [-0.48, 1]$ where $\bar{\xi}(\mu_c(c_1), c_1) = 0$. As can be read off from Fig. 5, the minimum of $\bar{\varepsilon}(c_1)$ is attained at

$$c_1^* \simeq 0.15 \quad \text{with} \quad \mu^* = \mu(c_1^*) = 8.61\Lambda_{\rm YM}. \tag{178}$$

Evaluating $\alpha_{\rm YM}(\mu^*) = g_{\rm YM}^2(\mu^*)/(4\pi) \simeq 0.27$ (to one-loop) at this scale confirms that the running coupling remains small enough to justify the perturbative treatment of the hard modes. [It exceeds $\alpha_{\rm YM}(\mu(c_1 = 0)) \simeq 0.26$ by less than 2%.] Similarly, the resulting $c_1^* \ll 1$ justifies our perturbative treatment of the $4U$ contributions. In addition, the rather small curvature of the critical line (126) around its maximum

$$\mu^{(\max)} = \mu(c_1 = 0) = \exp\left(\frac{24}{11}\right) \simeq 8.86\Lambda_{\rm YM} \tag{179}$$

at $c_1 = 0$ causes our dynamical IR mass scale $\mu^* \simeq 8.6\Lambda_{\rm YM}$ to be only about 3% smaller than $\mu^{(\max)}$. This

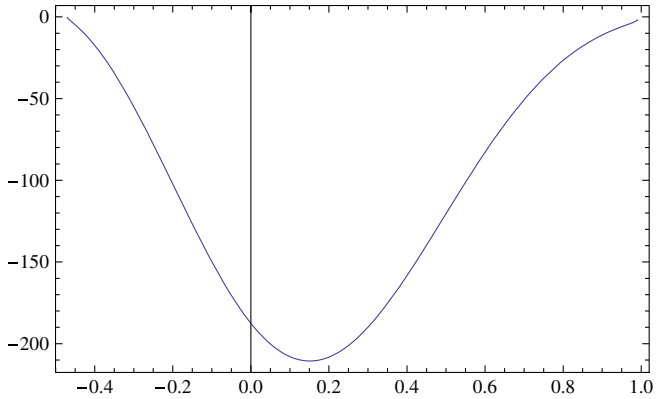

FIG. 5 (color online). The energy density $\bar{\varepsilon}(c_1) \equiv \bar{\varepsilon}(\mu_c(c_1), c_1)$ at the phase transition point μ_c in units of $\Lambda_{\rm YM}$.

has important consequences for the value of the gluon condensate to be discussed in Sec. VIII B and for other vacuum scales. The corresponding IR gluon mass, e.g., turns out to be

$$m_g^* = \frac{\mu(c_1^*)}{1 - c_1^*} \simeq 10.14\Lambda_{\mathrm{YM}}. \tag{180}$$

(For $\Lambda_{\mathrm{YM}} \simeq 0.15$ GeV [18] this value is somewhat larger than the potentially related mass $m_{\mathrm{LG}} \sim 1.1$ GeV extracted from the intermediate-momentum behavior of the Landau-gauge gluon propagator on the lattice (second reference of [41].)

The quantitative improvement of the vacuum description due to our generalized trial-functional basis can be measured in terms of the achieved variational bound on the Yang-Mills vacuum energy density. Comparing the minimum of our trial energy density (159),

$$\bar{\varepsilon}(c_1^*) \simeq -210.59\Lambda_{\mathrm{YM}}^4, \tag{181}$$

to the value $\bar{\varepsilon}(c_1 = 0) \simeq -187.52\Lambda_{\mathrm{YM}}^4$ generated by the lowest-order covariance $G_<^{-1}(k) = \mu$ shows that the c_1 corrections reduce the vacuum energy density by about 11%. Hence, variational optimization in our extended trial space has produced a rather substantial improvement of the vacuum functional. [The massive gluon propagator (24), on the other hand, is energetically disfavored: its IR behavior is approximately reproduced by $c_1 = -1/2$ and yields $\bar{\varepsilon}(c_1 = -1/2) \simeq 0$. We expect sizeable corrections to the $O(c_1)$ treatment of the $4U$ interactions for $c_1 = -1/2$, though, and further note that Eq. (24) does not match to the UV covariance (11) at $k = \mu$, in contrast to our IR covariance.]

B. Gluon condensate

Gluon condensates, i.e., the vacuum expectation values of gauge-invariant local operators composed of gluon fields, are among the key amplitudes which characterize the Yang-Mills ground state. The most important gluon condensate, which dominates the power corrections in the operator product expansion, e.g., of the glueball correlators [57], is the expectation value of the lowest-, i.e., four-dimensional gluonic operator $F^2 \equiv F^a_{\mu\nu}F^{a,\mu\nu} = -2(E^a_i E^a_i - B^a_i B^a_i)$. In our trial state, and to lowest order in the gauge coupling, this condensate becomes

$$\langle F^2 \rangle = 2[\langle B^2 \rangle - \langle E^2 \rangle], \tag{182}$$

$$= 2(N_c^2 - 1)\int \frac{d^3k}{(2\pi)^3}\theta(k^2 - \Lambda_{\mathrm{UV}}^2)\left[k^2 G(k) - \frac{3}{2}G^{-1}(k)\right] + (N_c^2 - 1)\int \frac{d^3k}{(2\pi)^3}[\theta(k^2 - \Lambda_{\mathrm{UV}}^2) - \theta(k^2 - \mu^2)] \times G^{-1}(k) - 2\langle E^2 \rangle_{U_<}, \tag{183}$$

where we used Eqs. (137)–(139) and again performed the Σ integrals in the saddle-point approximation. As anticipated above, the hard-mode (i.e., $k > \mu$) contributions to the chromo-electric and -magnetic parts cancel, which indicates that the gluon condensate (183) is renormalized at μ. After inserting the IR covariance (20) and the propagator (21) [with $c_{n\geq 2} = 0$, as before] the condensate becomes

$$\langle F^2 \rangle = 2(N_c^2 - 1)\int \frac{d^3k}{(2\pi)^3}\theta(k^2 - \mu^2) \times \left[k^2 G_<(k) - \frac{3}{2}G_<^{-1}(k)\right] - 2\langle E^2 \rangle_{U_<}, \tag{184}$$

$$= -\frac{N_c^2 - 1}{\pi^2}\frac{\mu^4}{\zeta c_1^2}\left[1 + \frac{c_1}{3} + \frac{1}{2}\zeta^2 c_1^2\left(1 - \frac{3}{5}c_1\right) - \frac{\operatorname{arctanh}\sqrt{c_1}}{\sqrt{c_1}}\right] - 2\langle E^2 \rangle_{U_<}. \tag{185}$$

At the border of the disordered phase, where $\bar{\xi}(\mu_c(c_1), c_1) = 0$ and where the energy becomes minimal (cf. Sec. VIII A), we furthermore have from the $\xi \to 0$ limit of Eq. (149) and the expressions for the integrals $\tilde{\imath}_n(0, c_1)$ and $\tilde{\jmath}_n(0, c_1)$ given in Appendix B 2 that

$$\langle E^2 \rangle_{U_<}(\mu_c(c_1), \bar{\xi}(\mu_c(c_1), c_1) = 0) = -\frac{(N_c^2 - 1)\zeta}{2\pi^2}\mu^4\left[\frac{1}{3} - \frac{c_1}{5} - \frac{2\gamma}{3\zeta}\left(1 - \frac{\operatorname{arctanh}\sqrt{c_1}}{\sqrt{c_1}}\right)\right]. \tag{186}$$

Combining the above results and specializing as before to $\zeta_{\mathrm{ct}} = (1 - c_1)^{-1}$ then results in our final expression

$$\langle F^2 \rangle = -\frac{N_c^2 - 1}{\pi^2}\mu^4\left[\frac{7c_1^3 - 20\gamma^* c_1^3 + 15c_1^2 + 20\gamma^* c_1^2 - 50c_1 + 30}{30c_1^2(1 - c_1)} - \left(\frac{1 - c_1}{c_1^2} + \frac{2\gamma^*}{3}\right)\frac{\operatorname{arctanh}\sqrt{c_1}}{\sqrt{c_1}}\right] \tag{187}$$

[$\gamma^* = g^2(\mu^*)N_c/\pi^2 \simeq 1.012$] for the gluon condensate. For small c_1 Eq. (187) expands into powers of c_1 as

$$\langle F^2 \rangle = \frac{N_c^2 - 1}{\pi^2}\mu^4\left[\frac{1}{30} - \left(\frac{13}{105} - \frac{2}{9}\gamma^*\right)c_1 + O(c_1^2)\right], \tag{188}$$

which shows that $\langle F^2 \rangle$ grows with c_1 when $c_1 \ll 1$. In the uncorrected case, with $c_1 = 0$ and the corresponding value $\alpha_{\mathrm{YM}}(\mu_c(c_1 = 0))/\pi = 1/(4N_c)$ or $\gamma^*(\mu_c(c_c = 0)) = 1$ [cf. Eq. (101)] for the gauge coupling as well as Eq. (179) for the IR scale, and furthermore setting $N_c^2 - 1 \sim N_c^2$, $N_c = 3$, one finds [18]

$$\left\langle \frac{\alpha}{\pi} F^2 \right\rangle^{(\mathrm{KK})} = \frac{N_c}{120\pi^2}\mu_c^4(c_c = 0) \simeq 15.62\Lambda_{\mathrm{YM}}^4. \quad (189)$$

Our improved value of the gluon condensate, on the other hand, is obtained by inserting the energy minimizing values $c_1^* \simeq 0.151$ and $\mu^* = 8.606\Lambda_{\mathrm{YM}}$ from the last section and the corresponding coupling $\gamma^* \simeq 1.012$. The result

$$\left\langle \frac{\alpha}{\pi} F^2 \right\rangle = 20.87\Lambda_{\mathrm{YM}}^4 \simeq 0.011\ \mathrm{GeV}^4 \quad (190)$$

is about 25% larger than the uncorrected value (189). In the second equation above we have specialized to $\Lambda_{\mathrm{YM}} \simeq 0.15$ GeV, which allows for comparison with the value range $\langle(\alpha/\pi)F^2\rangle = 0.0080 - 0.024\ \mathrm{GeV}^4$ obtained from QCD sum rules (for references see, e.g., Ref. [57]). (We refrain from using the currently preferred value for Λ_{QCD} which contains quark contributions.) Our condensate value prediction (190) lies comfortably within this standard range.

C. Vacuum-field distribution and quasigluon velocity

Our variationally optimized wave functional determines the distribution of the gauge-field modes $A_i(k)$ and thus contains new information about the field composition in the vacuum state. In our approximation, the IR covariance (20) with $c_{n\geq 2} = 0$ and Eq. (23) takes the form

$$G_<^{-1}(k) = \frac{\mu}{1 - c_1}\left(1 - c_1\frac{k^2}{\mu^2}\right)\theta(\mu^2 - k^2). \quad (191)$$

By construction, the covariance (191) is non-negative in the physical parameter range $\mu > 0$, $c_1 < 1$ and thus yields a normalizable wave functional. In addition, $G_<^{-1}(k)$ becomes larger (smaller) for positive (negative) values of c_1. This holds for each $k < \mu$ independently, but gets more pronounced for smaller k (cf. Fig. 1). Hence, the Gaussian weight factors

$$\exp[-(2\pi)^{-3}d^3kG_<^{-1}(k)A^2(k)/2], \quad (192)$$

which (when multiplied for all $k < \mu$) make up the IR part (10) of the unprojected core functional, become narrower (wider) in Fourier-mode space [58]. As a consequence, large $A_i^a(k)$ contributions to the IR part (10) of the unnormalized Gaussian vacuum functional, and thus to the functional integrands of any amplitude, are increasingly suppressed (enhanced) toward smaller $k \in [0, \mu]$.

Hence, our positive result $c_1^* = 0.15$ reshapes the vacuum-field population in a specific way: relative to the uncorrected case $c_1 \equiv 0$ the attractive IR interactions generate a depletion of the ultralong-wavelength $k \to 0$ modes and an enhancement of the $k \sim \mu$ modes. This effect helps to prevent the Savvidy instability which constant chromomagnetic fields experience in the Yang-Mills vacuum [59]. It also contributes to generating the expected average wavelength

$$\lambda \sim \Lambda_{\mathrm{YM}}^{-1} \quad (193)$$

of the vacuum fields. In contrast, the massive vector covariance (24) with $c_1 = -1/2$ would populate the medium-soft modes with $k \lesssim \mu$ less strongly (cf. Fig. 1) although this is energetically disfavored. (When comparing the overall weight of the $k < \mu$ modes associated with different covariances, the G^{-1} dependent normalization factor $\mathcal{N}_G$ has to be taken into account as well.) Since the higher-derivative soft-mode interactions in Eq. (43) do not affect the $k = 0$ modes, the above findings underline the importance of finite-momentum IR modes in shaping the vacuum structure.

Regarding Eq. (191) as the dispersion relation $\omega(k)$ of "quasigluon" modes in the vacuum, one may further relate the parameter c_1 to the dimensionless quasigluon group velocity

$$\vec{v}(\vec{k}) = \frac{\partial G_<^{-1}(\vec{k})}{\partial \vec{k}} = -2c_1\frac{m_g}{\mu}\frac{\vec{k}}{\mu} \overset{m_g=\mu(1-c_1)^{-1}}{\longrightarrow} -\frac{2c_1}{1-c_1}\frac{\vec{k}}{\mu}. \quad (194)$$

Since our approximate dispersion relation (191) is quadratic in the momentum, one may further define a (momentum-independent) effective kinetic gluon mass

$$\bar{m}_g = -\frac{\mu^2}{2c_1 m_g} = -\frac{1-c_1}{2c_1}\mu, \quad (195)$$

which relates velocity and momentum as $\vec{k} = \bar{m}_g\vec{v}$. Note that $\bar{m}_g$ is negative for $0 > c_1 > 1$. With $v(k) := |\vec{v}(\vec{k})|$ one further has

$$|c_1| = \frac{\mu}{2m_g}v(\mu), \quad (196)$$

which shows that c_1 is related to the quasigluon group velocity at the IR renormalization point $k = \mu$. Specializing to a continuous covariance by identifying $\mu/m_g = 1 - c_1$ then yields

$$|c_1| = \frac{v(\mu)}{v(\mu) + 2}. \quad (197)$$

This relation implies among other things that the velocity diverges toward the bound $c_1 \to 1$, and that the admissible velocity range is restricted to $\infty > v(\mu) = 2|c_1|/(1 - c_1) \geq -2$. Our result $c_1^* = 0.15$ corresponds to $v^* := v(\mu^*) = 0.35$.

The positive sign of c_1^* implies that the effective *kinetic* mass (195) is negative, i.e., that the quasigluon velocity in the vacuum is opposite to its momentum. Hence, these quasigluons decelerate when an external force is applied, in stark contrast to the behavior of free gluons. (An interesting and related issue is the vacuum response to external electric and magnetic background fields, cf., e.g., Ref. [31].) In this respect our IR dispersion relation is reminiscent of optical phonon branches in periodic structures over a Brillouin zone, or of the dispersion of electrons moving in such structures. In the latter example, the effect

is generated by the lattice exerting a large retarding force on the electron that counteracts and overcomes the applied force. Of course, in our aperiodic momentum space no Bloch-type oscillations are generated by external color-electric fields. Nevertheless, quasigluons (with their small scattering amplitudes) or quarks could show a negative differential resistance, in remarkable contrast to the impact of a simple infrared mass term of the type (24). The origin of these effects in the Yang-Mills dynamics should be investigated further. On a cautionary note, however, one has to keep in mind that not all properties of the gauge-*variant* core functional (3) play a physical role (cf. Sec. II B and Ref. [21]).

D. Phase structure and transition order

It is instructive to analyze some additional features of the $c_1 \neq 0$ interactions which have direct impact both on the phase structure of the soft-mode dynamics (42) and (43) and on the vacuum energy minimum. To begin with, we recall that the vacuum instability for $c_1 \geq 1$ is encoded in $c_1 \to 1$ singularities of the energy density and in zeros of the amplitude entering the gap equation. Hence, the constraint $c_1 < 1$ does not have to be imposed by hand but is automatically enforced by the diverging vacuum energy density and by the nontrivial saddle-point solution ceasing to exist. Since the energy density (159) decreases monotonically with μ, furthermore, its variational minimization could drive μ far below the validity range of the perturbative integration over the hard modes (cf. Sec. VII A), were it not stopped at a sufficiently large μ^* by the vanishing of the gap-equation solution $\bar{\xi}(\mu, c_1)$, i.e., by the order-disorder phase transition. This behavior generalizes to the c_1 dependence. Indeed, although the energy density (159) monotonically decreases with c_1 as well (cf. Fig. 4), the eventual vanishing of $\bar{\xi}$ prevents the variational solution to attain c_1 values too close to unity where our $O(c_1)$ treatment of the $4U$ interactions would break down. Hence, the bounded existence range of $\bar{\xi}(\mu, c_1) > 0$ solutions, inside the critical line of Fig. 2, is indispensable both for our approximations to remain valid and for the quantitatively reasonable size prediction of the gluon condensate (190) and other vacuum scales to emerge.

Another issue meriting discussion is the order of the transition between the strongly and weakly coupled vacuum phases. Above we found the (dis)order parameter $\bar{\xi}$ to vanish continuously at the phase boundary, which indicates a second-order transition. The same order was encountered in the Ref. [18], although lattice simulations predict a first-order transition [50]. In Ref. [18] this mismatch was argued to be a shortcoming of the mean-field approximation (which should break down close to the transition). Nevertheless, one may wonder whether the mean-field approximation could generate a first-order transition when the higher-derivative interactions corresponding to $c_n \neq 0$ are taken into account. One could imagine, for example, that the lowest-energy gap-equation solution $\bar{\xi} > 0$ may cease to exist for increasing μ before reaching zero and/or that a competing solution $\bar{\xi} \simeq 0$ may become energetically favorable before any of them vanishes. This raises the question whether more than one solution of the gap equation (119) could exist. In principle, this is indeed possible. An example can be constructed by treating the dominant $2U$ part of the $c_1 \neq 0$ interactions perturbatively to $O(c_1)$, instead of resumming it as we did in Eq. (74). In this case two solution branches of the gap equation would indeed emerge. One of them is not continuous in the $c_1 = 0$ limit, though, and the energy competition with the other one turns out to be unable to generate a first-order transition. In our case such scenarios are excluded from the outset, furthermore, since the nontrivial solution of our gap equation is unique.

E. Impact of the higher-gradient corrections

From Sec. V onward, we have restricted our practical calculations to contributions from the dominant higher-gradient interactions, associated with the low-momentum coupling c_1. Hence, a few comments on the expected impact of the subleading higher-gradient corrections (governed by the $c_{n\geq 2}$ couplings in the soft-mode Lagrangian (43)) may be useful. All c_n dependence originates from the expansion (13) of the infrared covariance. Through the generating functional (45) it then enters the soft-mode matrix elements [cf., e.g., Eq. (103)] and thereby any amplitude, both in terms of the propagators Δ^{-1} and $\bar{\Delta}^{-1}$ [cf. Eqs. (73) and (100)] and by virtue of the perturbative expansion (58) of the $4U$ contributions. In order to take the contributions from the $2(n+1)$-gradient interactions with $n \geq 2$ into account, one therefore has (i) to include the explicit c_n dependence from Eq. (20) in the expressions for the chromo-electric (137) and -magnetic (139) expectation values, (ii) to continue the expansion of the $4U$ contributions (58) to higher c_n, and (iii) to generalize the integrals (B1) and (B2), which summarize the impact of the c_n contributions on the $2U$ part of the soft-mode amplitudes, to

$$\tilde{\imath}_n(\xi, c_1, c_2, c_{3,\ldots}) := \int_0^1 \frac{\kappa^{2n}}{\kappa^2(1 - c_1\kappa^2 + c_2\kappa^4 - c_3\kappa^6 + \ldots) + \xi^2}\, d\kappa \qquad n \geq 1, \tag{198}$$

$$\tilde{j}_n(\xi, c_1, c_2, c_{3,\ldots}) := \int_0^1 \frac{\kappa^{2n}}{[\kappa^2(1 - c_1\kappa^2 + c_2\kappa^4 - c_3\kappa^6 + \ldots) + \xi^2]^2}\, d\kappa \qquad n \geq 1. \tag{199}$$

[The monotonicity properties of the integrals (198) and (199) are straightforward generalizations of those discussed in Appendix B.]

In Eqs. (198) and (199) the low-momentum constants c_n appear multiplied by $2n$ powers of the dimensionless momentum $\kappa \in [0, 1]$. This provides the basis for a consistent power counting. Indeed, the contributions from larger n are systematically suppressed and at least parametrically dominated by the four-derivative interactions associated with c_1. Since the c_n are furthermore bounded by the normalizability constraints (22) and since our optimal value $c_1^* \simeq 0.15$ keeps already the dominant contribution rather small, one may expect that a variational treatment of the $c_{n\geq 2}$ contributions would result in even substantially smaller corrections. [Vacuum energy, gluon condensate and other matrix elements could therefore be estimated by expanding the integrals (198) and (199) around $c_{n\geq 2} = 0$, incidentally, with the expansion coefficients determined by the integrals given in Appendix B.] With the above considerations in mind, we have not pursued the quantitative evaluation of $c_{n\geq 2}$ contributions in this paper, although our framework is fully equipped to take them into account. Another reason for neglecting these corrections was that their inclusion would reduce the transparency of our explorative study. (The visualization of the vacuum energy density and its minimum in Fig. 4, for instance, is possible only if $c_{n\geq 2} = 0$.)

F. Further physical implications and applications

We conclude our analysis by briefly reviewing several additional features of the resulting vacuum description. To begin with the UV physics, we note that the one-loop Yang-Mills β function can be recovered almost completely from the dynamics implemented in the UV covariance (11) [up to a missing 6% correction due to color screening [42]]. As already mentioned, the screening contribution may be accounted for as well, e.g., by generalizing the tensor structure of the UV covariance [19]. [We note in passing that Rayleigh-Schrödinger perturbation theory, even to higher orders of the gauge coupling, could be set up directly in our wave-functional basis (1) since it renders Gauss' law manifest.]

Turning to the IR physics content, we start by emphasizing that dimensional transmutation emerges naturally from gauge-invariant wave functionals (1) with Gaussian cores (3), and that it generates the infrared mass scale and the crucial mass gap dynamically. Since a Gaussian becomes the exact ground state of both massless and *massive* vector fields in the noninteracting limit, furthermore, one may expect it to yield an adequate description whenever the main net effect of the interactions is to create a quasiparticle-like self-energy. Similarly, it was argued in Ref. [18] that the Gaussian approximation should provide a reasonable description of Yang-Mills vacuum physics as long as the latter is dominated by a single gluon condensate (which QCD sum-rule analyses suggest especially in the glueball sector [57,60]).

An important advantage of the gauge-projected wave functionals (1) is that they incorporate the nontrivial topology of the gauge group and thereby of the gauge fields. In particular, they contain instanton effects [23,24] which play an especially important role in the spin-0 glueball sector [43,57,61] and emerge even in basic holographic duals for Yang-Mills theory [62]. Furthermore, the functional (1) comprises large classes of additional, gauge-invariant IR degrees of freedom which are often of topological origin as well [23]. Those are typically collective excitations gathered by gauge orbits of vacuum fields which were found to dominate the saddle-point expansion of the generating soft-mode functional (45) and to provide gauge-invariant physical interpretations, e.g., for merons and Faddeev-Niemi knots [23,25].

Another crucial consequence of the infrared fields populating the Yang-Mills vacuum, confinement, is characterized by the emergence of a linear potential between sufficiently far separated, static quark sources. Despite the rather direct access to the interquark potential provided in the Schrödinger representation [19,21] and heuristic arguments given in Refs. [18,19,21], however, it remains to be shown that gauge-averaged wave functionals (1) with a Gaussian core of the type (3) are capable of generating the confinement-induced area law for large, spacelike Wilson loops. Several cautionary lessons from three-dimensional, compact electrodynamics can be found in Ref. [22]. (The behavior of the adjoint Wilson loop would be of interest as well.) Explorations of confinement in Coulomb gauge encouragingly found a Gaussian wave functional, divided by the square root of the Faddeev-Popov determinant, to generate a linear heavy-quark potential [63].

In this context, one should further emphasize that confinement (as well as other crucial vacuum features) is expected to emerge in our framework only after gauge projection. In fact, Feynman had argued almost three decades ago [4] that for a mass gap to be generated in a non-Abelian gauge theory, all field configurations with nonvanishing support at "large" A should either be gauge equivalent to others with support only at "small" A or damped by their magnetic field energy. This argument is suggestive because then, in analogy with finite-dimensional quantum mechanics, the wave functionals of the ground and first-excited states cannot arbitrarily reduce their energy difference by favoring long-wavelength potentials A extending over all of space. As a consequence, the energy or (in the static case) mass gap cannot be closed. It would be important to check whether a gauge-projected Gaussian wave functional can realize this mechanism.

In order to simplify the analysis and to focus on the still rather poorly understood infrared gluon sector of QCD, we

have restricted our investigation to pure Yang-Mills theory without quarks. As the quenched approximation to lattice QCD, this provides stable and unmixed glueball states which set a benchmark for sorting out the QCD glueball spectrum. (For a first attempt to study glueball states on the basis of a gauge-invariant vacuum wave functional see Ref. [64].) However, static quark sources could be straightforwardly implemented into the gauge-invariant vacuum functional [21,22] and even the inclusion of light, dynamical quarks adds no conceptual problems, although a nonperturbative treatment of their interactions with the gluon sector appears challenging. (For a variational study of fermions in the $1+1$-dimensional Abelian Schwinger model see Ref. [65].)

We close this section by briefly discussing the improvement potential of our approach and by mentioning a few additional applications. The $O(g)$ treatment of the energy density and the $O(c_1)$ treatment of the $4U$ interactions could be systematically refined. In addition, one may evaluate the corrections due to higher-gradient contributions with couplings $c_{n\geq 2}$ in the effective soft-mode action (43). For the gauge group SU(2), the mean-field analysis of the integral over the auxiliary field Σ could alternatively be performed in quaternionic variables, as suggested in Ref. [19]. If this formulation could be generalized to higher N_c, it would keep the fluctuations around the mean field under control, and the corresponding saddle-point approximation may in fact become exact in the large-N_c limit [53]. One could further generalize the trial-functional basis by including both longitudinal and transverse mode contributions (potentially nonanalytic) to the covariance, or even allow for a nondiagonal color structure. Finally, one may consider to solve the nonlinear soft-mode dynamics (41) and its phase structure exactly on a lattice.

A particularly interesting class of Yang-Mills amplitudes are (equal-time) glueball correlation functions. They contain information on the whole spectrum and the decay constants of glueballs which was first explored variationally in Ref. [64] and is accessible in our framework as well. It could, e.g., be analyzed by comparison with results from lattice simulations [66], the operator product expansion [57,60] and holographic strong-coupling duals [62]. The pseudoscalar glueball correlator contains the topological susceptibility (in the zero-momentum limit), furthermore, whose evaluation would complement the analysis of the topological vacuum structure mentioned above. Another interesting type of amplitude which may become at least approximately accessible are the Bethe-Salpeter amplitudes of glueballs for which, e.g., lattice [66] and instanton liquid model [61] results are available. A further natural and interesting extension of our analysis would be its generalization to finite temperature, as pioneered in Ref. [67] for the minimal trial-functional family of Ref. [18]. This would open up several important applications, including the study of the deconfinement phase transition [68] as well as of properties of the currently intensely debated and potentially strongly coupled gluon plasma at temperatures of up to 2–3 times the critical temperature [69]. In the longer run, the potential of our Minkowski space formulation to describe quantum nonequilibrium physics should be exploited, too, e.g., by applying it to currently much discussed nonequilibrium processes in the early Universe as well as in the aftermath of ultrahigh-energy nuclear collisions (for a brief introduction see Sec. V of Ref. [10]). Hopefully, some of the above applications may also provide guidance for how to improve the Gaussian approximation (3) to the core wave functional.

IX. SUMMARY AND CONCLUSIONS

We have implemented and studied a gauge-invariant variational approximation scheme for the Yang-Mills vacuum wave functional. Our approach is based on minimizing the Yang-Mills Hamiltonian in a gauge-projected Gaussian trial-functional space that allows for an essentially general momentum distribution of the soft vacuum fields. This amounts to a substantial improvement upon previously used trial states which populated all infrared modes with identical, i.e., momentum-independent strength. Our extension of the trial basis rests on a controlled expansion of the infrared-mode dispersion relation (or covariance), which characterizes the vacuum wave functional, into powers of the soft momenta divided by the dynamically generated mass scale. The momentum dependence can then be systematically approximated by truncating the series, which allows us to restrict the quantitative part of our study to the leading-order corrections. After complementing the generalized soft vacuum-mode population by the leading perturbative ultraviolet modes, finally, one ends up with the largest gauge-invariant trial space for the Yang-Mills vacuum wave functional (in $3+1$ dimensions) which is currently available and which keeps the variational analysis analytically manageable.

The multifaceted vacuum physics emerging from energy minimization in this extended trial space turns out to be partly shaped by a subtle interplay between different parts of the dynamics. To begin with, the leading-order momentum distribution of the infrared modes is characterized by just one variational parameter. After translating the dynamical content of the wave functional into an effective Lagrangian for collective sets of soft gauge-field orbits, this parameter reappears as the coupling constant of the dominant higher-gradient interactions which modify the low-momentum dispersion of the vacuum modes. Moreover, it acquires an intuitive physical interpretation in terms of the group velocity of gauge-field quasiparticles in the vacuum. While this velocity vanishes in the unimproved ground state, one of our main findings is that it becomes finite in the improved one. The novel dispersion relation further reveals that the infrared quasigluons in the

vacuum decelerate when a force is applied to them. In other words, their ''effective kinetic mass'' is negative (analogous situations are encountered in several condensed matter systems) and their color conductivity can increase with increasing strength of an external color-electric field, implying a negative differential resistance of the vacuum.

The variationally optimized value of the higher-gradient coupling turns out to be positive. This sign may at first appear surprising since it is opposite to the one induced by the massive vector propagator which was previously adopted as a model for the infrared covariance. Its physical impact is quite intuitive, however, since it implies that soft gauge-field modes with larger momenta populate the vacuum more strongly than their longest-wavelength counterparts. Vacuum fields with constant color-magnetic field strength are thus energetically disfavored, in particular, which prevents the onset of the Savvidy instability. An energy barrier against larger quasigluon velocities preserves the normalizability of the vacuum wave functional and keeps the variationally determined value of the quasigluon velocity small. In addition, it implies the existence of a saddle-point solution for the disorder-parameter field at a dynamically generated mass scale which is consistent with lattice results for the Yang-Mills scale. (As a practical side benefit, the relatively small optimized coupling-parameter value also justifies a leading-order perturbative treatment of the four-soft-mode interactions.)

Moreover, the above findings indicate that the dimensional transmutation mechanism is an almost quantitatively robust feature of gauge-projected Gaussian core functionals (instead of emerging accidentally from an oversimplified trial space). As a consequence of this rather nontrivial result the lowest-dimensional gluon condensate, which scales with the fourth power of the dynamically generated infrared mass scale, acquires a magnitude well inside the range predicted by other sources. This observation further supports the conjecture that Gaussian trial functionals provide a reasonable vacuum description in dynamical situations where just one vacuum condensate dominates. While this holds, e.g., for the Cooper-pair condensate in the BCS theory of superconductivity, it is less well established in Yang-Mills theory where the lowest-dimensional gluon condensate provides the natural candidate. The main reasons for the robustness of the vacuum scales turn out to be that the nontrivial solution of the gap equation is unique and that the disordered vacuum phase exists only in a limited domain of all variational parameters. Even the soft-mode dynamics' order-disorder phase transition, where the vacuum energy attains its minimum, remains squarely of second order. This is in contrast to the first order predicted by lattice simulations and probably a shortcoming of the employed mean-field approximation near the transition. In any case, the improved dispersion generates a considerably larger attraction among the variationally optimized vacuum fields and lowers the vacuum energy density by more than 10%. This indicates that the nonvanishing quasigluon velocity provides a rather substantial overall improvement of the vacuum description.

Nevertheless, the gauge-invariant variational framework remains analytically tractable, the computational costs are comparable to those of fully gauge-fixed approaches, and the rather high degree of transparency owed to the explicit representation of the vacuum state is maintained. In combination, these qualities suggest considerable further potential of our approach as an intuitive theoretical laboratory for gaining insights into the nonperturbative real-time physics of Yang-Mills theories. The established framework provides, in particular, a privileged testing ground for the impact of topological vacuum excitations and their relation to the gauge symmetry. Indeed, both aspects are manifest in our effective soft-mode dynamics and should be explored further. In addition, our approach seems well suited to chart the maximal physics content which gauge-projected Gaussian core functionals can accommodate. In the longer run, this would allow to clarify the principal limitations of the Gaussian approximation and may help to trigger new ideas for going beyond it in a both systematic and analytically manageable way.

ACKNOWLEDGMENTS

The author would like to thank D. Ebert for a careful reading of the manuscript. Financial support from the Fundação de Amparo à Pesquisa do Estado de São Paulo (FAPESP) and from the Deutsche Forschungsgemeinschaft (DFG), as well as the hospitality of the Abdus Salam International Centre for Theoretical Physics (ICTP) in Trieste, Italy, are gratefully acknowledged.

APPENDIX A: EVALUATION OF VACUUM EXPECTATION VALUES

In the following appendix we review the general approach to calculating vacuum matrix elements in gauge-projected trial functionals of the type (1), following Ref. [18]. We recast this framework into the language of generating functionals and also derive several expressions which will be needed in the main text.

To begin with, consider local gauge-invariant operators $\mathcal{O}(A, E)$ composed of static gauge fields $A_i^a(\vec{x})$ and their canonically conjugate momenta $-E_i^a(\vec{x})$ (where E is the chromo-electric field) in the Hamiltonian formulation of SU(N_c) Yang-Mills theory, adopting temporal (or Weyl) gauge. In the Schrödinger coordinate representation, the canonical commutation relation $[E_i^a(\vec{x}), A_j^b(\vec{y})] = i\delta^{ab}\delta_{ij}\delta^3(\vec{x}-\vec{y})$ then implies that $E_i^a(\vec{x}) = i\delta/\delta A_i^a(\vec{x})$. Our aim is to calculate the (trial) vacuum expectation value of $\mathcal{O}$, i.e., the matrix element

$$\langle \mathcal{O}(A,E)\rangle = \frac{\int D\vec{A}\,\Psi_0^*[\vec{A}]\mathcal{O}(\vec{A}^a, \frac{i\delta}{\delta\vec{A}^a})\Psi_0[\vec{A}]}{\int D\vec{A}\,\Psi_0^*[\vec{A}]\Psi_0[\vec{A}]}, \tag{A1}$$

where the unrestricted linear measure $D\vec{A}$ comprises all gauge orbits and topological charges. (Recall that Gauss' law is enforced as a constraint on the physical states and, in particular, on the vacuum wave functional Ψ_0, cf. Sec. II A.)

1. Exact integration over the gauge field

After inserting the (residual) gauge-invariant, unnormalized wave functional (1) into Eq. (A1) [and interchanging the order of the A, $\bar{U}$ and $\tilde{U}$ integrations], the matrix element becomes

$$\langle \mathcal{O}(A,E)\rangle = \frac{\int D\bar{U}\int D\tilde{U}\int D\vec{A}\,\psi_0[\vec{A}^{\bar{U}}]\mathcal{O}(\vec{A}^a, \frac{i\delta}{\delta\vec{A}^a})\psi_0[\vec{A}^{\tilde{U}}]}{\int D\bar{U}\int D\tilde{U}\int D\vec{A}\,\psi_0[\vec{A}^{\bar{U}}]\psi_0[\vec{A}^{\tilde{U}}]}. \tag{A2}$$

Since $\mathcal{O}$ is gauge invariant, the integrand in the numerator can only depend on the relative transformation $U := \tilde{U}^{-1}\bar{U}$. Indeed, after changing the integration variable $A \to A' = A^{\bar{U}}$ (for fixed $\tilde{U}$), one has

$$\int D\vec{A}\,\psi_0[\vec{A}^{\bar{U}}]\mathcal{O}\left(\vec{A}, \frac{i\delta}{\delta\vec{A}}\right)\psi_0[\vec{A}^{\tilde{U}}] = \int D\vec{A}'\,\psi_0[A'^{\bar{U}^{-1}\bar{U}}]\mathcal{O}\left(\vec{A}', \frac{i\delta}{\delta\vec{A}'}\right)\psi_0[A'] \tag{A3}$$

and the analogous expression for the denominator. Making use of $\mathcal{O}(A) = \mathcal{O}(A')$ and $DA = DA'$, renaming A' to A and employing the translational invariance $D\bar{U} = DU$ of the Haar measure then yields

$$\int D\bar{U}\int D\vec{A}\,\psi_0[\vec{A}^{\bar{U}}]\mathcal{O}\left(\vec{A}, \frac{i\delta}{\delta\vec{A}}\right)\psi_0[\vec{A}^{\tilde{U}}] = \int DU\int D\vec{A}\,\psi_0[\vec{A}^{U}]\mathcal{O}\left(\vec{A}, \frac{i\delta}{\delta\vec{A}}\right)\psi_0[\vec{A}] \tag{A4}$$

(and the analogous expression for the denominator) which does not depend on $\tilde{U}$ since the latter was absorbed into the integration variable A. Hence, the factored (infinite) gauge-group volumes $\int D\tilde{U}$ in numerator and denominator cancel, leaving us with

$$\langle \mathcal{O}(A,E)\rangle = \frac{\int DU\int D\vec{A}\,\psi_0[\vec{A}^{U}]\mathcal{O}(\vec{A}^a, \frac{i\delta}{\delta\vec{A}^a})\psi_0[\vec{A}]}{\int DU\int D\vec{A}\,\psi_0[\vec{A}^{U}]\psi_0[\vec{A}]}. \tag{A5}$$

Now it is useful to define an effective bare action $\Gamma_b[U]$ and the associated nonlocal gauge-field correlators as

$$\exp\{-\Gamma_b[U]\} := \int D\vec{A}\,\psi_0[\vec{A}^{U}]\psi_0[\vec{A}] =: \int D\vec{A}e^{-\gamma[A,U]}, \tag{A6}$$

$$\langle\langle\langle \vec{A}\ldots\vec{A}\ldots\vec{E}\ldots\vec{E}\rangle\rangle\rangle\exp\{-\Gamma_b[U]\} := \int D\vec{A}\,\psi_0[\vec{A}^{U}]\vec{A}\ldots\vec{A}\ldots\frac{i\delta}{\delta\vec{A}}\ldots\frac{i\delta}{\delta\vec{A}}\,\psi_0[\vec{A}], \tag{A7}$$

where the triple bracket $\langle\langle\langle\ldots\rangle\rangle\rangle$ denotes (nondiagonal) matrix elements between U-rotated and unrotated core-functional states. [Note the symmetry $\Gamma_b[U] = \Gamma_b[g_L^\dagger U g_R]$ with $g_{L,R} \in \mathrm{SU}(N_c)$ which originates from the translational invariance of the two group integrations in Eq. (A2).] With the relation

$$\mathcal{O}\left(\vec{A}^a, \frac{i\delta}{\delta\vec{A}^a(\vec{x})}\right)\psi_0[\vec{A}] \equiv \bar{\mathcal{O}}[A]\psi_0[\vec{A}], \tag{A8}$$

which replaces the (quasi-) local, differential operator $\mathcal{O}$ by a nonlocal functional $\bar{\mathcal{O}}$ of the A fields only, one then arrives at

$$\langle \mathcal{O}(A,E)\rangle = \frac{\int DU\int D\vec{A}\,\psi_0[\vec{A}^{U}]\bar{\mathcal{O}}[A]\psi_0[\vec{A}]}{\int DU\int D\vec{A}\,\psi_0[\vec{A}^{U}]\psi_0[\vec{A}]} = \frac{\int DU\langle\langle\langle \mathcal{O}(A,E)\rangle\rangle\rangle\exp\{-\Gamma_b[U]\}}{\int DU\exp\{-\Gamma_b[U]\}}. \tag{A9}$$

Hence, the calculation of the matrix element is reduced to evaluating the vacuum expectation value of the expressions (A7), specialized to contain A fields only, in the U field dynamics determined by Γ_b.

Owing to the Gaussian nature of the wave functional (3), the effective bare action defined in Eq. (A6) and hence the matrix elements (A7) can be calculated exactly. In order to render the U dependence explicit, we write

$$\gamma[A,U] := -\ln\psi_0^*[\vec{A}^{U}]\psi_0[\vec{A}] = \tfrac{1}{2}[(A^U)^T G^{-1}A^U + A^T G^{-1}A] \tag{A10}$$

(in a triple matrix notation for the color, vector and spacial "indices"), where the rotated gauge field

$$(\vec{A}^U)^a = S^{ab}(\vec{x})\vec{A}^b + g^{-1}\vec{L}^a(\vec{x}) \tag{A11}$$

is expressed in terms of the homogeneous and inhomogeneous transformation functions

$$S^{ab}(\vec{x}) = \tfrac{1}{2}\mathrm{tr}\{\lambda^a U^\dagger(\vec{x})\lambda^b U(\vec{x})\}, \qquad \vec{L}^a(\vec{x}) = i\,\mathrm{tr}\{\lambda^a U^\dagger(\vec{x})\vec{\partial}U(\vec{x})\}. \tag{A12}$$

After inserting the representation (A11) into Eq. (A10), one finds that γ contains an A independent piece and a term which is bilinear in A,

$$\gamma[A,U] = \frac{1}{2}(A+a)^T\mathcal{M}(A+a) + \frac{1}{2g_b^2}L^T\mathcal{D}L. \tag{A13}$$

Above we have defined [18]

$$\mathcal{M} := S^T G^{-1}S + G^{-1} = \mathcal{M}^T, \qquad \vec{a} := g^{-1}\mathcal{M}^{-1}S^T G^{-1}\vec{L}, \tag{A14}$$

$$\mathcal{D} := G^{-1} - G^{-1} S \mathcal{M}^{-1} S^T G^{-1} = (G + SGS^{-1})^{-1}. \tag{A15}$$

(G^{-1} and $\mathcal{M}$ are symmetric in a, b, i, j and $\vec{x}$, $\vec{y}$, and transposition of $\vec{a}$ is understood to invert the direction of the derivatives in G^{-1} as well.) After performing the Gaussian integration over A, we arrive at the explicit form

$$\begin{aligned}\Gamma_b[U] &= \int d^3x \int d^3y \mathcal{L}_b(\vec{x}, \vec{y}) \\ &= -\ln \int D\vec{A} \exp\{-\gamma[A, U]\} \\ &= \frac{1}{2} \operatorname{Tr} \ln(\mathcal{M}) + \frac{1}{2g_b^2} L^T \mathcal{D} L \end{aligned} \tag{A16}$$

of the bare action which is a nonlocal, nonlinear σ model. (The regularization by the ultraviolet cutoff Λ_{UV} is implicit in the definition of the wave functional.) This dynamics sums up the self-interaction of the "background" field U which the gauge fields induce through the vector $\vec{a}[U]$ and the propagator $\mathcal{M}^{-1}[U]$. In the following we will omit the first term $\propto \operatorname{Tr} \ln(\mathcal{M})$ in Eq. (A16) since it is of $O(g^2)$ relative to the second one and does not contain U derivatives [18,42].

The connected (equal-time) n-point functions at fixed U,

$$\begin{aligned}&\langle\langle\langle A_{i_1}^{a_1}(\vec{z}_1) A_{i_2}^{a_2}(\vec{z}_2) \ldots A_{i_n}^{a_n}(\vec{z}_n) \rangle\rangle\rangle \\ &= \frac{\int D\vec{A}\, \psi_0[\vec{A}^U] A_{i_1}^{a_1}(\vec{z}_1) A_{i_2}^{a_2}(\vec{z}_2) \ldots A_{i_n}^{a_n}(\vec{z}_n) \psi_0[\vec{A}]}{\int D\vec{A}\, \psi_0[\vec{A}^U] \psi_0[\vec{A}]}, \end{aligned} \tag{A17}$$

specialize the definition (A7) exclusively to A fields and can now be evaluated by means of the generating functional

$$\begin{aligned}&\int D\vec{A}\, \psi_0[\vec{A}^U] \psi_0[\vec{A}] \exp(-\vec{J}\,\vec{A}) \\ &= \int D\vec{A} \exp(-\gamma[\vec{A}, U] - \vec{J}\,\vec{A}), \end{aligned} \tag{A18}$$

$$= \exp(\tfrac{1}{2}\vec{J}\mathcal{M}^{-1}\vec{J} + \vec{J}\,\vec{a}) \exp(-\Gamma_b[U]), \tag{A19}$$

as

$$\begin{aligned}&\langle\langle\langle A_{i_1}^{a_1}(\vec{z}_1) A_{i_2}^{a_2}(\vec{z}_2) \ldots A_{i_n}^{a_n}(\vec{z}_n) \rangle\rangle\rangle \\ &= \frac{(-1)^n \delta^n \exp(\frac{1}{2}\vec{J}\mathcal{M}^{-1}\vec{J} + \vec{J}\,\vec{a})}{\delta J_{i_1}^{a_1}(\vec{z}_1) \ldots \delta J_{i_n}^{a_n}(\vec{z}_n)} \Bigg|_{\vec{J}=0}. \end{aligned} \tag{A20}$$

This expression reproduces the Wick expansion for correlators of a vector field $\vec{A}$ with nontrivial propagator $\mathcal{M}^{-1}$ in the background of the U and $\vec{a}$ fields. [In contrast to free or mean-field correlators, it does not factorize $2n$-point functions into products of n 2-point functions, however, and also generates finite $(2n+1)$-point functions.] Explicit expressions for the 2-, 3-, and 4-point functions needed in the main text are

$$\langle\langle\langle A_{i_1}^{a_1}(\vec{z}_1) A_{i_2}^{a_2}(\vec{z}_2) \rangle\rangle\rangle = \mathcal{M}_{i_1 i_2}^{-1 a_1 a_2}(\vec{z}_1, \vec{z}_2) + a_{i_1}^{a_1}(\vec{z}_1) a_{i_2}^{a_2}(\vec{z}_2) \tag{A21}$$

and (in shorthand notation for arguments and indices)

$$\begin{aligned}\langle\langle\langle A(1)A(2)A(3) \rangle\rangle\rangle = -[&\mathcal{M}^{-1}(2,3)a(1) + \mathcal{M}^{-1}(1,3)a(2) \\ &+ \mathcal{M}^{-1}(1,2)a(3) + a(1)a(2)a(3)], \end{aligned} \tag{A22}$$

as well as

$$\begin{aligned}\langle\langle\langle A(1)A(2)A(3)A(4) \rangle\rangle\rangle = {}& \mathcal{M}^{-1}(1,2)\mathcal{M}^{-1}(3,4) + \mathcal{M}^{-1}(1,3)\mathcal{M}^{-1}(2,4) + \mathcal{M}^{-1}(1,4)\mathcal{M}^{-1}(2,3) + \mathcal{M}^{-1}(1,2)a(3)a(4) \\ &+ \mathcal{M}^{-1}(2,3)a(1)a(4) + \mathcal{M}^{-1}(3,4)a(1)a(2) + \mathcal{M}^{-1}(1,4)a(2)a(3) + \mathcal{M}^{-1}(1,3)a(2)a(4) \\ &+ \mathcal{M}^{-1}(2,4)a(1)a(3) + a(1)a(2)a(3)a(4). \end{aligned} \tag{A23}$$

Hence, the above results reduce the calculation of the matrix element (A2) to integrating over the nonlocally interacting $U(\vec{x})$ fields according to Eq. (A9). This integral will be performed in the next two sections.

2. Perturbative integration over the hard U modes

Since we are interested in amplitudes with soft external momenta $|\vec{p}_i| \ll \mu$ (where μ is a typical hadronic scale, e.g., the lowest glueball mass), the integrations over U in Eq. (A9) can be approximately done in two steps [18]: after integrating out the hard modes $U_>$ (containing momenta $k \geq \mu$) perturbatively, one performs the integral over the remaining soft modes $U_<$ (which contain the momenta $k < \mu$) in the saddle-point approximation. In preparation for this procedure, we factor the integration variable U in a group-structure preserving manner as

$$U(\vec{x}) = U_<(\vec{x}) U_>(\vec{x}), \qquad U_>(\vec{x}) = \exp(-ig\phi^a(\vec{x})\lambda^a/2). \tag{A24}$$

Note that the soft modes vary only weakly over distances $|\vec{x} - \vec{y}| < \mu^{-1}$, i.e., $U_<(\vec{x}) \simeq U_<(\vec{y})$. Since asymptotic freedom is manifest in the high-momentum covariance (11), the bare coupling g_b is small at the large cutoff scale $\Lambda_{\mathrm{UV}} \gg \Lambda_{\mathrm{YM}}$ where the theory is defined. Hence, the hard modes can be integrated perturbatively, e.g., by Wilson's momentum-shell technique [70], down to the infrared scale μ chosen such that the renormalized coupling $g(\mu)$ remains sufficiently small. The functional measure factorizes

according to Eq. (A24) as

$$DU = DU_< DU_> \propto DU_< D\phi^a. \tag{A25}$$

As a consequence, the bare action becomes a functional of the ϕ and $U_<$ fields,

$$\Gamma_b[\phi, U_<] = \Gamma_{b,>}[\phi] + \Gamma_{b,<>}[\phi, U_<] + \Gamma_{b,<}[U_<], \tag{A26}$$

and Eq. (A9) for the matrix element turns into

$$\langle \mathcal{O}(A,E)\rangle = \frac{\int DU_< \int D\phi \langle\langle\langle \mathcal{O}(A,E)\rangle\rangle\rangle \exp\{-\Gamma_b[\phi, U_<]\}}{\int DU_< \int D\phi \exp\{-\Gamma_b[\phi, U_<]\}}. \tag{A27}$$

As long as $g^2(\mu) \ll 1$, the ϕ field can be integrated perturbatively to one-loop in the bare coupling (where the integrals over loop momenta are regularized by the cutoff Λ_{UV}). The result has the form

$$\begin{aligned}&\langle\langle \mathcal{O}(A,E)\rangle\rangle \exp\{-\Gamma_<[U_<]\} \\ &:= \int D\phi \langle\langle\langle \mathcal{O}(A,E)\rangle\rangle\rangle \exp\{-\Gamma_b[\phi, U_<]\},\end{aligned} \tag{A28}$$

where we defined the soft-mode action $\Gamma_<[U_<]$ as

$$\exp\{-\Gamma_<[U_<]\} := \int D\phi \exp\{-\Gamma_b[\phi, U_<]\}, \tag{A29}$$

made use of $\Gamma_{b,<>}[U_<, \phi] = 0$ to leading order in the coupling, and assumed that the (one-loop) anomalous dimension of $\mathcal{O}$ vanishes. [This is appropriate for the conserved Yang-Mills Hamiltonian density (131) which we consider in the bulk of the paper.] The expression (A27) for the matrix element is then further reduced to the soft-mode integral

$$\langle \mathcal{O}(A,E)\rangle = \frac{\int DU_< \langle\langle \mathcal{O}(A,E)\rangle\rangle \exp\{-\Gamma_<[U_<]\}}{\int DU_< \exp\{-\Gamma_<[U_<]\}}. \tag{A30}$$

In order to exhibit the (approximate) $U_<$ dependence of $\Gamma_<[U_<]$ and $\langle\langle \mathcal{O}(A,E)\rangle\rangle$, we now exploit the smallness of the bare coupling to truncate the expansion of $U_>$ in powers of g. Up to corrections of $O(g^3)$ one finds

$$\begin{aligned}U_> &= \exp\left(-ig\phi^a \frac{\lambda^a}{2}\right) \\ &= 1 - ig\phi^a \frac{\lambda^a}{2} - \frac{g^2}{8}(\phi^a \lambda^a)^2 + O(g^3),\end{aligned} \tag{A31}$$

$$\begin{aligned}\lambda^a_{>,i} &= \partial_i \phi^a + O(g^3), \\ S^{ab}_> &= \delta^{ab} + g f^{abc}\phi^c - \frac{g^2}{2} f^{ace} f^{bde} \phi^c \phi^d + O(g^3),\end{aligned} \tag{A32}$$

$$\begin{aligned}\lambda^a_i &= S^{ab}_> \lambda^b_{<,i} + \lambda^a_{>,i} \\ &= \lambda^a_{<,i} + \partial_i \phi^a + g f^{abc} \lambda^b_{<,i} \phi^c \\ &\quad - \frac{g^2}{2} f^{ace} f^{bde} \lambda^b_{<,i} \phi^c \phi^d + O(g^3).\end{aligned} \tag{A33}$$

[Above we have rescaled the Cartan-Maurer form (35) as $\lambda^a_i := L^a_i / g$ in order to facilitate explicit power counting in g. The spacial index should avoid confusion with the SU(N_c) generators.] To the same order, the operator (A15) expands as

$$\begin{aligned}\mathcal{D}^{ab}(\vec{x}, \vec{y}) = \frac{G^{-1}(\vec{x} - \vec{y})}{2} \delta^{ab} \Big\{ 1 + \frac{g^2}{N^2 - 1} [\phi^a(\vec{x})\phi^a(\vec{x}) \\ - 2\phi^a(\vec{x})\phi^a(\vec{y}) + \phi^a(\vec{y})\phi^a(\vec{y})] \Big\} + O(g^3).\end{aligned} \tag{A34}$$

(Note that $\mathcal{D}$ is independent of $U_<$, as a consequence of $S_< G S_<^{-1} \simeq G$ which holds because $S_<$ varies slowly over distances $|\vec{x} - \vec{y}| \lesssim \mu^{-1}$ over which the decaying G remains non-negligible.) Inserting the above expansions into the bare action (A16), one finds the associated Lagrangian

$$\mathcal{L}_b(\vec{x}, \vec{y}) = \mathcal{L}_{b,>}(\vec{x}, \vec{y}) + \mathcal{L}_{b,<}(\vec{x}, \vec{y}) + \mathcal{L}_{b,<>}(\vec{x}, \vec{y}) + O(g^3), \tag{A35}$$

with the bilinear parts

$$\mathcal{L}_{b,>}(\vec{x}, \vec{y}) = \tfrac{1}{4} \partial_i \phi^a(\vec{x}) G^{-1}(\vec{x} - \vec{y}) \partial_i \phi^a(\vec{y}), \tag{A36}$$

$$\mathcal{L}_{b,<}(\vec{x}, \vec{y}) = \tfrac{1}{4} \lambda^a_{<,i}(\vec{x}) G^{-1}(\vec{x} - \vec{y}) \lambda^a_{<,i}(\vec{y}) \tag{A37}$$

and the hard-soft-mode interactions [after using $G^{-1}(\vec{x} - \vec{y}) = G^{-1}(\vec{y} - \vec{x})$ and anticipating the exchange symmetry $\vec{x} \leftrightarrow \vec{y}$ after integration over $\vec{x}$ and $\vec{y}$]

$$\begin{aligned}\mathcal{L}_{b,<>}(\vec{x}, \vec{y}) = \frac{g}{2} f^{abc} \lambda^b_{<,i}(\vec{x}) G^{-1}(\vec{x} - \vec{y}) \phi^c(\vec{x}) \partial_i \phi^a(\vec{y}) \\ + \frac{g^2}{8} \left(\frac{N_c \delta^{ab} \delta^{cd}}{N^2 - 1} - 2 f^{ace} f^{bde} \right) \\ \times \lambda^b_{<,i}(\vec{x}) G^{-1}(\vec{x} - \vec{y}) \lambda^a_{<,i}(\vec{y}) \\ \times [\phi^c(\vec{x})\phi^d(\vec{x}) - \phi^c(\vec{x})\phi^d(\vec{y})].\end{aligned} \tag{A38}$$

(Note that $\mathcal{L}_b$ is invariant under $\phi \to -\phi$.) To leading order in g the hard and soft modes decouple, and the higher-order interactions $\mathcal{L}_{b,<>}$ can be treated perturbatively. [The $O(g)$ term in $\mathcal{L}_{b,<>}$ contributes neither to the β function nor to the soft-mode action.] Writing further

$$\begin{aligned}\Gamma_b[U] = \Gamma_{b,<}[U_<] + \Gamma_{b,>}[\phi] + g\Gamma_1[\phi, U_<] \\ + g^2 \Gamma_2[\phi, U_<] + O(g^3)\end{aligned} \tag{A39}$$

renders the bare-coupling dependence of the action explicit. In terms of the kinetic operator

$$K^{ab}(\vec{x} - \vec{y}) \equiv \tfrac{1}{2} \delta^{ab} [\partial_{yi} \partial_{xi} G^{-1}(\vec{x} - \vec{y})]_{p^2 > \mu^2} \tag{A40}$$

of the Lagrangian (A36), furthermore, the hard-mode action becomes

$$\Gamma_{b,>}[\phi] = \int d^3x \int d^3y \mathcal{L}_{>,b}(\vec{x},\vec{y}) = \frac{1}{2}\int d^3x \int d^3y \phi^a(\vec{x}) K^{ab}(\vec{x}-\vec{y})\phi^b(\vec{y}) + O(g) \tag{A41}$$

$$= \frac{1}{4}\frac{d^3k}{(2\pi)^3}[\theta(\Lambda_{\mathrm{UV}}^2 - k^2) - \theta(\mu^2 - k^2)]\tilde{\phi}^a(\vec{k}) \times G^{-1}(k)k^2\tilde{\phi}^a(-\vec{k}) \tag{A42}$$

from which one reads off the static ϕ^a propagator

$$\langle \phi^a(\vec{x})\phi^b(\vec{y})\rangle \equiv \frac{\int D\phi_{\mu<k<\Lambda_{\mathrm{UV}}} \phi^a(\vec{x})\phi^b(\vec{y})\exp\{-\Gamma_{b,>}[\phi]\}}{\int D\phi \exp\{-\Gamma_{,>}[\phi]\}} = K^{-1ab}(\vec{x}-\vec{y}), \tag{A43}$$

$$= \int \frac{d^3k}{(2\pi)^3}[\theta(\Lambda_{\mathrm{UV}}^2 - k^2) - \theta(\mu^2 - k^2)] \times e^{i\vec{k}(\vec{x}-\vec{y})}\frac{2G_>(k)}{k^2}\delta^{ab}. \tag{A44}$$

The nonstandard kinetic term of the high-momentum σ model (A42) thus generates a propagator with large-k asymptotics $K^{-1}(k) \propto G_>(k)/k^2 \sim 1/k^3$ (instead of the standard $1/k^2$ behavior which impedes perturbative renormalizability in three dimensions). Hence, the high-momentum dynamics (A42) is renormalizable (the tadpole diagram diverges only logarithmically) and asymptotically free, with a perturbative β function very similar to that of Yang-Mills theory [42].

From the definition (A29) and the decomposition (A35) of the bare action one then has

$$\exp\{-\Gamma_<[U_<]\} = \exp\{-\Gamma_{b,<}[U_<]\}\int D\phi \times \exp\{-\Gamma_{b,>}[\phi] - \Gamma_{,<>}[U_<,\phi]\}, \tag{A45}$$

$$= \exp\{-\Gamma_{b,<}[U_<] - \langle\Gamma_{b,<>}[U_<,\phi]\rangle_{\Gamma_{b,>}} + O(g^2)\} \tag{A46}$$

(where the average $\langle\ldots\rangle_{\Gamma_{b,>}}$ over ϕ is weighted by $\exp(-\Gamma_{b,>}[\phi])$) which yields the renormalized soft-mode action

$$\Gamma_<[U_<] = -\Gamma_{b,<}[U_<] - \langle\Gamma_{b,<>}[\phi,U_<]\rangle_{\Gamma_{b,>}} + O(g^2), \tag{A47}$$

$$= \frac{1}{4g^2(\mu)}\int d^3x \int d^3y L^a_{<,i}(\vec{x})G_<^{-1}(\vec{x}-\vec{y})L^a_{<,i}(\vec{y}) + O(g^2). \tag{A48}$$

To the considered order [and for $G_>(k) = k^{-1}$], $\Gamma_<$ has therefore the same form as the bare soft-mode action $\Gamma_{b,<}$, but with the bare coupling replaced by the renormalized one,

$$g(\mu) = g_b + \frac{g_b^3 N_c}{(2\pi)^2}\ln\frac{\Lambda_{\mathrm{UV}}}{\mu} + O(g_b^5), \tag{A49}$$

which was calculated in Ref. [42]. This renormalization of the soft-mode interactions compensates for the removal of the hard $U_>$ modes from amplitudes with external momenta $p^2 \ll \mu^2$. Analogously, the ϕ mode contributions

$$\langle\langle\mathcal{O}(A,E)\rangle\rangle = \frac{\int D\phi\langle\langle\langle\mathcal{O}(A,E)\rangle\rangle\rangle\exp\{-\Gamma_b[U_<,\phi]\}}{\int D\phi\exp\{-\Gamma_b[U_<,\phi]\}} \tag{A50}$$

can be integrated out perturbatively by rewriting

$$\langle\langle\mathcal{O}(A,E)\rangle\rangle = \frac{\exp\{-\Gamma_{b,<}[U_<]\}}{\exp\{-\Gamma_<[U_<]\}}\int D\phi\langle\langle\langle\mathcal{O}(A,E)\rangle\rangle\rangle \times \exp\{-\Gamma_{b,<>}[U_<,\phi]\}\exp\{-\Gamma_{b,>}[\phi]\}, \tag{A51}$$

$$\simeq \frac{\int D\phi\langle\langle\langle\mathcal{O}(A,E)\rangle\rangle\rangle\exp\{-\Gamma_{b,>}[\phi]\}}{\int D\phi\exp\{-\Gamma_{b,>}[\phi]\}}. \tag{A52}$$

[To the considered order the anomalous dimension of $\mathcal{O}(A,E)$ arising from the perturbative interactions $\Gamma_{b,<>}[U_<,\phi]$ can be neglected. This approximation becomes exact for the operator considered in the main text, i.e., the conserved Yang-Mills Hamiltonian density (131) in temporal gauge.] After introducing another generating functional

$$z_>[j] := \int D\phi\exp[-\Gamma_{b,>}[\phi] - \int d^3x j^a(\vec{x})\phi^a(\vec{x})], \tag{A53}$$

$$= z_>[0]\exp\left[\frac{1}{2}\int d^3x\int d^3y j^a(\vec{x})K^{-1ab}(\vec{x}-\vec{y})j^b(\vec{y})\right], \tag{A54}$$

the ϕ^a fields in $\langle\langle\langle\mathcal{O}(A,E)\rangle\rangle\rangle$ can be replaced by derivatives $-\delta/\delta j^a$ with respect to the source j^a, which yields

$$\langle\langle\mathcal{O}(A,E)\rangle\rangle \simeq \frac{1}{z_>[0]}\left\langle\left\langle\left\langle\mathcal{O}\left(U_<,\frac{-\delta}{\delta j}\right)\right\rangle\right\rangle\right\rangle z_>[j]|_{j=0} \tag{A55}$$

and shows that this intermediate matrix element is a functional of G^{-1} and $U_<$ only.

3. Saddle-point integration over the soft U modes

With the result (A55) for the intermediary matrix element $\langle\langle \mathcal{O}(A,E)\rangle\rangle$ at hand, it remains to perform the functional integral

$$\langle \mathcal{O}(A,E)\rangle = \frac{\int DU_< \langle\langle \mathcal{O}(A,E)\rangle\rangle \exp\{-\Gamma_<[U_<]\}}{\int DU_< \exp\{-\Gamma_<[U_<]\}} \tag{A56}$$

over the soft modes $U_<$. In order to prepare for this last step, we integrate over a complex matrix field V and represent the unitarity constraint $U_< U_<^\dagger = 1$ by inserting a delta functional. The latter is rendered explicit by the additional integration over an auxiliary Hermitian field $\Sigma(\vec{x})$ which acts as a Lagrange multiplier, as explained in Sec. IV A. The result is

$$\langle \mathcal{O}(A,E)\rangle = \frac{\int D\Sigma \int DV \langle\langle \mathcal{O}(A,E)\rangle\rangle \exp\{-\Gamma_<[V] - \Gamma_\Sigma[V,\Sigma]\}}{\int D\Sigma \int DV \exp\{-\Gamma_<[V] - \Gamma_\Sigma[V,\Sigma]\}}, \tag{A57}$$

where the integration contour for $\Sigma(\vec{x})$ runs parallel to the imaginary axis and where

$$\Gamma_\Sigma[V,\Sigma] \equiv \frac{m_g}{2g^2}\int d^3x\, \mathrm{tr}\{\Sigma(V^\dagger V - 1)\}. \tag{A58}$$

[Note that Σ is Hermitian since $VV^\dagger$ is. The unimodularity constraint $\det U_< = 1$ could additionally be implemented by integrating over a minimally coupled $U(1)$ gauge field [18]. We refrain from doing so because the impact of the difference between $\mathrm{SU}(N_c)$ and $U(N_c)$ is of order $1/N_c^2$.] The matrix element (A57) can then be obtained from the soft-mode generating functional (47), i.e.,

$$Z[j,j^\dagger] = \int D\Sigma \int DV \exp[-\Gamma_<[V] - \Gamma_\Sigma[V,\Sigma] - \int d^3z\, \mathrm{tr}\{jV^\dagger + j^\dagger V\}], \tag{A59}$$

after replacing the $U_<$ and $U_<^\dagger$ fields in $\langle\langle \mathcal{O}(A,E)\rangle\rangle$ by derivatives with respect to the matrix sources $j^\dagger$ and j:

$$\langle \mathcal{O}(A,E)\rangle \simeq \frac{1}{Z[0,0]}\left\langle\left\langle \mathcal{O}\left(\frac{-\delta}{\delta j},\frac{-\delta}{\delta j^\dagger}\right)\right\rangle\right\rangle Z[j,j^\dagger]|_{j,j^\dagger=0}. \tag{A60}$$

The unconstrained integral over V in Eq. (A59) is Gaussian and can be done exactly (cf. Sec. IV A), and the remaining integral over Σ can be performed in the saddle-point (or mean-field) approximation, as detailed in Sec. IV B. To leading order, this just amounts to substituting the solution $\bar{\Sigma}$ of the gap equation (62) into the integrand of Eq. (A59).

Given an explicit expression for the covariance, as in our case Eq. (13), the soft-mode action $\Gamma_<[U_<]$ [cf. Eq. (41)] and the amplitudes (A60) are thus uniquely determined functionals of $G_<^{-1}$. In the (trial) vacuum expectation value $\langle \mathcal{H}_{\mathrm{YM}}\rangle$ of the Yang-Mills Hamiltonian, in particular, $G_<^{-1}$ plays the role of a variational trial function. By means of the parametrization (20), $\langle \mathcal{H}_{\mathrm{YM}}\rangle$ becomes a function of the variational parameters μ, m_g, and $\{c_i\}$ with respect to which it has to be minimized according to the Rayleigh-Ritz procedure. (The bare cutoff $\Lambda_{\mathrm{UV}} \gg \Lambda_{\mathrm{YM}}$, on the other hand, has been traded for Λ_{YM} which will be fixed from lattice data, cf. Sec. VIII.)

APPENDIX B: COINCIDENCE LIMIT INTEGRALS

The coincidence limit of the soft-mode correlators calculated in Secs. IV and V is (for $c_{n\geq 2} = 0$) determined by integrals of the type

$$\tilde{\imath}_n(\xi,c_1) := \int_0^1 \frac{\kappa^{2n}}{\kappa^2(1-c_1\kappa^2)+\xi^2}\,d\kappa \qquad n \geq 1, \tag{B1}$$

$$\tilde{\jmath}_n(\xi,c_1) := \int_0^1 \frac{\kappa^{2n}}{[\kappa^2(1-c_1\kappa^2)+\xi^2]^2}\,d\kappa \qquad n \geq 1, \tag{B2}$$

with $c_1 < 1$ (which ensures normalizability of the vacuum wave functional). In the following we list pertinent properties of these integrals and derive analytic expressions to be used, e.g., for the numerical solution of the gap equation and for the evaluation of the vacuum energy. To start with, we note the obvious relations

$$\tilde{\imath}_n(\xi,c_1) > \tilde{\imath}_{n+1}(\xi,c_1), \tag{B3}$$

$$\tilde{\jmath}_n(\xi,c_1) > \tilde{\jmath}_{n+1}(\xi,c_1), \tag{B4}$$

which hold point by point. Furthermore, for the physically required $c_1 < 1$ all integrals (B1) and (B2) are nonnegative. They decrease monotonically with increasing $\xi \geq 0$ and increase monotonically with increasing c_1 in the allowed range $-\infty < c_1 < 1$ (where $1 - c_1\kappa^2 \geq 0$ decreases with increasing c_1 for any $\kappa \in [0,1]$). All integrals are regular at $c_1 = 0$ and at $\xi = 0$, with the exception of $\tilde{\jmath}_1$ which contains a single pole at $\xi = 0$ (see below). Because of the factors of κ^2 in the numerator, all integrands have most of their support close to $\kappa \to 1$, i.e., at momenta $k \sim \mu$.

1. Analytical expressions

An efficient strategy for evaluating the integrals $\tilde{\imath}_n(\xi,c_1)$ analytically starts from the identity

$$\frac{1}{\kappa^2(1-c_1\kappa^2)+\xi^2} = \frac{1}{\sqrt{1+4c_1\xi^2}}\left(\frac{1}{\kappa^2-\kappa_2^2} - \frac{1}{\kappa^2-\kappa_1^2}\right), \tag{B5}$$

which exhibits poles at the positions

$$\kappa^2_{1,2}(\xi, c_1) = \frac{1}{2c_1}(1 \pm \sqrt{1 + 4c_1\xi^2}). \tag{B6}$$

Hence, the evaluation of

$$\tilde{\imath}_n(\xi, c_1) = \frac{1}{\sqrt{1 + 4c_1\xi^2}} \int_0^1 \kappa^{2n}\left(\frac{1}{\kappa^2 - \kappa_2^2} - \frac{1}{\kappa^2 - \kappa_1^2}\right)d\kappa \tag{B7}$$

is reduced to the calculation of one-pole integrals. The simple identity

$$\frac{\kappa^{2n}}{\kappa^2 - x^2} = x^2\frac{\kappa^{2(n-1)}}{\kappa^2 - x^2} + \kappa^{2(n-1)} \tag{B8}$$

implies the recursion relation

$$\int_0^1 \frac{\kappa^{2n}}{\kappa^2 - x^2}d\kappa = \frac{1}{2n-1} + x^2\int_0^1 \frac{\kappa^{2(n-1)}}{\kappa^2 - x^2}d\kappa \tag{B9}$$

and allows to reduce the $\tilde{\imath}_n(\xi, c_1)$ to analytic expressions involving only

$$\int_0^1 \frac{1}{\kappa^2 - x^2}d\kappa = -\frac{1}{2x}\ln\frac{x+1}{x-1} = -\frac{1}{x}\operatorname{arctanh}\left(\frac{1}{x}\right) \quad \text{(for } x^2 \notin]0, 1[\text{)}. \tag{B10}$$

[Note that our $\kappa^2_{1,2}$ ensure $x^2 \notin]0, 1[$ inside the κ integration range (except at $\xi = 0$).]From the recursion relation one then finds (for $x^2 \notin]0, 1[$)

$$\int_0^1 \frac{\kappa^2}{\kappa^2 - x^2}d\kappa = 1 - x\operatorname{arctanh}\left(\frac{1}{x}\right), \tag{B11}$$

$$\int_0^1 \frac{\kappa^4}{\kappa^2 - x^2}d\kappa = \frac{1}{3} + x^2 - x^3\operatorname{arctanh}\left(\frac{1}{x}\right), \tag{B12}$$

$$\int_0^1 \frac{\kappa^6}{\kappa^2 - x^2}d\kappa = \frac{1}{5} + \frac{1}{3}x^2 + x^4 - x^5\operatorname{arctanh}\left(\frac{1}{x}\right), \ldots \tag{B13}$$

and so on. Combining the above results one obtains for the first four $\tilde{\imath}_n$, which are needed in the main text, the following expressions:

$$\tilde{\imath}_1(\xi, c_1) = \frac{\kappa_1\operatorname{arctanh}(\frac{1}{\kappa_1}) - \kappa_2\operatorname{arctanh}(\frac{1}{\kappa_2})}{\sqrt{1 + 4c_1\xi^2}}, \tag{B14}$$

$$\tilde{\imath}_2(\xi, c_1) = \frac{\kappa_2^2[1 - \kappa_2\operatorname{arctanh}(\frac{1}{\kappa_2})] - \kappa_1^2[1 - \kappa_1\operatorname{arctanh}(\frac{1}{\kappa_1})]}{\sqrt{1 + 4c_1\xi^2}}, \tag{B15}$$

$$\tilde{\imath}_3(\xi, c_1) = \frac{\kappa_2^2[\frac{1}{3} + \kappa_2^2 - \kappa_2^3\operatorname{arctanh}(\frac{1}{\kappa_2})] - \kappa_1^2[\frac{1}{3} + \kappa_1^2 - \kappa_1^3\operatorname{arctanh}(\frac{1}{\kappa_1})]}{\sqrt{1 + 4c_1\xi^2}}, \tag{B16}$$

$$\tilde{\imath}_4(\xi, c_1) = \frac{\kappa_2^2[\frac{1}{5} + \frac{\kappa_2^2}{3} + \kappa_2^4 - \kappa_2^5\operatorname{arctanh}(\frac{1}{\kappa_2})] - \kappa_1^2[\frac{1}{5} + \frac{\kappa_1^2}{3} + \kappa_1^4 - \kappa_1^5\operatorname{arctanh}(\frac{1}{\kappa_1})]}{\sqrt{1 + 4c_1\xi^2}}. \tag{B17}$$

[Note that the main ξ and c_1 dependence of these expressions originates from the pole positions $\kappa_{1,2}(\xi, c_1)$, cf. Eq. (B6).]

Analytical solutions for the integrals $\tilde{j}_n(\xi, c_1)$ can either be derived from those for the $\tilde{\imath}_n(\xi, c_1)$ by using the identity

$$\tilde{j}_n(\xi, c_1) = -\frac{1}{2\xi}\frac{\partial}{\partial\xi}\tilde{\imath}_n(\xi, c_1), \tag{B18}$$

or again by direct integration of the pole decomposition. Following the latter path, we have from the square of relation (B5)

$$\tilde{j}_n(\xi, c_1) = \frac{1}{1 + 4c_1\xi^2}\int_0^1\left(\frac{\kappa^{2n}}{(\kappa^2 - \kappa_1^2)^2} - \frac{2\kappa^{2n}}{(\kappa^2 - \kappa_1^2)(\kappa^2 - \kappa_2^2)} + \frac{\kappa^{2n}}{(\kappa^2 - \kappa_2^2)^2}\right)d\kappa, \tag{B19}$$

which we evaluate further with

$$\int_0^1 \frac{\kappa^2}{(\kappa^2 - x^2)^2}d\kappa = \frac{1}{2}\frac{1}{x^2 - 1} - \frac{1}{2x}\operatorname{arctanh}\frac{1}{x}, \tag{B20}$$

$$\int_0^1 \frac{\kappa^2}{(\kappa^2 - x_1^2)(\kappa^2 - x_2^2)}\, d\kappa = \frac{x_2 \operatorname{arctanh}\frac{1}{x_2} - x_1 \operatorname{arctanh}\frac{1}{x_1}}{x_1^2 - x_2^2}, \tag{B21}$$

and

$$\int_0^1 \frac{\kappa^4}{(\kappa^2 - x^2)^2}\, d\kappa = \frac{1}{2}\frac{3x^2 - 2}{x^2 - 1} - \frac{3}{2} x \operatorname{arctanh}\frac{1}{x}, \tag{B22}$$

$$\int_0^1 \frac{\kappa^4}{(\kappa^2 - x_1^2)(\kappa^2 - x_2^2)}\, d\kappa = 1 - \frac{x_1^3 \operatorname{arctanh}\frac{1}{x_1} - x_2^3 \operatorname{arctanh}\frac{1}{x_2}}{x_1^2 - x_2^2}, \tag{B23}$$

as well as

$$\int_0^1 \frac{\kappa^6}{(\kappa^2 - x^2)^2}\, d\kappa = \frac{2 + 10x^2 - 15x^4}{6(1 - x^2)} - \frac{5}{2} x^3 \operatorname{arctanh}\frac{1}{x}, \tag{B24}$$

$$\int_0^1 \frac{\kappa^6}{(\kappa^2 - x_1^2)(\kappa^2 - x_2^2)}\, d\kappa = \frac{1}{3} + (x_1^2 + x_2^2) - \frac{x_1^5 \operatorname{arctanh}\frac{1}{x_1} - x_2^5 \operatorname{arctanh}\frac{1}{x_2}}{x_1^2 - x_2^2} \tag{B25}$$

(all for $x^2 \notin]0, 1[$), and so on.

This yields

$$\tilde{j}_1(\xi, c_1) = \frac{1}{1 + 4c_1\xi^2}\left[\frac{1}{2}\frac{1}{\kappa_1^2 - 1} + \frac{1}{2}\frac{1}{\kappa_2^2 - 1} + \left(\frac{2\kappa_1}{\kappa_1^2 - \kappa_2^2} - \frac{1}{2\kappa_1}\right)\operatorname{arctanh}\frac{1}{\kappa_1} - \left(\frac{2\kappa_2}{\kappa_1^2 - \kappa_2^2} + \frac{1}{2\kappa_2}\right)\operatorname{arctanh}\frac{1}{\kappa_2}\right] \tag{B26}$$

and

$$\tilde{j}_2(\xi, c_1) = \frac{1}{1 + 4c_1\xi^2}\left[\frac{1}{2}\frac{3\kappa_1^2 - 2}{\kappa_1^2 - 1} + \frac{1}{2}\frac{3\kappa_2^2 - 2}{\kappa_2^2 - 1} - 2 - \left(\frac{3}{2}\kappa_1 - \frac{2\kappa_1^3}{\kappa_1^2 - \kappa_2^2}\right)\operatorname{arctanh}\frac{1}{\kappa_1} - \left(\frac{3}{2}\kappa_2 + \frac{2\kappa_2^3}{\kappa_1^2 - \kappa_2^2}\right)\operatorname{arctanh}\frac{1}{\kappa_2}\right] \tag{B27}$$

and

$$\tilde{j}_3(\xi, c_1) = \frac{1}{1 + 4c_1\xi^2}\left[\frac{1}{6}\frac{15\kappa_1^4 - 10\kappa_1^2 - 2}{\kappa_1^2 - 1} + \frac{1}{6}\frac{15\kappa_2^4 - 10\kappa_2^2 - 2}{\kappa_2^2 - 1} - \frac{2}{3}\frac{\kappa_1^2 + 3\kappa_1^4 - \kappa_2^2 - 3\kappa_2^4}{\kappa_1^2 - \kappa_2^2} - \left(\frac{5}{2}\kappa_1^3 - \frac{2\kappa_1^5}{\kappa_1^2 - \kappa_2^2}\right)\operatorname{arctanh}\frac{1}{\kappa_1} - \left(\frac{5}{2}\kappa_2^3 + \frac{2\kappa_2^5}{\kappa_1^2 - \kappa_2^2}\right)\operatorname{arctanh}\frac{1}{\kappa_2}\right] \tag{B28}$$

and

$$\tilde{j}_4(\xi, c_1) = \frac{1}{1 + 4c_1\xi^2}\left[\frac{1}{30}\frac{6 + 14\kappa_1^2 + 70\kappa_1^4 - 105\kappa_1^6}{1 - \kappa_1^2} + \frac{1}{30}\frac{6 + 14\kappa_2^2 + 70\kappa_2^4 - 105\kappa_2^6}{1 - \kappa_2^2} - \frac{2}{15}\frac{3\kappa_1^2 + 5\kappa_1^4 + 15\kappa_1^6 - 3\kappa_2^2 - 5\kappa_2^4 - 15\kappa_2^6}{\kappa_1^2 - \kappa_2^2} - \left(\frac{7}{2}\kappa_1^5 - \frac{2\kappa_1^7}{\kappa_1^2 - \kappa_2^2}\right)\operatorname{arctanh}\frac{1}{\kappa_1} - \left(\frac{7}{2}\kappa_2^5 + \frac{2\kappa_2^7}{\kappa_1^2 - \kappa_2^2}\right)\operatorname{arctanh}\frac{1}{\kappa_2}\right] \tag{B29}$$

and finally

$$\tilde{j}_5(\xi, c_1) = \frac{1}{1 + 4c_1\xi^2}\left[\frac{1}{70}\frac{10 + 18\kappa_1^2 + 42\kappa_1^4 + 210\kappa_1^6 - 315\kappa_1^8}{1 - \kappa_1^2} + \frac{1}{70}\frac{10 + 18\kappa_2^2 + 42\kappa_2^4 + 210\kappa_2^6 - 315\kappa_2^8}{1 - \kappa_2^2} - \frac{2}{105}\frac{15\kappa_1^2 + 21\kappa_1^4 + 35\kappa_1^6 + 105\kappa_1^8 - 15\kappa_2^2 - 21\kappa_2^4 - 35\kappa_2^6 - 105\kappa_2^8}{\kappa_1^2 - \kappa_2^2} - \left(\frac{9}{2}\kappa_1^7 - \frac{2\kappa_1^9}{\kappa_1^2 - \kappa_2^2}\right)\operatorname{arctanh}\frac{1}{\kappa_1} - \left(\frac{9}{2}\kappa_2^7 + \frac{2\kappa_2^9}{\kappa_1^2 - \kappa_2^2}\right)\operatorname{arctanh}\frac{1}{\kappa_2}\right] \tag{B30}$$

[the $\kappa_{1,2}(\xi, c_1)$ are defined in Eq. (B6)] which we needed to evaluate the matrix elements derived in the main text.

2. Limits

When analyzing the soft-mode contributions to gap equation and energy density, it is useful to consider the $\xi \to 0$ and $c_1 \to 0$ limits. This boils down to finding the limits of the $\tilde{\imath}_n$ and $\tilde{\jmath}_n$ integrals which we provide in the present section. The $\xi \to 0$ limits are (for $c_1 \leq 1$, as before)

$$\tilde{\imath}_n(\xi = 0, c_1) = \int_0^1 \frac{\kappa^{2n-2}}{1 - c_1\kappa^2} d\kappa = \frac{1}{2n-1} {}_2F_1\left(1, n - \frac{1}{2}, n + \frac{1}{2}, c_1\right), \quad \text{(B31)}$$

$$\overset{c_1 \to 0}{\to} \frac{1}{2n-1} \quad \text{(B32)}$$

for $n > 1/2$ and

$$\tilde{\jmath}_n(\xi = 0, c_1) = \int_0^1 \frac{\kappa^{2n-4}}{(1 - c_1\kappa^2)^2} d\kappa = \frac{1}{2n-3} {}_2F_1\left(2, n - \frac{3}{2}, n - \frac{1}{2}, c_1\right), \quad \text{(B33)}$$

$$\overset{c_1 \to 0}{\to} \frac{1}{2n-3} \quad \text{(B34)}$$

for $n > 3/2$. [The hypergeometric functions ${}_2F_1(a, b, c, z)$ are defined, e.g., in Ref. [71].] Note that only $\tilde{\jmath}_1$, which does not appear in the coincidence limit of the soft-mode correlation functions, contains a $\xi \to 0$ divergence [cf. Eq. (B38)]. The $\xi \to 0$ limit of the $\tilde{\imath}_n$ integrals can be re-expressed via continued partial integration as

$$\tilde{\imath}_n(\xi = 0, c_1) = -\frac{1}{c_1^{n-1}}\left(\sum_{k=0}^{n-2} \frac{c_1^k}{2k+1} - \frac{\operatorname{arctanh}\sqrt{c_1}}{\sqrt{c_1}}\right), \quad \text{(B35)}$$

which yields

$$\tilde{\imath}_1(\xi = 0, c_1) = \frac{\operatorname{arctanh}\sqrt{c_1}}{\sqrt{c_1}} \overset{c \to 0}{\to} 1, \quad \text{(B36)}$$

$$\tilde{\imath}_2(\xi = 0, c_1) = -\frac{1}{c_1}\left(1 - \frac{\operatorname{arctanh}\sqrt{c_1}}{\sqrt{c_1}}\right), \quad \text{(B37)}$$

etc. Furthermore,

$$\tilde{\jmath}_1(\xi, c_1) \overset{\xi \to 0}{\to} \frac{\pi}{4}\frac{1}{\xi} - \frac{1}{2}\left(\frac{2 - 3c_1}{1 - c_1} - 3\sqrt{c_1}\operatorname{arctanh}\sqrt{c_1}\right) - \frac{15\pi}{8} c_1 \xi + O(\xi^2), \quad \text{(B38)}$$

as well as

$$\tilde{\jmath}_2(\xi = 0, c_1) = \frac{1}{2}\left(\frac{1}{1 - c_1} + \frac{\operatorname{arctanh}\sqrt{c_1}}{\sqrt{c_1}}\right), \quad \text{(B39)}$$

$$\tilde{\jmath}_3(\xi = 0, c_1) = \frac{1}{2c_1}\left(\frac{1}{1 - c_1} - \frac{\operatorname{arctanh}\sqrt{c_1}}{\sqrt{c_1}}\right), \quad \text{(B40)}$$

$$\tilde{\jmath}_4(\xi = 0, c_1) = \frac{1}{2c_1^2}\left(\frac{3 - 2c_1}{1 - c_1} - 3\frac{\operatorname{arctanh}\sqrt{c_1}}{\sqrt{c_1}}\right), \quad \text{(B41)}$$

$$\tilde{\jmath}_5(\xi = 0, c_1) = \frac{1}{6c_1^3}\left(\frac{15 - 10c_1 - 2c_1^2}{1 - c_1} - 15\frac{\operatorname{arctanh}\sqrt{c_1}}{\sqrt{c_1}}\right). \quad \text{(B42)}$$

This implies, in particular,

$$e(\xi, c_1) := \tilde{\imath}_2 - 2c_1\tilde{\imath}_3 + c_1^2\tilde{\imath}_4 + 2c_1\frac{\gamma}{\zeta}\tilde{\imath}_2(\tilde{\jmath}_3 - 2c_1\tilde{\jmath}_4 + c_1^2\tilde{\jmath}_5), \quad \text{(B43)}$$

$$\overset{\xi = 0}{=} \frac{1}{3} - \frac{c_1}{5} - \frac{2\gamma}{3\zeta}\left(1 - \frac{\operatorname{arctanh}\sqrt{c_1}}{\sqrt{c_1}}\right) \quad \text{(B44)}$$

for the combination of integrals which appears in the electric soft-mode contribution (149) to the vacuum energy density (159).

We further examine the $c_1 \to 0$ limits

$$\tilde{\imath}_n(\xi) := \tilde{\imath}_n(\xi, c_1 = 0) = \int_0^1 \frac{\kappa^{2n}}{\kappa^2 + \xi^2} d\kappa, \qquad n \geq 1, \quad \text{(B45)}$$

$$\tilde{\jmath}_n(\xi) := \tilde{\jmath}_n(\xi, c_1 = 0) = \int_0^1 \frac{\kappa^{2n}}{(\kappa^2 + \xi^2)^2} d\kappa, \qquad n \geq 1, \quad \text{(B46)}$$

which we distinguish from the general integrals (B1) and (B2) only by their arguments. Both $\tilde{\imath}_n(\xi)$ and $\tilde{\jmath}_n(\xi)$ decay monotonically in $\xi \in [0, \infty]$, starting from the (finite) values

$$\tilde{\imath}_n(0) = \frac{1}{2n-1}, \qquad n \geq 1, \quad \text{(B47)}$$

$$\tilde{\jmath}_n(0) = \frac{1}{2n-3}, \qquad n \geq 2, \quad \text{(B48)}$$

except for

$$\tilde{\jmath}_1(\xi) \overset{\xi \to 0}{\to} \frac{\pi}{4}\frac{1}{\xi} - 1 + \frac{2}{3}\xi^2 - \frac{3}{5}\xi^4 + O(\xi^6), \quad \text{(B49)}$$

which exhibits the already mentioned pole divergence at $\xi \to 0$. The $\tilde{\imath}_n(\xi)$, $\tilde{\jmath}_n(\xi)$ further satisfy the recursion relations

$$\tilde{\imath}_n'(\xi) \equiv \frac{d\tilde{\imath}_n(\xi)}{d\xi} = -2\xi\tilde{\jmath}_n(\xi) \leq 0, \quad \text{(B50)}$$

$$\tilde{j}'_n(\xi) \equiv \frac{d\tilde{j}_n(\xi)}{d\xi} = -4\xi\tilde{k}_n(\xi) \leq 0, \tag{B51}$$

and

$$\tilde{\imath}_n(\xi) = \frac{1}{2n-1} - \xi^2\tilde{\imath}_{n-1}(\xi), \tag{B52}$$

$$\tilde{j}_n(\xi) = \frac{1}{2n-3}\left[\frac{1}{1+\xi^2} - (2n-1)\xi^2\tilde{j}_{n-1}\right](n>1), \tag{B53}$$

which may be summed up into a finite power series and a transcendental piece,

$$\tilde{\imath}_n(\xi) = \sum_{k=0}^{n-2}\frac{(-1)^k\xi^{2k}}{2n-2k-1} + (-1)^{n+1}(1-\xi\arctan\frac{1}{\xi})\xi^{2n-2}. \tag{B54}$$

Explicit expressions for the first few $\tilde{\imath}_n(\xi)$ and $\tilde{j}_n(\xi)$, which appear in the main text, are thus

$$\tilde{\imath}_1(\xi) = 1 - \xi\arctan\frac{1}{\xi}, \tag{B55}$$

$$\tilde{\imath}_2(\xi) = \frac{1}{3} - \xi^2 + \xi^3\arctan\frac{1}{\xi}, \tag{B56}$$

$$\tilde{\imath}_3(\xi) = \frac{1}{5} - \frac{1}{3}\xi^2 + \xi^4 - \xi^5\arctan\frac{1}{\xi}, \tag{B57}$$

$$\tilde{\imath}_4(\xi) = \frac{1}{7} - \frac{1}{5}\xi^2 + \frac{1}{3}\xi^4 - \xi^6 + \xi^7\arctan\frac{1}{\xi} \tag{B58}$$

as well as

$$\tilde{j}_1(\xi) = \frac{1}{2}\left(-\frac{1}{1+\xi^2} + \frac{1}{\xi}\arctan\frac{1}{\xi}\right), \tag{B59}$$

$$\tilde{j}_2(\xi) = \frac{1}{2}\left(3 - \frac{1}{1+\xi^2} - 3\xi\arctan\frac{1}{\xi}\right), \tag{B60}$$

$$\tilde{j}_3(\xi) = \frac{1}{2}\left(\frac{5}{3} - 5\xi^2 - \frac{1}{1+\xi^2} + 5\xi^3\arctan\frac{1}{\xi}\right), \tag{B61}$$

$$\tilde{j}_4(\xi) = \frac{1}{2}\left(\frac{7}{5} - \frac{7}{3}\xi^2 + 7\xi^4 - \frac{1}{1+\xi^2} - 7\xi^5\arctan\frac{1}{\xi}\right), \tag{B62}$$

$$\tilde{j}_5(\xi) = \frac{1}{2}\left(\frac{9}{7} - \frac{3}{5}(3 - 5\xi^2 + 15\xi^4)\xi^2 - \frac{1}{1+\xi^2} + 9\xi^7\arctan\frac{1}{\xi}\right). \tag{B63}$$

Finally, we note that the $\tilde{\imath}_n(\xi)$, $\tilde{j}_n(\xi)$ (and their analogs with additional powers of the integrand's denominator) determine the coefficients of the expansion of the integrals $\tilde{\imath}_n(\xi; c_1)$ and $\tilde{j}_n(\xi; c_1)$ in powers of c_1. For example, from

$$\frac{1}{\kappa^2(1-c_1\kappa^2)+\xi^2} = \frac{1}{\kappa^2+\xi^2} + \frac{\kappa^4}{(\kappa^2+\xi^2)^2}c_1 + \frac{\kappa^8}{(\kappa^2+\xi^2)^3}c_1^2 + O(c_1^3), \tag{B64}$$

$$\frac{1}{(\kappa^2(1-c_1\kappa^2)+\xi^2)^2} = \frac{1}{(\kappa^2+\xi^2)^2} + \frac{2\kappa^4}{(\kappa^2+\xi^2)^3}c_1 + \frac{3\kappa^8}{(\kappa^2+\xi^2)^4}c_1^2 + O(c_1^3), \tag{B65}$$

one has [with $\tilde{k}_n(\xi) := \int_0^1 \kappa^{2n}/(\kappa^2+\xi^2)^3 d\kappa$]

$$\tilde{\imath}_n(\xi; c_1) = \tilde{\imath}_n(\xi) + \tilde{j}_{n+2}(\xi)c_1 + \tilde{k}_{n+4}(\xi)c_1^2 + O(c_1^3), \tag{B66}$$

$$\tilde{j}_n(\xi; c_1) = \tilde{j}_n(\xi) + 2\tilde{k}_{n+2}(\xi)c_1 + O(c_1^2). \tag{B67}$$

[1] E. Schrödinger, Ann. Phys. (Leipzig) **79**, 361 (1926); **79**, 489 (1926); **80**, 437 (1926); **81**, 8 (1926).

[2] See, e.g., *Proceedings of the International Workshop Variational Calculations in Quantum Field Theory, Wangerooge, Germany*, edited by L. Polley and D. E. L. Pottinger (World Scientific, Singapore, 1988); See also J. O. Akeyo, H. F. Jones, and C. S. Parker, Phys. Rev. D **51**, 1298 (1995) for a corresponding lattice ansatz of the trial action.

[3] J. Greensite, Nucl. Phys. **B158**, 469 (1979).

[4] R. P. Feynman, Nucl. Phys. **B188**, 479 (1981).

[5] J. Cornwall, Phys. Rev. D **38**, 656 (1988).

[6] A. K. Kerman and D. Vautherin, Ann. Phys. (N.Y.) **192**, 408 (1989).

[7] R. Jackiw, in *Field Theory and Particle Physics, Proceedings of the 5th Jorge Andre Swieca Summer School, Campos do Jordao, Brazil*, edited by O. J. P. Eboli, M. Gomes, and A. Santoro (World Scientific, Singapore 1990), p. 731.

[8] O. Eboli, R. Jackiw, and S.-Y. Pi, Phys. Rev. D **37**, 3557 (1988).

[9] Nonequilibrium processes of particular current interest in high-energy physics are those in the early Universe and in the aftermath of ultrarelativistic nuclear collisions at the

RHIC and the CERN LHC (for a brief discussion see, e.g., Sec. V of Ref. [10]).
[10] R. Fariello and H. Forkel, Phys. Rev. D **80**, 025021 (2009).
[11] See, for example, A. Kerman and R. Jackiw, Phys. Lett. **71A**, 158 (1979); Y. Tsue and Y. Fujiwara, Prog. Theor. Phys. **86**, 443 (1991); **86**, 469 (1991).
[12] R. P. Feynman, in *Proceedings of the Workshop Variational Calculations in Quantum Field Theory, Wangerooge, Germany, 1987*, edited by L. Polley and D. Pottinger (World Scientific, Singapore, 1988).
[13] K. Symanzik, Nucl. Phys. **B190**, 1 (1981).
[14] M. Lüscher, Nucl. Phys. **B254**, 52 (1985).
[15] A. P. Szczepaniak, Phys. Rev. D **69**, 074031 (2004).
[16] C. Feuchter and H. Reinhardt, Phys. Rev. D **70**, 105021 (2004).
[17] N. H. Christ and T. D. Lee, Phys. Rev. D **22**, 939 (1980); Phys. Scr. **23**, 970 (1981).
[18] I. I. Kogan and A. Kovner, Phys. Rev. D **52**, 3719 (1995).
[19] D. I. Diakonov, Surv. High Energy Phys. **14**, 29 (1999).
[20] A. Jaffe and E. Witten, http://www.claymath.org/Millennium Prize Problems/Yang-Mills Theory/objects/Official Problem Description.
[21] K. Zarembo, Phys. Lett. B **421**, 325 (1998).
[22] A. Kovner and B. Svetitsky, Phys. Rev. D **60**, 105032 (1999).
[23] H. Forkel, Phys. Rev. D **73**, 105002 (2006).
[24] W. E. Brown, J. P. Garrahan, I. I. Kogan, and A. Kovner, Phys. Rev. D **59**, 034015 (1999).
[25] H. Forkel, Int. J. Mod. Phys. E **16**, 2789 (2007).
[26] It may, for example, shed new light on the interplay between gauge symmetry and topological vacuum properties, which emerge transparently in the Schrödinger picture [7,23], and on microscopic aspects of the confinement mechanism [4,12].
[27] Perturbation theory, on the other hand, becomes more complex in temporal gauge (or other axial gauges) [28].
[28] G. C. Rossi and M. Testa, Nucl. Phys. **B163**, 109 (1980); **B176**, 477 (1980); **B237**, 442 (1984).
[29] A. M. Polyakov, Phys. Lett. **72B**, 477 (1978); L. Susskind, Phys. Rev. D **20**, 2610 (1979); B. Svetitsky, Phys. Rep. **132**, 1 (1986); M. Lüscher, R. Narayanan, P. Weisz, and U. Wolff, Nucl. Phys. **B384**, 168 (1992).
[30] The gauge transformations of Yang-Mills theory without matter span the coset $\mathrm{SU}(N_c)/Z_{N_c}$ since center elements of $\mathrm{SU}(N_c)$ act trivially on the gauge fields. Following Ref. [18] we will refrain from making the deviation of the gauge group from $\mathrm{SU}(N_c)$ manifest, although it could be implemented by gauging the action (34) and may become relevant, e.g., for the discussion of center vortices.
[31] C. Heinemann, E. Iancu, C. Martin, and D. Vautherin, Phys. Rev. D **61**, 116008 (2000).
[32] H. Leutwyler, Nucl. Phys. **B179**, 129 (1981).
[33] The dynamical mass gap and other nonperturbative features of 2 + 1-dimensional compact photodynamics are described exactly by a Gaussian vacuum wave functional as well [34].
[34] I. I. Kogan and A. Kovner, Phys. Rev. D **51**, 1948 (1995); D. Nolland, arXiv:hep-th/0408075.
[35] M. Consoli and G. Preparata, Phys. Lett. B **154**, 411 (1985).
[36] T. H. Hansson, K. Johnson, and C. Peterson, Phys. Rev. D **26**, 2069 (1982).
[37] W. E. Brown, Int. J. Mod. Phys. A **13**, 5219 (1998).
[38] As pointed out in Ref. [18], minimizing the mode energy by using the more general power ansatz $G_>(k) = \alpha k^\beta$ for the UV covariance results in $\alpha = 1$, $\beta = -1$, i.e., precisely the covariance (11) required by asymptotic freedom.
[39] Adopting Eq. (11) for *all* momenta $0 \leq k \leq \Lambda_{\mathrm{UV}}$, on the other hand, would turn the functional (1) into the exact ground state of $N_c^2 - 1$ copies of $U(1)$ photodynamics (since averaging over the gauge group $[U(1)]^{N_c}$ removes the longitudinal gauge-field modes).
[40] A. Cucchieri and T. Mendes, Proc. Sci., CONFINEMENT8 (2008) 040; I. L. Bogolubsky, E.-M. Ilgenfritz, M. Müller-Preussker, and A. Sternbeck, Phys. Lett. B **676**, 69 (2009); O. Oliveira and P. J. Silva, arXiv:0911.1643; see also A. C. Aguilar, A. A. Natale, and P. S. Rodrigues da Silva, Phys. Rev. Lett. **90**, 152001 (2003); D. Dudal, J. A. Gracey, S. P. Sorella, N. Vandersickel, and H. Verschelde, Phys. Rev. D **78**, 065047 (2008); A. C. Aguilar, D. Binosi, and J. Papavassiliou, Phys. Rev. D **78**, 025010 (2008).
[41] T. Iritani, H. Suganuma, and H. Iida, Phys. Rev. D **80**, 114505 (2009); P. J. Silva and O. Oliveira, Nucl. Phys. **B690**, 177 (2004).
[42] W. E. Brown and I. I. Kogan, Int. J. Mod. Phys. A **14**, 799 (1999).
[43] T. Schaefer and E. V. Shuryak, Rev. Mod. Phys. **70**, 323 (1998); D. I. Diakonov, Prog. Part. Nucl. Phys. **51**, 173 (2003); For an elementary introduction to instantons, see H. Forkel, arXiv:hep-ph/0009136.
[44] M. F. Atiyah and N. S. Manton, Phys. Lett. B **222**, 438 (1989).
[45] V. de Alfaro, S. Fubini, and G. Furlan, Phys. Lett. **65B**, 163 (1976); **72B**, 203 (1977); C. G. Callan, R. G. Dashen, and D. J. Gross, Phys. Lett. **66B**, 375 (1977); Phys. Rev. D **17**, 2717 (1978); **19**, 1826 (1979); F. Lenz, J. W. Negele, and M. Thies, Phys. Rev. D **69**, 074009 (2004); Nucl. Phys. B, Proc. Suppl. **140**, 629 (2005).
[46] G. 't Hooft, in *High Energy Physics*, edited by A. Zichichi (Editrice Compositori, Bologna, 1976); S. Mandelstam, Phys. Rep. **23C**, 245 (1976); G. 't Hooft, Nucl. Phys. **B190**, 455 (1981); A. Kronfeld, G. Schierholz, and U. J. Wiese, Nucl. Phys. **B293**, 461 (1987); G. Ripka, *Dual Superconductor Models of Color Confinement*, Lecture Notes in Physics, Vol. 639 (Springer, Berlin, 2004).
[47] L. D. Faddeev, in *Proceedings of 18th International Conference on High Energy Physics, Tbilisi, USSR, 1976* (Steklov Math. Institute and Institute for Advanced Study Report No. IAS-75-0570 1976).
[48] L. D. Faddeev and A. J. Niemi, Nature (London) **387**, 58 (1997); Phys. Rev. Lett. **82**, 1624 (1999).
[49] F. R. Brown *et al.*, Phys. Rev. Lett. **65**, 2491 (1990); Phys. Lett. B **251**, 181 (1990).
[50] J. B. Kogut, M. Snow, and M. Stone, Nucl. Phys. **B200**, 211 (1982).
[51] R. Pisarski and F. Wilczek, Phys. Rev. D **29**, 338 (1984).
[52] In the weakly coupled phase (RG-improved) perturbation theory should work, while the mean-field approximation becomes increasingly reliable with growing coupling in

the strongly coupled phase (at least as long as the mass gap is large enough to effectively suppress fluctuations). It is well known, however, that the above saddle-point approximation does not become exact at large N_c [53]. An improved saddle-point expansion could be developed if a practicable analog of the SU(2) quaternion representation could be found for $N_c \geq 3$ [19]. However, for the value $N_c = 3$ of interest in the context of QCD the ensuing large-N_c suppression of deviations from the mean field might still be rather weak.

[53] A. M. Polyakov, *Gauge Fields and Strings* (Harwood Academic, Chur, Switzerland 1987).

[54] Alternatively, one could trade the $4U$ interactions for another composite field of the form $\chi_{ik} = (\partial_i \partial_k U^\dagger)U$ and treat its contributions at the mean-field level.

[55] The first-order transition expected from the ε expansion and lattice simulations may be prevented by limitations of the mean-field approximation [18].

[56] Numerical studies [50] show that the phase transition in the nonlinear σ model (42) (i.e., for $c_n = 0$) is strongly first order and occurs when $\langle U \rangle \gtrsim 0.5$, indicating that perturbation theory should remain qualitatively reliable down to the transition point.

[57] H. Forkel, Phys. Rev. D **71**, 054008 (2005); in *Seventh Workshop on Continuous Advances in QCD, Minneapolis, May 11-14, 2006* (World Scientific, Singapore, 2007), p. 283.

[58] The contributions of the Fourier modes to the vacuum wave functional are of course also affected by the (c_1 dependent) normalization $Z^{-1/2} = (\int D\vec{A}\Psi[\vec{A}]\Psi[\vec{A}])^{-1/2}$. This overall factor does not change the relative weight of the $A_i^a(k)$ for different k, however.

[59] G. K. Savvidy, Phys. Lett. B **71**, 133 (1977).

[60] S. Narison, Nucl. Phys. **B509**, 312 (1998).

[61] T. Schaefer and E. V. Shuryak, Phys. Rev. Lett. **75**, 1707 (1995).

[62] H. Forkel, Phys. Rev. D **78**, 025001 (2008); arXiv: 0808.0304; Proc. Sci., CONFINEMENT8 (**2008**) 184.

[63] H. Reinhardt and D. Epple, Phys. Rev. D **76**, 065015 (2007); M. Pak and H. Reinhardt, Phys. Rev. D **80**, 125022 (2009).D. Campagnari, A. Weber, H. Reinhardt, F. Astorga, and W. Schleifenbaum, arXiv:0910.4548.

[64] B. M. Gripaios, Int. J. Mod. Phys. A **18**, 85 (2003).

[65] W. E. Brown, J. P. Garrahan, I. I. Kogan, and A. Kovner, Phys. Rev. D **62**, 016004 (2000).

[66] R. Gupta *et al.*, Phys. Rev. D **43**, 2301 (1991); P. de Forcrand and K.-F. Liu, Phys. Rev. Lett. **69**, 245 (1992); C. Morningstar and M. Peardon, Phys. Rev. D **60**, 034509 (1999); W. Lee and D. Weingarten, Phys. Rev. D **61**, 014015 (1999); G. Bali *et al.* (SESAM and TxL Collaborations), Phys. Rev. D **62**, 054503 (2000); A. Hart and M. Teper, Phys. Rev. D **65**, 034502 (2002); N. Ishii, H. Suganuma, and H. Matsufuru, Phys. Rev. D **66**, 094506 (2002); B. Lucini, M. J. Teper, and U. Wenger, J. High Energy Phys. 06 (2004) 012; H. B. Meyer and M. J. Teper, Phys. Lett. B **605**, 344 (2005); M. Loan and Y. Ying, Prog. Theor. Phys. **116**, 169 (2006); Y. Chen *et al.*, Phys. Rev. D **73**, 014516 (2006); H. B. Meyer, J. High Energy Phys. 01 (2009) 071.

[67] I. Kogan, A. Kovner, and J. G. Milhano, J. High Energy Phys. 12 (2002) 017.

[68] B. M. Gripaios and J. G. Milhano, Phys. Lett. B **564**, 104 (2003).

[69] E. Shuryak, J. Phys. G **30**, S1221 (2004).

[70] K. G. Wilson and J. B. Kogut, Phys. Rep. **12**, 75 (1974); for a textbook exposition see M. E. Peskin and D. V. Schroeder, *An Introduction to Quantum Field Theory* (Addison-Wesley, Reading, MA, 1995).

[71] M. Abramowitz and I. A. Stegun, *Handbook of Mathematical Functions*, National Bureau of Standards Applied Mathematics Series 55 (U.S. GPO, Washington, DC, 1972).